ELECTROCHEMICAL ASPECTS OF THE AQUEOUS OXIDATION OF COPPER SULPHIDES

BY

ARLETTE ETIENNE

Ingénieur civil métallurgiste (Université de Liège, 1965)
M.A.Sc. (Université de Montréal, 1966)

A THESIS SUBMITTED IN PARTIAL FULFILMENT OF THE REQUIREMENTS FOR THE DEGREE OF

DOCTOR OF PHILOSOPHY

in the Department

of

METALLURGY

We accept this thesis as conforming to the required standard

THE UNIVERSITY OF BRITISH COLUMBIA

November, 1970

In presenting this thesis in partial fulfilment of the requirements for an advanced degree at the University of British Columbia, I agree that the Library shall make it freely available for reference and study. I further agree tha permission for extensive copying of this thesis for scholarly purposes may be granted by the Head of my Department or by his representatives. It is understood that copying or publication of this thesis for financial gain shall not be allowed without my written permission.

Department of Metallurgy

The University of British Columbia
Vancouver 8, Canada

Date November 26, 1970

ACKNOWLEDGEMENTS

The author wishes to express sincere thanks to Dr. E. Peters for his support and criticism during the course of this work.

Special thanks are due to Dr. A. Mitchell for providing many parts of the experimental equipment.

The assistance of the technical staff, during the experimental program, has been greatly appreciated.

Financial assistance in the form of a Canada Council Scholarship and a National Research Council Scholarship is gratefully acknowledged.

ABSTRACT

The Cu-S binary system was subjected to electrochemical studies at temperatures below 100°C in acid solution. Three types of electrochemical experiments were conducted:

a) Measurements of electromotive force were made on the galvanic cell,

$$Cu \mid 0.1\ M\ CuSO_4,\ 0.1\ M\ H_2SO_4 \mid Cu_yS$$

across the Cu-S system (y variable). The range of copper activity corresponding to the zone of stability of digenite ($\sim Cu_{1.8}S$) was accurately determined. From these measurements and the existing thermodynamic data on covellite (CuS), the standard free enthalpy of formation of digenite ($\sim Cu_{1.8}S$) and djurleite ($Cu_{1.965}S$) was calculated.

b) Copper sulphides were grown on a copper anode from an acidic solution saturated with H_2S at constant current. The thickening of the copper sulphide film was accounted for by electrolytic transport in the scale. The diffusion coefficient of cuprous ions in low chalcocite (Cu_2S) and low digenite ($\sim Cu_{1.8}S$) was calculated from the slope of the electrode potential versus time relationship.

c) Galvanostatic polarization of rotating disk anodes of digenite and covellite was studied at 55°C in 0.1 M $CuSO_4$-0.1 M H_2SO_4 solutions. The resistances arising during the anodic dissolution of these sulphides were assessed from the dependence of the electrode potential on time and current density.

The above polarization experiments were correlated with the electrolysis of copper matte anodes and the leaching experiments in acidic ferric solutions described in the literature.

RESUME

Cette thèse constitue une étude du système binaire Cu-S en solution acide, en dessous de 100°C. Trois types d'expériences, utilisant des méthodes de mesure électrochimiques, ont été realisées:

a) On a mesuré la force électromotrice de la cellule galvanique,

$$Cu \mid 0.1\ M\ CuSO_4,\ 0.1\ M\ H_2SO_4 \mid Cu_yS$$

pour des sulfures de cuivre de diverses compositions et déterminé, avec précision, les valeurs de l'activité du cuivre qui correspondent aux limites de la zone de stabilité de la digénite ($\sim Cu_{1.8}S$). Ces mesures et les données thermodynamiques sur la covelline qui existent dans littérature, ont permis de calculer l'enthalpie libre standard de formation de la digénite ($\sim Cu_{1.8}S$) et de la djurléite ($Cu_{1.965}S$).

b) On a fabriqué des sulfures de cuivre par oxydation, à courant constant d'une anode de cuivre plongée dans une solution acide saturée en H_2S. Un modèle de transport électrolytique dans la couche de sulfure a été proposé pour expliquer la croissance du film. La pente du potentiel de l'électrode en fonction du temps a permis de calculer le coefficient de diffusion des ions cuivreux dans la chalcosine inférieure (Cu_2S) et dans la digénite inférieure ($\sim Cu_{1.8}S$).

c) On a étudié la polarisation galvanostatique de disques tournants du digénite et de covelline à 55°C, en solution 0.1 M $CuSO_4$-0.1 M H_2SO_4. Les variations du potentiel d'électrode en fonction du temps et de la densité de courant ont permis de déterminer les résistances associées à la dissolution anodique de ces sulfures.

On a établi la corrélation entre les expériences précédentes, l'électrolyse d'anodes de mattes de cuivre et les expériences de lixiviation en solutions ferriques décrites par plusieurs auteurs.

TABLE OF CONTENTS

Page

Page

LIST OF FIGURES

LIST OF TABLES

LIST OF FREQUENTLY USED SYMBOLS

a_i = activity of species i

B_i = mobility of species i, $cm^2 sec^{-1} J^{-1}$

C_i = concentration of species i, mole cm^{-3}

D_i = diffusivity of species i, $cm^2 sec^{-1}$

d = specific weight, g cm^{-3}

E = electrode potential, V

E_o = rest potential of an electrode, V

$E_s = E_o + \eta_s$ = surface potential, V

F = Faraday constant, 96,484 clb $eqgr^{-1}$

i = current, A

I = total current density, A cm^{-2}

I_i = current density carried by species i, A cm^{-2}

J_i = flux of species i, mole $cm^{-2} sec^{-1}$

ℓ = thickness of a sulphide layer, cm

M = molecular weight

$M_{ii} = M_i$ = Onsager coefficient, $cm^{-1} sec^{-1} J^{-1}$

q_i = charge carried by particle i, clb

R = gas constant, 8.31439 J $°K^{-1} mole^{-1}$

S = surface area, cm^2

T = absolute temperature, °K

t = time, sec

t_o = reference for time, sec

x = abscissa at time t, cm

x_o = abscissa at time t_o

y = number of copper atoms per sulphur atom in compound Cu_yS

δ = thickness of a diffusion boundary layer, cm

ΔF = free enthalpy change, cal $mole^{-1}$

ΔH = enthalpy change, cal $mole^{-1}$

ΔS = entropy change, e.u.

ε_o = standard electrode potential, V

η_t = charge-transfer overvoltage, V

η_D = diffusion overvoltage, V

η_C = crystallization overvoltage, V

$\eta_S = \eta_C + \eta_t$ = surface overvoltage, V

η_Ω = ohmic potential drop, V

η = total overvoltage, V

μ_i = chemical potential of species i, J $mole^{-1}$

ν = kinematic viscosity of a liquid, $cm^2 sec^{-1}$

σ_1 = partial conductivity due to species i, $\Omega^{-1} cm^{-1}$

σ = total conductivity, $\Omega^{-1} cm^{-1}$

ω = angular velocity, rad. sec^{-1}

τ = transition time, sec

CHAPTER 1

LITERATURE SURVEY AND INTRODUCTION

A. DIRECT LEACHING OF COPPER SULPHIDES

Heap leaching of copper sulphide ores has been practised at Rio Tinto in Spain for over 200 years, but the study of the problems related to the direct oxidation of copper sulphides in acidic aqueous solutions has received attention only in the past 20 years. In spite of the interest manifested by several copper companies for such a process, none of the laboratory attempts has, so far, resulted in industrial application.

The reported works deal with ground minerals, sintered synthetic disks or cast specimens. Direct leaching is carried out in sulphuric, hydrochloric or perchloric solutions, using ferric ions, oxygen or chlorine as oxidising agent. The experiments cover a range of temperature between 15°C and 200°C.

The variety of conditions make the comparison between these experimental results difficult. Only part of the parameters which affect the leaching of sulphides are controlled or determined and the discussion of mechanisms and rate controlling steps is left open to conjecture (1). A review of the literature published on the subject will none the less sum up our knowledge of the copper sulphide behaviour during oxidation in acidic aqueous solutions.

1.1. Stoichiometry of the leaching reactions

Oxidation of copper sulphides in acidic solutions yields, ultimately, a combination of elemental sulphur, dissolved copper and sulphate ions. Nevertheless, suphate is the only oxidized form of sulphur to be stable in these conditions, and the reaction

$$3Cu^{++} + 4H_2O + 4S^\circ \longrightarrow 3CuS + HSO_4^- + 7H^+$$

is thermodynamically favourable. The standard free enthalpy change is equal to $\Delta F^\circ = -19{,}402 - 51.9\ T$, (2), which corresponds to an equilibrium constant of 3.74×10^{25} at 25°C. Thus, a $CuS\text{-}HSO_4^-\text{-}Cu^{++}$ system is more stable than a $S^\circ\text{-}HSO_4^-\text{-}Cu^{++}$ system, and the elemental sulphur eventually formed during the reaction could subsequently react to form CuS and HSO_4^-. Loewen (3) observed, however, that elemental sulphur was not oxidized to sulphate in 0.36 M cupric perchlorate-0.25 M perchloric acid solution under 60.3 p.s.i. of oxygen at 125°C, conditions which led to sulphate formation from covellite (CuS). Elemental sulphur, therefore, would not be an intermediate product in the formation of sulphate, but sulphur and sulphate would be produced simultaneously by oxidation processes which follow at least two different paths.

Sullivan (4) established experimentally that the oxidation of covellite minerals in acidified ferric sulphate solutions at 35°C produces cupric ions in solution and elemental sulphur according to the reaction

$$CuS + 2Fe^{+++} \longrightarrow Cu^{++} + 2Fe^{++} + S^\circ \qquad (1.1)$$

The molar percentages of copper dissolved and elemental sulphur liberated were nearly the same. The molar ratio of copper to sulphur in the residue after a carbon disulphide wash, which removed elemental sulphur, was approximately 1:1. The quantities of ferrous and cupric salts produced by the oxidation were also in a ratio corresponding to the stoichiometry of reaction (1.1).

Thomas and Ingraham (5) leached pure synthetic CuS in acidic ferric sulphate solutions between 25 and 80°C. They found that the ferrous to cupric ion ratio and the cupric ion to elemental sulphur ratio did not exceed 2.1:1 and 1.1:1 respectively. In addition, when leaching tests were carried out in acidic ferric chloride solutions, only 4% of the covellite which had reacted was found to have been converted to sulphate. The foregoing observations confirm that equation (1.1) represents the predominant leaching reaction of covellite in acidic ferric solutions below 100°C.

Jackson and Strickland (6) reported that the reaction of oxidation of chalcocite (Cu_2S) and covellite (CuS) by chlorine in acid solution at 50°C produced almost exclusively elemental sulphur.

Oxygen pressure leaching of copper sulphides yields elemental sulphur and sulphate in various proportions depending on the experimental conditions. These reactions are described by the two following equations:

$$CuS + 1/2O_2 + 2H^+ \rightarrow Cu^{2+} + S^\circ + H_2O, \qquad (1.2)$$

$$CuS + 2\,O_2 \rightarrow Cu^{2+} + SO_4^{2-}. \qquad (1.3)$$

Warren (7), leaching purified covellite (CuS) in sulphuric acid between the melting point of sulphur and 180°C, observed that small quantities of sulphur were produced in experiments carried at high acidity (pH = 0.75, p_{O_2} = 100 p.s.i.).

Loewen (3) leached chalcocite (Cu_2S) at 125°C with 60.3 p.s.i. of oxygen and determined that the fraction of sulphur oxidized to sulphate varied from 15 to 72% as the acidity of the starting solution was decreased from 4 M to 0.5 M perchloric acid.

Dahms, Gerlach and Pawlek (8) changed the concentration of sulphuric acid from 0.204 M to 0.816 M during the leaching of chalcocite under 10 atm. of oxygen at 130°C. The extraction of copper was completed in 2 hours when using 0.204 M sulphuric acid solution. The quantity of copper leached decreased rapidly as the acid content was raised to 0.4 M and remained constant at higher acidity. The quantity of sulphate produced dropped rapidly as the acid concentration was increased to 0.4 M, then it decreased more slowly till it remained unchanged for initial acidities larger than 0.7 M. The sulphur to sulphate molar ratio reached its maximum value of 1:1 for the latter condition.

1.2 Two stage leaching of chalcocite and digenite

Experimental evidence indicates that the oxidation of chalcocite (Cu_2S) and digenite ($Cu_{1.8}S$) occurs in two stages.

Sullivan (9), Thomas, Ingraham and MacDonald (10) leached chalcocite with dilute ferric solution below 50°C and noticed that the reaction slowed down markedly after 50% of the copper was dissolved.

The residue was then identified to be CuS. The first step of the leaching reaction involved copper oxidation according to the equation

$$Cu_2S + 2Fe^{+++} \longrightarrow 2Fe^{++} + Cu^{++} + CuS \qquad (1.4)$$

The second step proceeded with the oxidation of covellite.

Leaching chalcocite at 200°C under 60 p.s.i. of oxygen, Warren (7) noticed a pH increase during the first half of the reaction. This increase was the result of the reaction

$$Cu_2S + 1/2O_2 + 2H^{+} \longrightarrow Cu^{2+} + CuS + H_2O \qquad (1.5)$$

The acidity remained constant during the second half of the reaction.

Copper extraction-time curves obtained by Dahms et al. (8) during oxygen leaching (p_{O_2} = 10 atm.) of various copper sulphides of composition intermediate between Cu_2S and $Cu_{1.8}S$ clearly exhibited two distinct steps. The quantity of copper extracted at the end of the first stage depended upon the initial composition of the sulphide and corresponded to its conversion into CuS. Very little sulphate, if any, was produced during that first stage.

1.3 Kinetics of dissolution of copper sulphides in acidic chlorine solutions

In the leaching experiments conducted by Jackson and Strickland (6) in acidic chlorine solutions, the dissolution rates of copper sulphides were controlled by chlorine diffusion in the solution.

1.4 Kinetics of dissolution of copper sulphides in acidic ferric solutions

The copper-sulphur binary phase diagram (Fig. 1) indicates that the oxidation of chalcocite should result in the appearance of new phases following the sequence: djurleite, digenite, covellite and finally sulphur. However, unstable compositions of these phases or metastable phases may be favoured by the oxidation kinetics (12).

King (13) and Burkin (14) studied the solid state transformations occurring during the oxidation of synthetic chalcocite by acidic ferric chloride solutions between 40 and 80°C. Optical microscopy, X-ray diffraction and electron microprobing techniques were used to study the solid residues recovered after leaching. The electron microprobe analysis suggested that, as copper was leached from Cu_2S, the composition of the resulting solid varied continuously until the molar ratio of copper to sulphur became 1:1; the covellite (CuS) produced by the reaction extended its range of composition up to $Cu_{0.8}S$ at 40°C. These authors observed also that the material was porous and cracked, that the sample could not be polished: these features reduce considerably the significance of microprobe readings. Leaching residues of composition intermediate between Cu_2S and CuS were analysed chemically and by X-ray diffraction. Residues of composition $Cu_{1.8}S$ and CuS exhibited X-ray diffraction patterns in good agreement with those of low temperature digenite and covellite, respectively, as given in the A.S.T.M. index file. A regular shift of the lines on the X-ray photographs was interpreted as an extension of the composition range of these sulphides: digenite would exist from

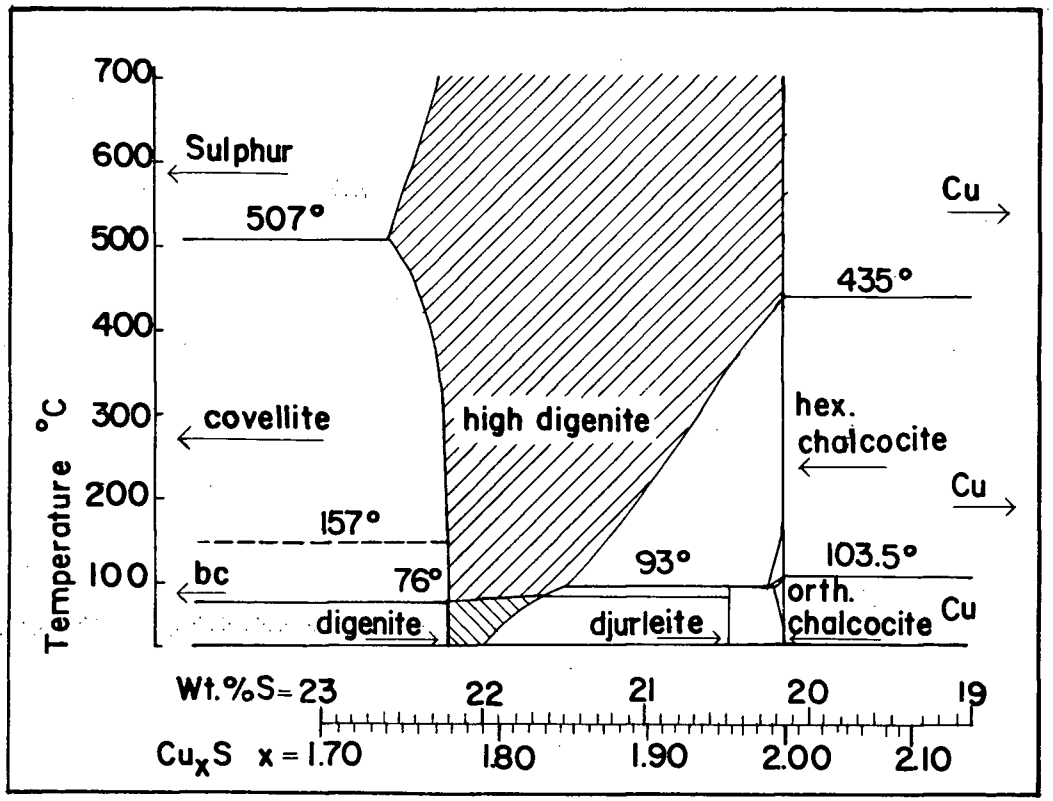

Figure 1. Portion of the phase diagram of the binary Cu-S system taken from Roseboom (11).

$Cu_{1.8}S$ to $Cu_{1.5}S$ and covellite from $Cu_{1.5}S$ to CuS or even down to $Cu_{0.8}S$.

The results of King (13) and Sullivan (9) showed that the oxidation of copper sulphides proceeded with similar rates in hydrochloric and in sulphuric solutions (anionic concentrations <1 M).

Changing the acid content of the solution did not affect significantly the oxidation rate.

Except in very dilute solutions where the leaching rate was controlled by the diffusion of ferric ions, varying the ferric ion concentration did not appear to alter the first stage of the chalcocite dissolution, but affected the covellite dissolution to some extent (5,9,10,13).

The activation energy calculated for the first stage of the chalcocite and digenite leaching varies betwen 0.8 and 5 kcal. $mole^{-1}$, this value being considered indicative of a transport controlled reaction (10,13,14). The activation energy calculated for the second stage of the chalcocite leaching (13,14) and for the covellite leaching (5) is between 22 and 25 $kcal.mole^{-1}$, a range usually associated with processes controlled by an interface reaction. Yet Sullivan's experiments showed that the second step of the leaching of chalcocite was 3 to 4 times faster than the leaching of covellite in otherwise identical conditions (4,9). Furthermore, the rate of oxidation of chalcocite was not dependent on the particle size, though that of covellite was directly proportional to the particle surface.

1.5 Kinetics of dissolution of copper sulphides during oxygen pressure leaching

Leaching chalcocite in 1 M perchloric acid at 110°C under 74 p.s.i.

of oxygen, Loewen (3) found oxygen consumption rates equivalent to 6.3 mA cm^{-2} and 0.8 mA cm^{-2} for the first and second step, respectively. Thomas and al. (10) measured copper dissolution rates equivalent to 18 mA cm^{-2} for the first stage of leaching of chalcocite, and 2 mA cm^{-2} for the leaching of covellite, at 55°C in 0.1 M Fe^{3+}-0.1 M H_2SO_4 solutions. It follows that copper sulphide leaching is much faster with ferric salts than with oxygen, below the melting point of sulphur.

As stated earlier, copper sulphide leaching with oxygen takes place by way of at least two distinct parallel mechanisms, leading to sulphur and sulphate formation. This makes the oxidation kinetics all the more difficult to resolve. The following questions remain largely unanswered, although they have been examined experimentally. Does the sulphur result from the direct electrochemical oxidation of the sulphide or from the oxidation of the hydrogen sulphide evolved by the mineral? Is the sulphate formed by way of an electrochemical or chemical mechanism? What is the influence of the fusion of sulphur (above 119°C) on the oxidation kinetics? What is the relative importance of the various components of the reaction?

Raising the initial acidity of the solution increases the ratio of elemental sulphur to sulphate produced by the reaction. The first stage of the leaching of chalcocite is accompanied by H^+ consumption (Eq. 1.5) and there is a minimum initial acidity required to prevent the subsequent precipitation of basic salts. Warren (7) observed that (T = 160°C, p_{O_2} = 40 p.s.i.) the copper dissolution rate increased as the concentration of sulphuric acid was raised from 30 g/l to 40 g/l. Any further increase of the acidity resulted in a decrease of the

leaching rate. The results obtained by Dahms and al. (8) have already been reported during the discussion of the stoichiometry of the leaching reactions (Section 1.1). The largest leaching rate was obtained for the minimum acidity, 0.204 M H_2SO_4 (T = 130°C, p_{O_2} = 10 atm.). Any further increase of the acidity reduced the copper dissolution rate.

In all these experiments, the oxidation rates increased with the partial pressure of oxygen. Dahms and al. (8) observed that the rate of the first leaching step became independent of the oxygen partial pressure above 10 atm. and that the rate of the second leaching step varied as the 1/3 power of the oxygen partial pressure. This relationship was explained by means of oxygen adsorption on the mineral surface.

The discrepancies between the above works are revealed in the activation energies calculated from the reaction rates. Warren (7) estimated the activation energies associated with the dissolution rates of copper to be 6.6 and 1.8 kcal.mole^{-1} for the first and second stage of the leaching of chalcocite, respectively (p_{O_2} = 40 p.s.i., 30 g/l H_2SO_4, 100-200°C) and 11.8 kcal.mole^{-1} for the leaching of covellite (pH = 0.75, p_{O_2} = 100 p.s.i., 120-180°C). Loewen (3) determined from the oxygen consumption rates that the activation energies were 1.8 and 11.4 kcal.mole^{-1} for the first and second leaching steps of chalcocite, respectively (1 M $HClO_4$, 110-140°C).

Dahms and al. (8) investigated the second leaching step of chalcocite (0.4 M H_2SO_4, p_{O_2} = 10 atm.) between 40 and 140°C. They found two distinct rate-temperature dependences: below 80°C, the dissolution rate of copper was associated with an activation energy of

1.9 kcal.mole^{-1} and above 120°C, with an activation energy of 20.77 kcal.mole^{-1}. Similar activation energies were calculated from the rate of sulphate formation. This type of temperature dependence could be related to a reaction which takes place by two distinct parallel paths. As the temperature is increased, the lightly activated mechanism gives way to the highly activated one.

B. DIRECT ELECTROREFINING OF COPPER MATTE

1.6 Laboratory attempts and related industrial practices

The electrolysis of copper matte anodes was first attempted by Andre in 1877 (15). This trial as well as later attempts were unsuccessful. The development by the International Nickel Co. of Canada of an electrolytic refining process for nickel matte anodes, which went into plant operation at Thompson (Manitoba) in 1961 (16,17), revived the interest for a similar copper matte refining process.

At Inco, nickel matte anodes (76.0% Ni, 2.6% Cu, 0.5% Co, 0.5% Fe, 20.0% S) are electrolysed in a sulphate-chloride solution (composition of the purified electrolyte: Ni^{++}=60 g.p.l., NaCl=100 g.p.l., $SO_4^=$ 100 g.p.l., H_3BO_3=20 g.p.l.). The current density is 20.7 mA cm^{-2}, and the cell voltage, which is about 2.3 V on the first day, gradually rises to about 5 V near the end of the life of a 2 inch thick anode. The porous and granular anode slime is strongly adherent and contains approximately 95% of elemental sulphur.

The sulphide anodes corrode at approximately 94% current efficiency. The remaining 6% of the anodic current is consumed by oxygen evolution which results in an increase of the anolyte acidity. No significant

oxidation of sulphur can be detected. The difference between the cathodic and anodic current efficiencies leads to a slight depletion of the electrolyte in nickel.

Recently, several researchers investigated the feasibility of the copper matte anode electrolysis on laboratory scale (15,18,19,20).

Data on the industrial practice of copper electrorefining are summed up in Table 1 to allow the comparison between the conditions of the electrolysis of copper and copper matte anodes.

Table 1

Copper electrorefining practice (21,22)

Electrolyte composition:		
Cu,	34-52	g.p.l.
H_2SO_4,	125-230	g.p.l.
Cl,	0.02-0.052	g.p.l.
Fe,	0.2-6	g.p.l.
Electrolyte-temperature	55-70	°C
Power:		
Max. cathode current density,	16-25	mA cm^{-2}
	up to 32	mA cm^{-2}
Current efficiency,	89-98	%
Cell voltage,	0.17-0.40	V

At 20°C, the electrolysis of copper matte anodes is accompanied by an important increase in the bath voltage which reaches, in some cases, the prohibitive value of 8 V (20) and is characterized by a very low anode yield (15).

The electrolysis of Cu_2S anodes ($CuSO_4$ = 30 g.p.l., H_2SO_4 = 100 g.p.l., T = 55°C) at a current density of 15 mA cm^{-2} yields a bath voltage of 0.9 V during the first 14 hours, then a sharp potential increase develops to a maximum of 2.1 V; the bath voltage finally oscillates between 1.5 and 1.8 V (15). The first part of the electrolysis corresponds to CuS formation. During the second part, S° formation, O_2 evolution and eventually SO_4 formation supplement the initial reaction (15). The Cu content of the bath remains constant during the first part of the electrolysis, then it decreases linearly; after 5 days, the solution is depleted of 30% of its copper, with a corresponding increase in acidity (15).

The slimes, granular and porous, remain adherent on the anode; they are composed of a mixture of CuS and S° (15,18,19,20). Kuxmann and Biallass (15) observed that the copper content of the slime was decreasing from 20% in electrolyte containing 100 g.p.l. of H_2SO_4 to 14% in electrolyte containing 250 g.p.l. of H_2SO_4. The increase in acidity resulted also in a small decrease in the anodic and cathodic current efficiencies.

The amount of elemental sulphur oxidized to sulphate varies widely with the experimental conditions and from author to author. Habashi and al. (20) claimed that the elemental sulphur-sulphide balance closed within 3% (Cu = 30 g.p.l., H_2SO_4 = 100 g.p.l., I = 10 mA cm^{-2}, T = 20°C) but Venkatachalam and al. (19) (Cu = 30 g.p.l., H_2SO_4 = 150 g.p.l., I = 10 mA cm^{-2}, T = 33°C) and Loshkarev and al. (18) (Cu = 35 g.p.l., H_2SO_4 = 200 g.p.l., I = 10 mA cm^{-2}, T = 15°C) described measurements indicating that 55% of the sulphur was oxidized to sulphate. Kuxmann and al. (15) determined that the amount of sulphur oxidized to

sulphate varied between 4 and 10% (Cu = 30 g.l.p., H_2SO_4 = 100-250 g.p.l., I = 15 mA cm^{-2}, T = 55°C).

These investigations show that the direct electrorefining of copper matte is heavily penalized by the copper loss in the anode slime (2.8% of the anode Cu content in 250 g.p.l. H_2SO_4 electrolyte (15)), by the impoverishment of the electrolyte in copper and by the acid build up resulting from the relatively low anode efficiency (≃ 89% (15)).

To compensate for these drawbacks, Kuxmann and al. (15) added HNO_3 continuously to the electrolyte (up to 0.1 g. p. Amp.hr.). This reduced the copper loss in the slime to 0.4% of the copper contained in the anode and reduced the variation of the copper and acid content of the electrolyte. The presence of nitric acid effectively reduced the cathode current efficiency from 98 to approximately 92% as a result of the reaction

$$3Cu + 2NO_3^- + 8H^+ \longrightarrow 2NO + 3Cu^{2+} + 4H_2O,$$

and increased slightly the anode current efficiency according to the equation (15)

$$3CuS + 2NO_3^- + 8H^+ \longrightarrow 3Cu^{2+} + 3S^\circ + 2NO + 4H_2O,$$

The presence of nitric acid did not appear to affect markedly the sulphate formation (sulphur oxidized to sulphate remained below 10% in all cases). The addition of nitric acid to the electrolytic bath seems to improve the feasibility of the direct electrorefining of copper

mattes but represents the consumption of a reagent at some additional cost.

C. ELECTROCHEMICAL ASPECTS OF THE AQUEOUS OXIDATION OF COPPER SULPHIDES

1.7 Scope of the present work

In all cases, the oxidation of copper sulphides imposes a series of solid state transformations releasing copper ions in solution and leading to elemental sulphur formation. This basic reaction sequence is sometimes accompanied by sulphate formation. The development of the oxidation reactions results from the driving force imposed on the system, the mobility of the various interfaces, and the rate of transport of copper through the reaction products. The knowledge of the resistances arising from every reaction step should allow the prediction of the overall oxidation rates.

Copper sulphides are electronic conductors; chalcocite is a p-type semiconductor, the conductivity of which increases notably with copper deficiency ($\sigma \simeq 10^{-2}$ to 50 $\Omega^{-1}cm^{-1}$ at room temperature) (23,24), digenite and covellite are almost metallic in character ($\sigma = 2 \times 10^{4}$ $\Omega^{-1}cm^{-1}$ at room temperature) (23,25). Thus, electrode potential measurements can be used to monitor the solid state transformations resulting from the oxidation. Since electrode potentials are very sensitive to the presence of a second phase and of impurities, the following electrochemical study was performed on pure, synthetic copper sulphides.

Prior to any dynamic study, the knowledge of electrode rest potentials is desired. The stability of the electrode-electrolyte system can then be ascertained and the existence of a thermodynamic

equilibrium potential considered. This study began with the measurements of the electromotive force of the cell

$$Cu \mid 0.1\ M\ CuSO_4,\ 0.1\ M\ H_2SO_4 \mid Cu_yS, \qquad I$$

which has been established to correspond to the equilibrium relationship

$$E = -RT \ln a_{Cu}(Cu_yS)$$

The sulphide composition was selected to produce a two-phase electrode having a fixed copper activity.

The existing thermodynamic data on the Cu-S system were relevant only to the two terminal compounds, Cu_2S and CuS (2,26). The stability ranges of the various copper sulphides, Cu_2S, $Cu_{1.965}S$, $\simeq Cu_{1.8}S$, CuS, (Fig. 1) were to be determined. Measurements of cell I e.m.f. with a high impedance electrometer ($10^{13}\ \Omega$ input resistance) allowed the accurate determination of the copper activity in digenite-covellite and digenite-djurleite mixtures. The standard free enthalpy of formation of digenite and djurleite was calculated from these measurements and the thermodynamic data on CuS, available in the literature (Chapter 2).

The contribution of the solid state diffusion to the transport of copper ions through the oxidation products can be assessed from the range of the copper activities corresponding to the zone of stability of the oxidation products and from the diffusion coefficients of copper ions in these solid phases. The following experiment was designed in order to measure the copper ionic diffusivity in copper sulphides. An

ionic current of copper was forced through a copper sulphide membrane and the associated voltage drop determined. In the absence of surface overvoltages and electronic short-circuits, the ionic resistivity is directly measured by the potential difference across the membrane. The method proved to be inapplicable to digenite, and the irreversibility of the reactions at the covellite electrode obscured these measurements (Appendix 1).

More valid results were obtained with the following electrochemical experiments which allowed the indirect determination of the desired diffusion coefficients. A copper anode was oxidized in H_2S saturated acid solutions, at constant current. The analysis of the electrode potential versus time relationship permitted the calculation of the copper ion diffusivity in low chalcocite and low digenite. The experiment could not, however, be extended until the formation of a layer of covellite (Chapter 3).

The apparent electrochemical mechanism of some leaching reactions of copper sulphides (27) suggested that anodic polarization studies could provide useful information on the behaviour of these sulphides during oxidation. Galvanostatic polarization studies of rotating disk anodes of digenite and covellite were thus undertaken. The rotating disk electrode technique was adopted because the well defined geometry and hydrodynamic regime of this system permits the calculation of the ohmic voltage drop in solution and of transport rates in the electrode boundary layer. The relation of the electrode potentials versus time and current density allowed the magnitude and effects of the resistances associated with the dissolution reaction to be assessed (Chapter 4).

The behaviour of chalcocite during similar polarization experiments is derived from the above results with the help of theoretical considerations and correlated with actual experiments done by other researchers.

Leaching rates calculated from information obtained in the present work are consistent with experimental rates observed by other investigators using ferric oxidants in similarly designed leaching experiments. The general features of the leaching of copper sulphides in acidic ferric solution can be accounted for by the oxidation mechanisms proposed in the present work (Chapter 5).

CHAPTER 2.

THERMODYNAMIC MEASUREMENTS IN THE Cu-S SYSTEM

2.1 Measurement method

Many investigations of chemical reactions involving copper sulphides have been explained on the basis of the existence of only the two compounds, Cu_2S and CuS. However, the phase diagram of the Cu-S system as published by Roseboom (11) leads to a more accurate interpretation of these reactions. Four copper sulphides exist in a stable form at room temperature and have been observed as minerals: chalcocite (Cu_2S), djurleite ($Cu_{1.965}S$), digenite ($\sim Cu_{1.8}S$) and covellite (CuS). The only existing thermodynamic data on the Cu-S system are relative to the two terminal compounds. The thermodyanmic properties of the intermediate copper sulphides, which are electronic conductors (23,24, 25), may be investigated by electrode potential measurements.

The equilibrium potential of a two-component electrode, such as a copper sulphide, depends on the particular composition of the solid and on the process of charge-transfer between the electrode and the electrolyte; this charge-transfer can take place through the cation, the anion or a redox. couple present in the solution. When two or more different charge-transfer processes occur independently of each other, at the same electrode surface, currents of opposite sign flow across the electrode-electrolyte boundary, resulting in a change of the chemical composition of the system. The rest potential, which is measured in the absence of an external flow of current, is then a mixed potential. Charge-transfer processes involving both the Cu and the S species could occur at the surface of a Cu_yS electrode in contact with a $CuSO_4$

electrolyte; this would result in a subsequent alteration of the composition of the solid and of the solution (Fig.2).

Studies of the rest potentials of electrodes of synthetic and natural, chalcocite and covellite established that the potential of these electrodes varied with the activity of cupric ions in solution, in a way identical to a copper electrode, and that they were not affected by the presence of sulphate (15,28,29,30). The standard potential of a Cu_2S electrode in cupric solution, at 25°C, was derived from these experiments as 486 mV (15), 490 mV (28) and 505 mV (29). The standard potential of a CuS electrode in cupric solution, at 25°C, was calculated to be 597 mV (30) and 567 mV (29).

Further evidence that the $S°-SO_4^{--}$ couple is inert has been otained by Loewen (3), who verified that elemental sulphur did not oxidize to sulphate in cupric perchlorate solution at 125°C under 60.3 p.s.i. of oxygen. Sullivan (4,9), who studied the oxidation of copper sulphides in acidic ferric solution below 100°C, established that the final products of oxidation were cupric ions and elemental sulphur, though sulphate was the most stable sulphur species in his experimental conditions. Therefore the potential difference between the sulphide electrode and the cupric sulphate electrolyte is determined by the reaction

$$(Cu)_{Cu_yS} \longrightarrow Cu^{++} + 2e$$

The electromotive force of the galvanic cell

$$Cu/0.1\ M\ CuSO_4,\ 0.1\ M\ H_2SO_4/Cu_yS \qquad (I)$$

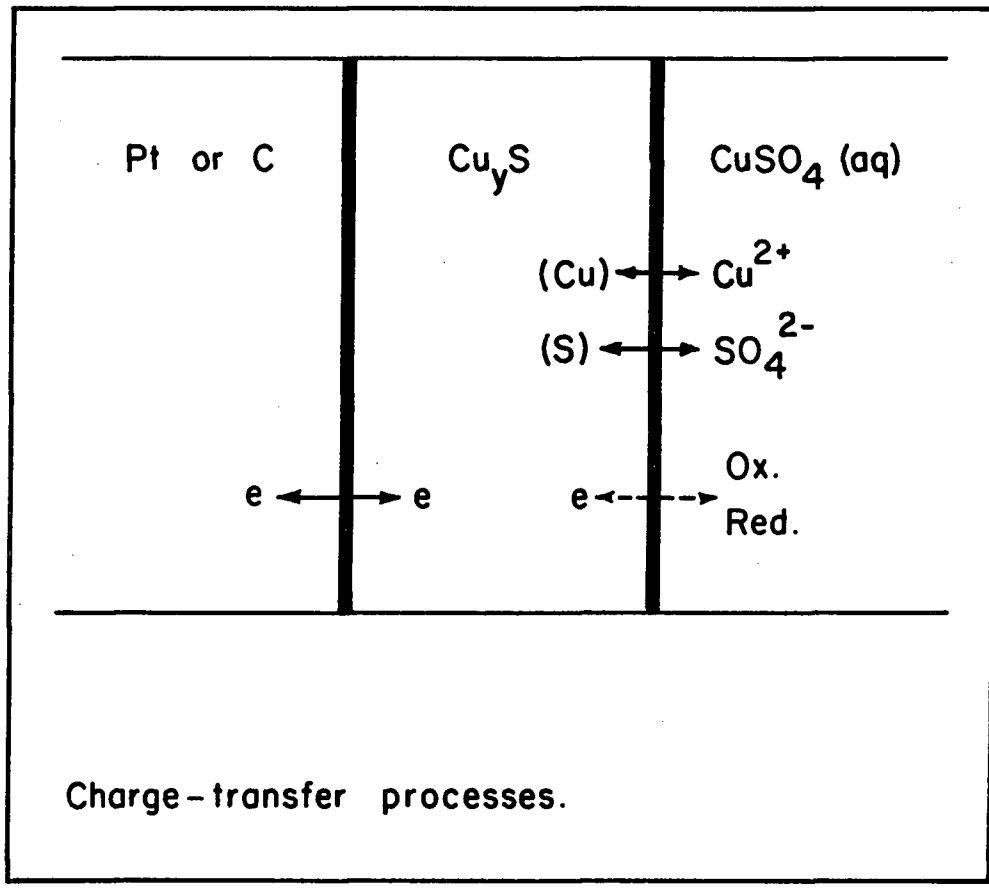

Figure 2. Charge-transfer processes between a Cu_yS electrode and a $CuSO_4$ electrolyte.

is a direct measurement of the copper activity in the sulphide,

$$-2\Delta E\ F = \mu_{Cu}(Cu_yS) - \mu^{o}_{Cu} = RT\ \ln\ a_{Cu}$$

Cell I may be considered as a double cell involving the two individual cells

$$Cu/0.1\ M\ CuSO_4,\ 0.1\ M\ H_2SO_4/S.C.E.\ (25°C), \qquad (II)$$

$$S.C.E.\ (25°C)/0.1\ M\ CuSO_4,\ 0.1\ M\ H_2SO_4/Cu_yS, \qquad (III)$$

and both the Cu and Cu_yS potentials are measured separately versus S.C.E. (25°C).

2.2 Experimental

Copper sulphides of appropriate Cu to S ratio were synthesized at 400°C in sealed quartz tubes from 99.999% pure Cu and S purified according to the method of Bacon and Fanelli (31). The product was pressed under vacuum into a disk, 13 mm in diameter by 1 mm thick. The sulphide was cemented to a platinum foil with epoxy resin made conductive by the addition of graphite powder. The specimen was then mounted in acrylic resin (Koldmount) and polished. The electrolyte (0.1 M $CuSO_4$, 0.1 M H_2SO_4) was kept free from oxygen by continuously bubbling helium, which had been previously saturated with the same solution. The cell was immersed in an oil thermostat.

The cell e.m.f. was measured by a high impedance electrometer

(Keithley 630). The reference electrode was a saturated calomel electrode at 25°C: corrections calculated from de Bethune, Licht and Swendeman's data (32) were made to compensate for the temperature fluctuations of the reference electrode. The Pt-Cu lead contacts were at room temperature. The solution was analysed by electrogravimetry for copper after each final measurement.

2.3. Results

2.3.1. Electrode potential measurements

The results of the measurements of the Cu electrode potentials are reported in Fig. 3 as a function of temperature. Measurements were made after an anodizing or cathodizing treatment on electrodes of different purity, some being annealed under H_2. The experimental values follow a linear relationship in the temperature range, 35-75°C.

$$E = (70.45 \pm 0.33) \times 10^{-3} + (0.632 \pm 0.025) \times 10^{-3} \ (T - 328) \quad (V)$$

The equation and the errors were calculated by the classical method of the linear regression for a probability of 98%.

Electrodes of composition $Cu_{1.37}S$ were then studied. An X-ray diffraction pattern confirmed the existence of the two phases, digenite and covellite. Covellite is reported to be stoichiometric, digenite in equilibrium with covellite has the composition $Cu_{1.765}S$, this composition limit remaining constant up to 200°C (11). A sample synthesized at high temperature should still be in equilibrium after cooling down to room temperature.

To appreciate the reversibility of the electrode reaction, the digenite-covellite mixture was subjected to anodizing and cathodizing

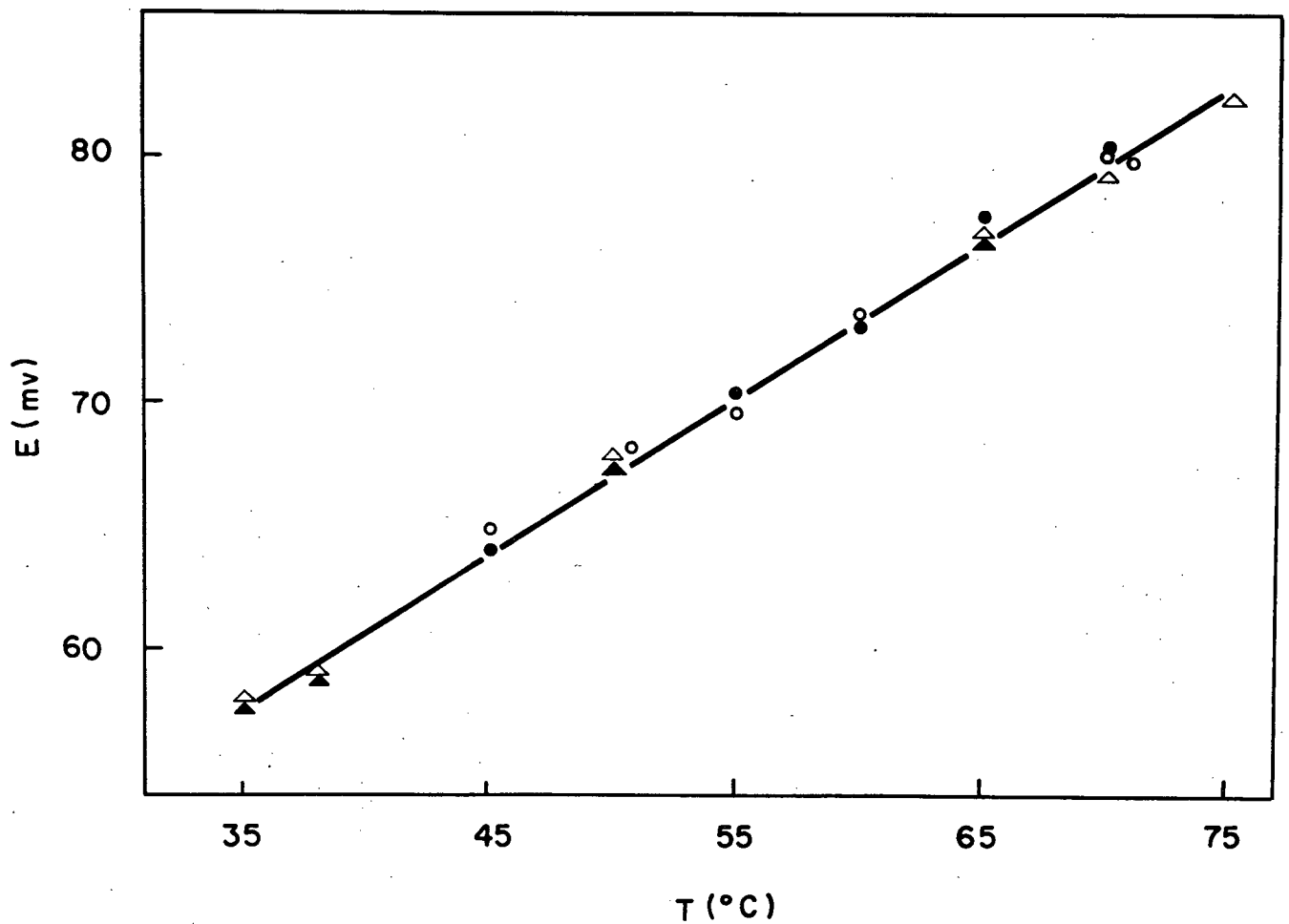

Figure 3. Temperature dependence of the e.m.f. of the cell
S.C.E. (25°C) | 0.1 M $CuSO_4$-0.1 M H_2SO_4 | Cu

○ △ after anodization ● ▲ after cathodization △ ▲ H_2 annealed

current. The amount of current passed through the specimen resulted in a variation of 0.3% of its average Cu content. After switching off, the electrode potential was recorded as a function of time. The stabilized electrode was then subjected to a current of opposite sign and the rest potential recorded. A series of these relaxation curves is shown on Fig. 4. Though the relaxation curves obtained after successive anodization and cathodization on the same sample were not symmetrical, the relaxation curves obtained after anodization and cathodization of two fresh specimens were symmetrical and more convergent. The gap between any set of two curves decreased with increasing temperature, as it appears from the comparison of Fig. 4 and 5.

Forcing current in or out of the electrode forces the following reaction to the right or to the left,

$$CuS + 0.765Cu \rightleftharpoons Cu_{1.765}S,$$

unless one of the sulphides takes care of the Cu by composition changes. The whole specimen homogenizes by diffusion.

The equilibrium electrode potential was chosen in the middle of the gap between two corresponding relaxation curves. The results are plotted on Fig. 6 as a function of temperature. They are expressed by a linear relationship in the temperature range, 40-70°C,

$$E = (251.50 \pm 0.35) \times 10^{-3} + (0.765 \pm 0.035) \times 10^{-3} (T - 328) \text{ (V)}$$

The equation and the errors were calculated by the classical method

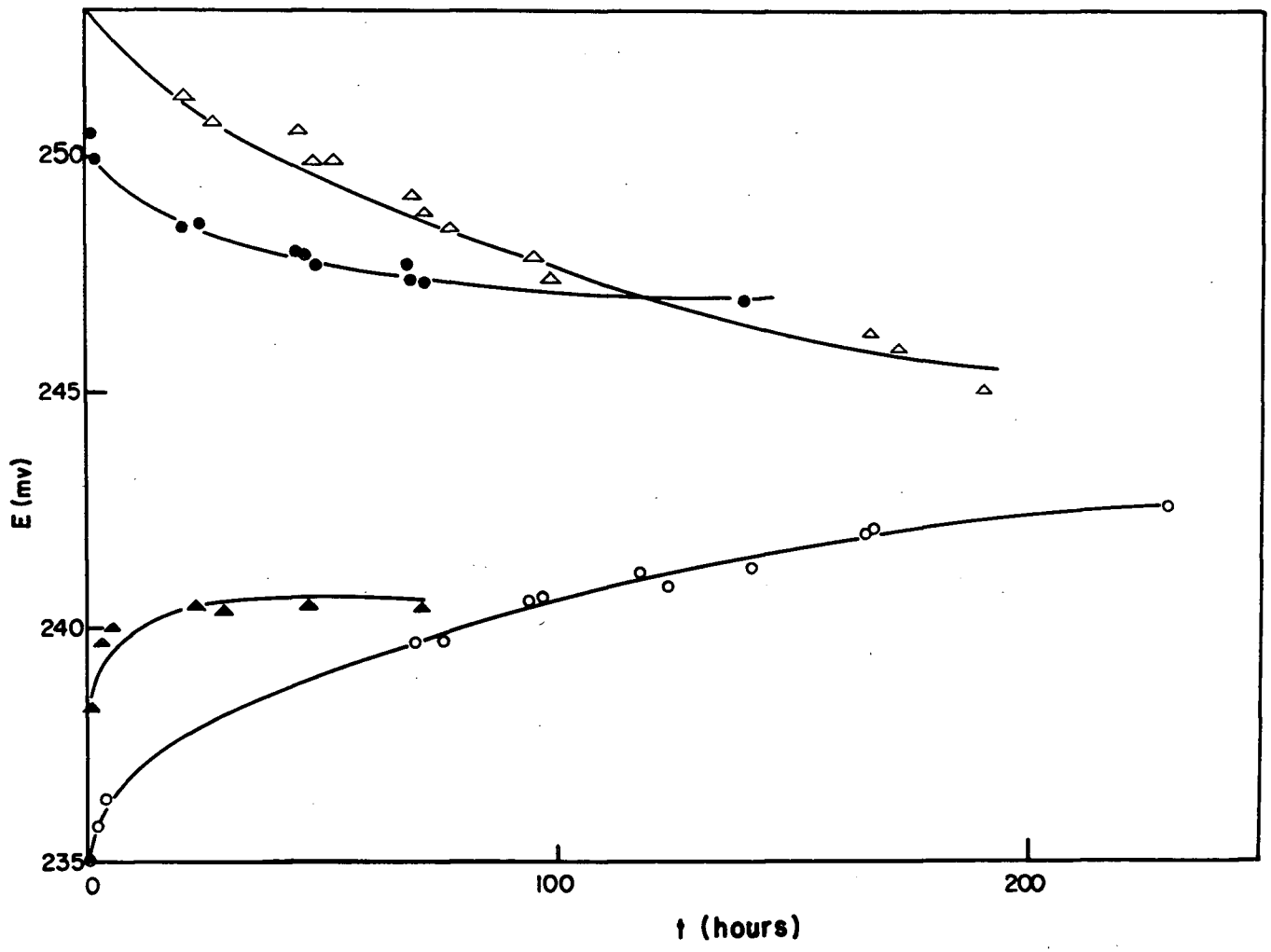

Figure 4. Relaxation curves obtained at 45°C after anodization or cathodization of CuS-$Cu_{1.765}S$ electrodes.

▲ ○ after cathodization

△ ● after anodization

△ ○ treatment on fresh electrode

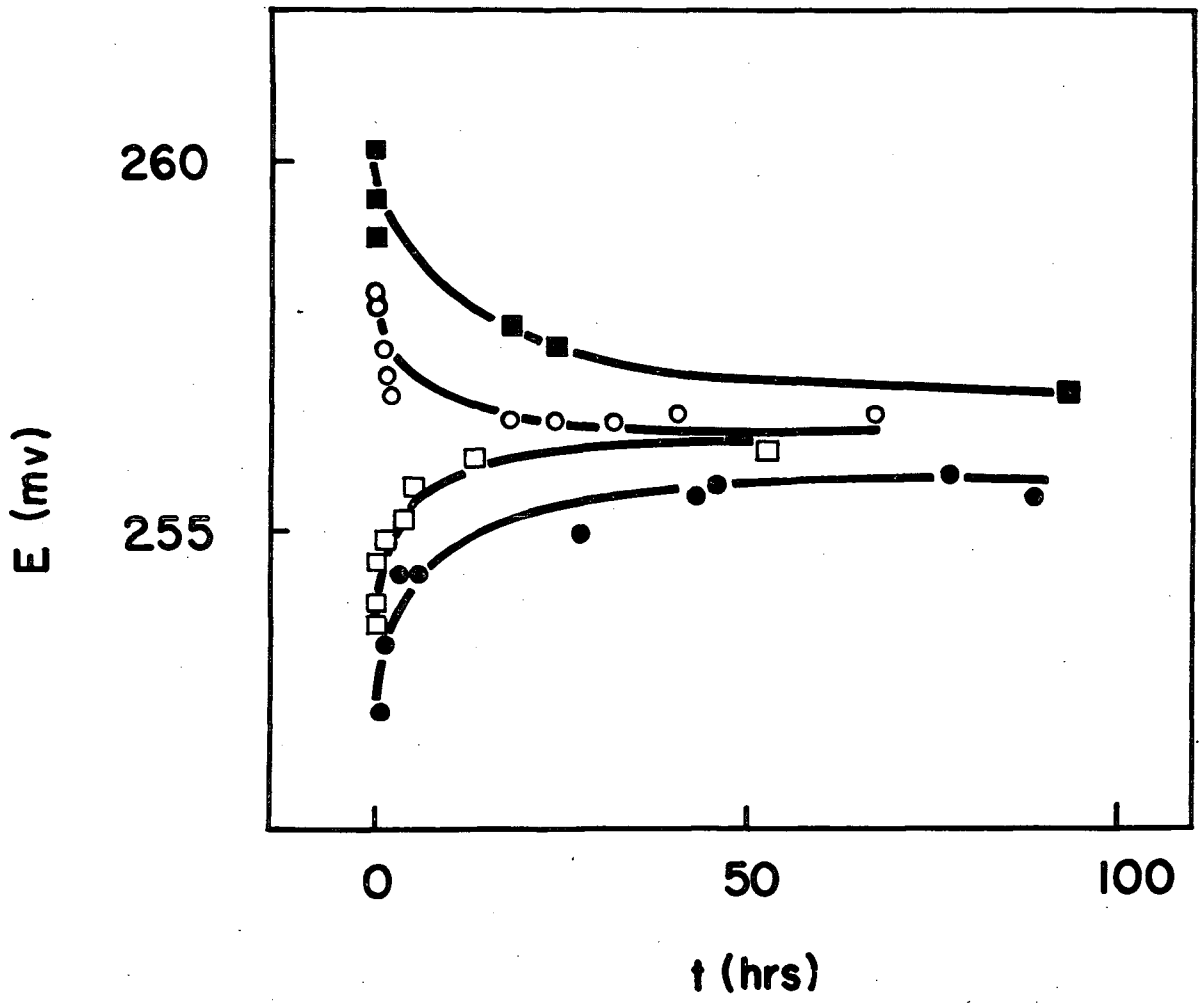

Figure 5. Relaxation curves of CuS-$Cu_{1.765}S$ electrodes, at 60°C.

■ ○ after anodization

□ ● after cathodization

○ □ treatment on fresh electrode

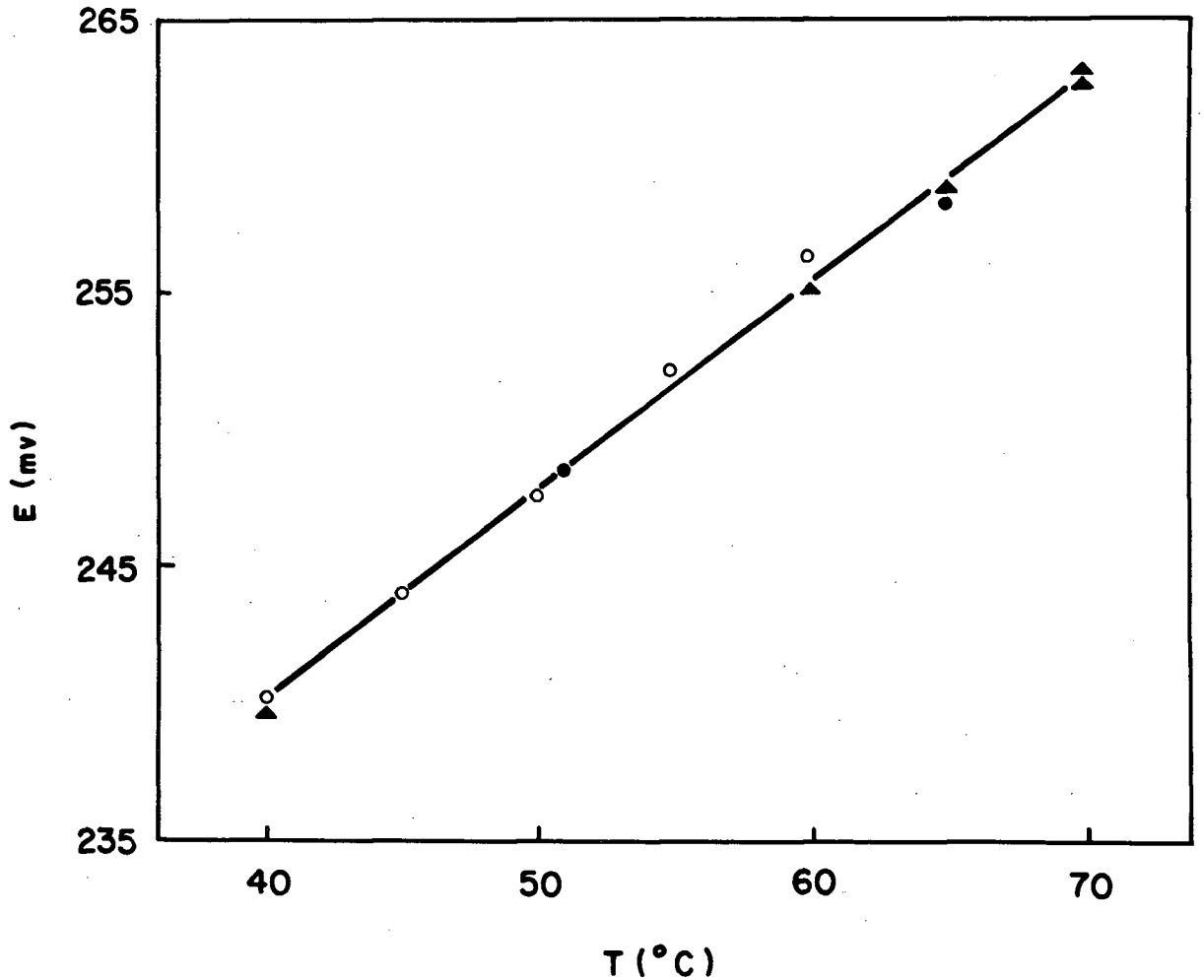

Figure 6. Temperature dependence of the e.m.f. of the cell
S.C.E. (25°C) | 0.1 M $CuSO_4$-0.1 M H_2SO_4 | $CuS-Cu_{1.765}S$

▲ no preliminary electrolysis

o ● different batches of sulphides

of the linear regression for a probability of 98%.

Sulphides of composition $Cu_{1.84}S$ and $Cu_{1.88}S$ were synthesized. X-ray diffraction provided evidence for the presence of both digenite and djurleite. According to Roseboom (11) the Cu rich limit of digenite varies with temperature, going from $Cu_{1.79}S$ at room temperature to $Cu_{1.83}S$ at 83°C where digenite inverts its crystal structure.

The electrode potential of the digenite-djurleite mixture was measured during heating and cooling cycles. A period from 24 to 96 hours was allowed for equilibration at each temperature. The experimental results are reported on Fig. 7 as a function of temperature. The values can be accommodated by a straight line relationship,

$$E = (242.20 \pm 0.45) \times 10^{-3} + (0.62 \pm 0.06) \times 10^{-3} \ (t - 343) \ (V)$$

The equation and the errors were calculated by the classical linear regression for a probability of 98%.

It appears that the reaction

$$Cu_yS + (1.965 - y)Cu \longrightarrow Cu_{1.965}S^*$$

takes place quite readily above 70°C but becomes sluggish below 55°C. This is consistent with Roseboom's (11) observation that the djurleite formation is reversible at 93°C.

---

* Cu_yS represents the Cu rich limit of digenite, y is a function of temperature, $1.79 < y < 1.83$.

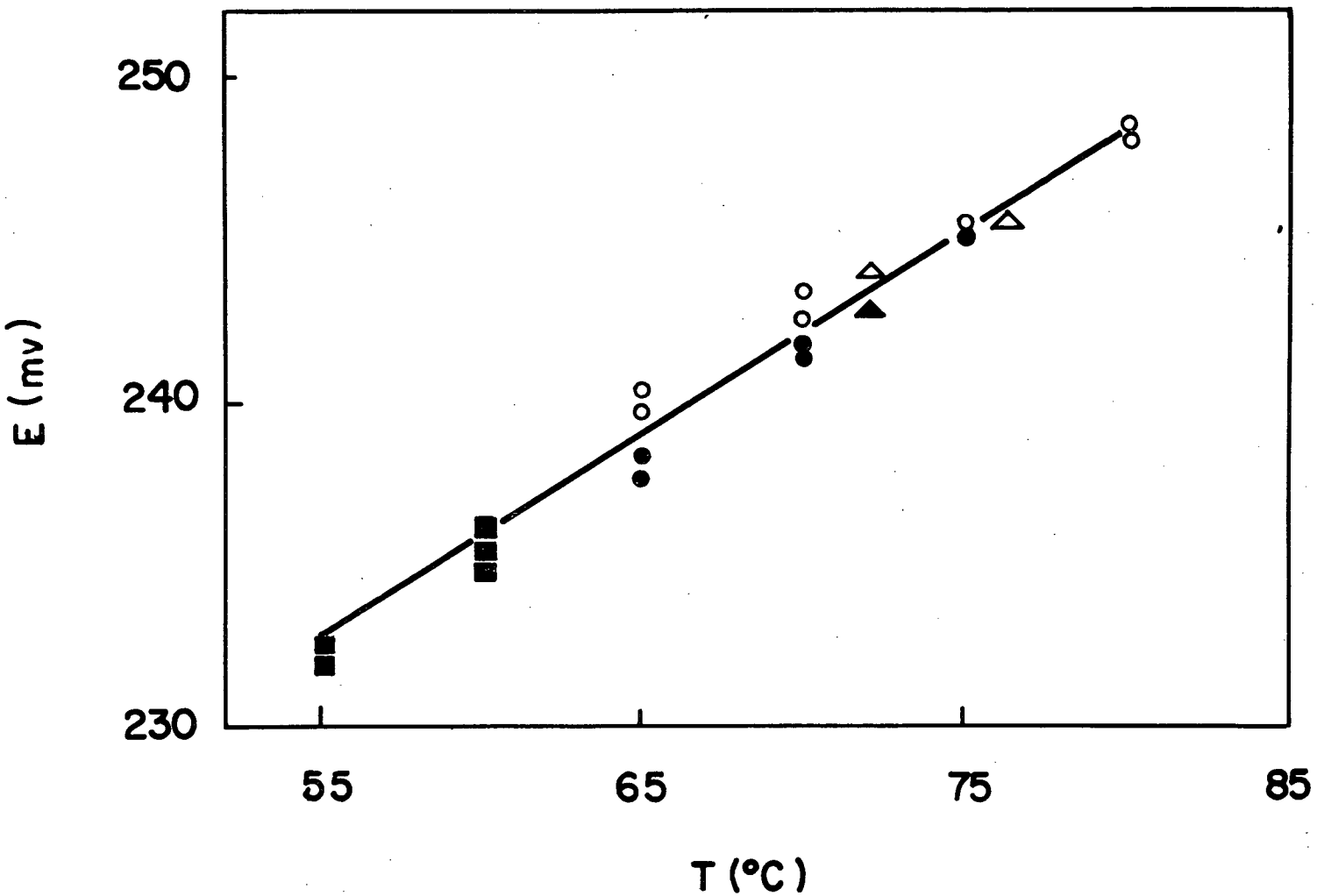

Figure 7. Temperature dependence of the e.m.f. of the cell
S.C.E. (25°C) | 0.1 M $CuSO_4$-0.1 M H_2SO_4 | Cu_yS-$Cu_{1.965}S$

○ △ different compositions, after heating

● ▲ different compositions, after cooling

■ excluded from the linear regression.

Specimens of composition $Cu_{1.98}S$ produced, in spite of a cooling rate of 10°C per day, a mixture of chalcocite and metastable tetragonal djurleite identified by X-ray diffraction. Tetragonal djurleite is often reported to be present in sulphide of composition intermediate between chalcocite and digenite synthesized at high temperature (11,33).

From the reported set of experimental data, the standard free enthalpy of formation of low digenite and djurleite can be calculated. The standard states are pure Cu, pure orthorhombic S and the pure copper sulphide of the stated composition.

2.3.2. Standard free enthalpy of formation of low digenite

The activity of copper in a covellite-digenite mixture in equilibrium is directly related to the standard free enthalpy of the reaction

$$CuS + 0.765Cu \longrightarrow Cu_{1.765}S,$$

which depends only on the standard free enthalpy of formation of CuS and $Cu_{1.765}S$,

$$\Delta F^\circ (Cu_{1.765}S) = \Delta F^\circ (CuS) + 0.765\ RT\ \ln a_{Cu}.$$

Von Wartenberg (34) measured the heat of formation of CuS at 25°C,

$$\Delta H^\circ_{298°K} (CuS) = -11{,}610 \pm 400\ cal.mole^{-1}\ ^*,$$

---

* .1 cal. = 4.1840 J.

and Kubaschewsky and Weibke (35) assessed the experimental error. Anderson (36) calculated the entropy of CuS at 20°C from specific heat measurements. His value has been selected by K.K. Kelley as the most probable (37).

$$\Delta S^{\circ}_{298°K}\ (CuS) = 0.3 \pm 0.45\ \text{cal. mole}^{-1}\ °K^{-1}$$

These are the only data on CuS resulting from direct measurements. Any value obtained by extrapolation from high temperature measurements, supposing the existence of an equilibrium between CuS and Cu_2S are obviously doubtful. However, Kubaschewsky, Evans and Alcock (26) are in favour of a more negative heat of formation for CuS.

In the temperature range, 40-70°C, the standard free enthalpy of formation of Cu-poor digenite is then calculated to be

$$\Delta F^{\circ}\ (Cu_{1.765}S) = (-18{,}140 \pm 525) - (4.90 \pm 2.50)(T - 328)\ \text{cal.mole}^{-1}.$$

2.3.3. Variation of the standard free enthalpy of formation of digenite with composition

The effect of composition variations on the standard free enthalpy of formation of digenite can be calculated,

$$yCu + S \longrightarrow Cu_yS$$

The free enthalpy of the system can be expressed in terms of the chemical potential of its constituents,

$$\Delta F^{\circ}(Cu_yS) = y(\mu_{Cu} - \mu^{\circ}_{Cu}) + \mu_s - \mu^{\circ}_s$$

The total derivative of the free enthalpy with respect to y is equal to

$$d[\Delta F^{\circ}(Cu_yS)] = (\mu_{Cu} - \mu^{\circ}_{Cu})dy + y\, d(\mu_{Cu} - \mu^{\circ}_{Cu}) + d(\mu_s - \mu^{\circ}_s) \tag{3.1}$$

This expression of Eq (3.1) can be simplified to

$$d[\Delta F^{\circ}(Cu_yS)] = (\mu_{Cu} - \mu^{\circ}_{Cu})dy \tag{3.2}$$

by utilizing the Gibbs-Duhem relationship

$$y\, d(\mu_{Cu} - \mu^{\circ}_{Cu}) + d(\mu_s - \mu^{\circ}_s) = 0$$

Integration of Eq. (3.2) between the composition limits of digenite yields the corresponding difference of the standard free enthalpy of formation,

$$\Delta F^{\circ}(Cu_{y_2}S) - \Delta F^{\circ}(Cu_{y_1}S) = \int_{y_1}^{y_2} (\mu_{Cu} - \mu^{\circ}_{Cu})dy$$

The right hand side of this equation is equal to the area bounded by the integration limits and located below the experimental curve, $\mu_{Cu} - \mu^{\circ}_{Cu} = f(y)$, which has not been determined. As the chemical potential of a component in a stable compound is a continuously increasing function of composition, this area is intermediate between

the surfaces of the rectangles $(y_2-y_1)(\mu_{Cu} - \mu^\circ_{Cu})_{y_2}$ and $(y_2-y_1)(\mu_{Cu} - \mu^\circ_{Cu})_{y_1}$. In the digenite case, these two values differ by approximately 12% and the variation of the standard free enthalpy of formation can be approximated by

$$\Delta F^\circ(Cu_{y_2}S)-\Delta F^\circ(Cu_{y_1}S)=(y_2-y_1)\frac{\mu_{Cu}(y_1)+\mu_{Cu}(y_2)}{2}$$

$$= \frac{y_2-y_1}{2} RT[\ln a_{Cu}(y_1) + \ln a_{Cu}(y_2)$$

introducing an error < 6%.

This information makes the calculation of the standard free enthalpy of formation of djurleite possible.

2.3.4. Standard free enthalpy of formation of djurleite

In a digenite-djurleite mixture in equilibrium,

$$Cu_yS + (1.965 - y)\ Cu \rightarrow Cu_{1.965}S,$$

the Cu activity is related to the standard free enthalpy change of the reaction. In this case, the coefficient multiplying the Cu chemical potential is temperature dependent. The standard free enthalpy of formation of djurleite is given by

$$\Delta F^\circ(Cu_{1.965}S) = \Delta F^\circ(Cu_yS) + (1.965 - y)RT \ln a_{Cu},$$

and in the temperature range, 55-80°C, it has been calculated to be

$$\Delta F^\circ(Cu_{1.965}S) = (-19{,}700 \pm 550) - (5.5 \pm 3.1)(T - 343) \text{ cal mole}^{-1}.$$

2.4. Discussion

At 93°C, djurleite decomposes into digenite ($Cu_{1.84}S$) and chalcocite ($Cu_{1.99}S$) (11,38),

$$0.166Cu_{1.840}S + 0.833Cu_{1.990}S \longrightarrow Cu_{1.965}S.$$

This equilibrium acts as a reference point for correlating the present measurements with the existing data on the system. The standard free enthalpy of formation of djurleite is derived from the measurements performed in this work, $\Delta F^\circ_{366°K}(Cu_{1.965}S) = 19{,}830 \pm 600$ cal mole^{-1}. The standard free enthalpy of formation of high digenite can be extrapolated from the present measurements, $\Delta F^\circ_{366°K}(Cu_{1.84}S) = -18{,}900 \pm 600$ cal mole^{-1}.

Von Wartenberg (34) determined the heat of formation of Cu_2S at 298°K, $\Delta H^\circ_{298°K}(Cu_2S) = 18{,}970$ cal mole^{-1}. Kubaschewsky and Weibke (35) in their discussion on the Cu-S data selected this value as the most probable, assessing the experimental error to 500 cal mole^{-1}. Cu_2S has been studied in detail by Richardson et al. (39) using H_2-H_2S equilibrium in the temperature range 800-1000°K, by Brook (40) in the temperature range 500-1000°K and by J.B. Wagner et al. (41) using e.m.f. measurements at 500°K. Its standard free enthalpy of formation seems to be accurately established in that temperature range, but extrapolation of these values to room temperature can only lead to high

errors because of the inaccuracy of the specific heat data. For that reason, Von Wartenberg's data seems more applicable than the value proposed by Kubaschewsky, Evans and Alcock (26). Anderson's (36) and Kelley's (37) data on the entropy of Cu_2S yield, along with Von Wartenberg's data for $\Delta H°$, $\Delta F°_{366°K}(Cu_2S) = 20,900 \pm 800$ cal $mole^{-1}$.

In these conditions the two sets of data converge within 700 cal. $mole^{-1}$, a gap which sits in the middle of the experimental error of 1400 cal. $mole^{-1}$.

The enthalpies, entropies and free enthalpies of the copper sulphides below 100°C are summarized in table 2. The digenite and djurleite values are based on measurements described in this work, the covellite and chalcocite values are selected on the basis of the best low temperature data shown in the literature. The major component (90%) of the final error on the values calculated from the present measurements originates from the error associated with the existing data on CuS.

The variation of Cu and S chemical potentials across the Cu-S system can then be assessed at any temperature (Fig. 8). However, the value proposed for the djurleite-chalcocite equilibrium is conjectural: it was not measured directly and the accuracy of the existing data did not allow its calculation. The difference in free enthalpy of formation between djurleite and chalcocite is much smaller than the experimental error on any of these values. Though the Cu chemical potential in the djurleite-chalcocite system is known at 93°C from the present measurements, the uncertainty on the entropy change of the reaction (0.1 ± 0.3) e.u. does not allow any extrapolation.

Table 2

Thermodynamic data of the copper sulphides below 100°C

Composition	$\Delta F^\circ / _{cal\ mole^{-1}}$	$\Delta S^\circ / _{cal\ mole^{-1}\ ^\circ K^{-1}}$	Ref.
CuS (C.).	$(-11{,}610 \pm 400) - (0.3 \pm 0.45)T$	0.3 ± 0.45	34,35,36,37
$Cu_{1.765}S$ (D.).	$(-18{,}140 \pm 520) - (4.9 \pm 2.5(T-328)$	4.9 ± 2.5	this work
Cu_yS (D.).	$(-18{,}140 \pm 520) - (4.9 \pm 2.5(T-328) + (y - 1.765)[(-7{,}910 \pm 40) - (3.2 \pm 3.5)(T-328)$		this work
$Cu_{1.965}S$ (Dj.).	$(-19{,}700 \pm 550) - (5.5 \pm 3.1)(T-343)$	5.5 ± 3.1	this work
Cu_2S (Ch.).	$-(18{,}970 \pm 500) - (5.3 \pm 0.8)T$	5.3 ± 0.8	34,35,36,37

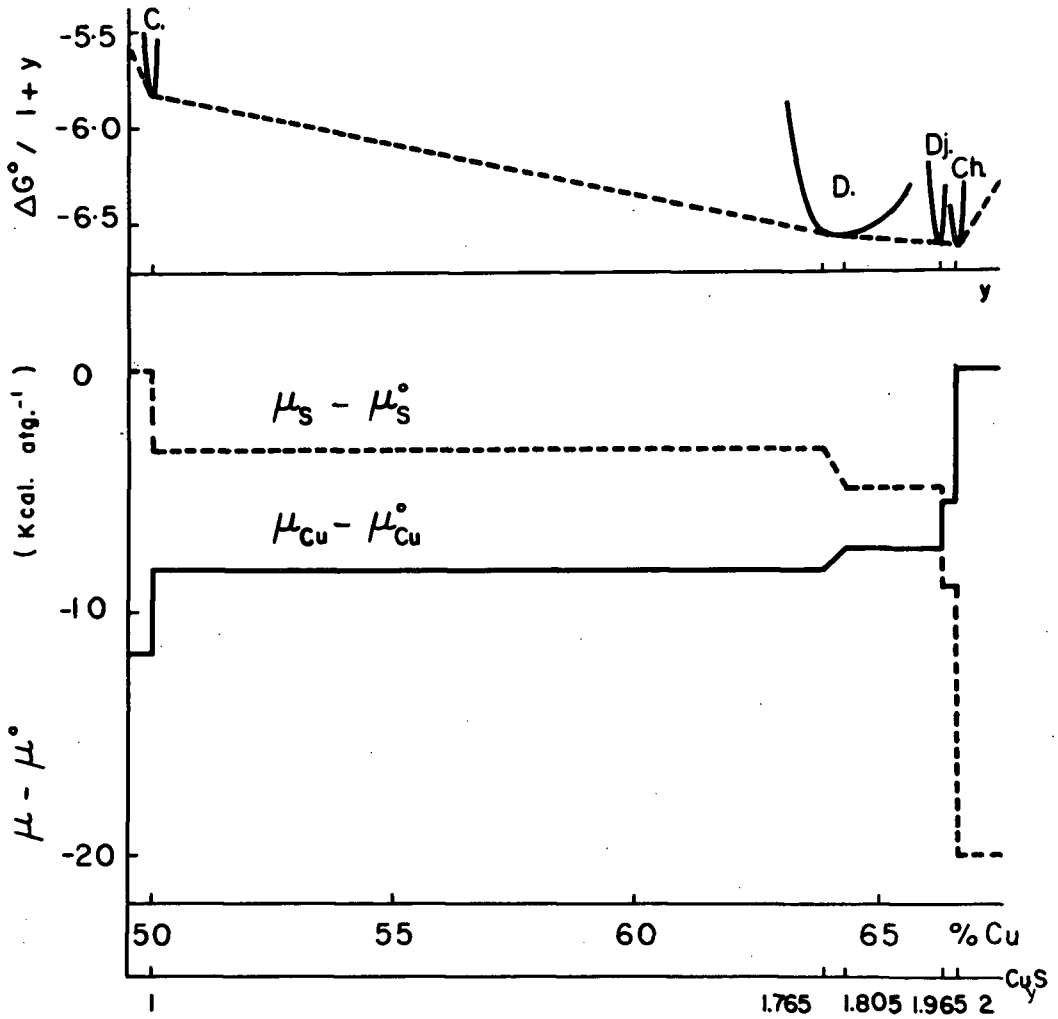

Figure 8. Variation of standard free enthalpy of formation and of chemical potentials across the Cu-S system at 55°C.

CHAPTER 3.

AN ELECTROCHEMICAL METHOD OF MEASURING THE COPPER IONIC DIFFUSIVITY IN A COPPER SULPHIDE SCALE

3.1. Principle of the method

Copper sulphides can be grown on a copper anode from an acidic solution saturated with H_2S. If the operation is conducted at constant current, different sulphide layers of decreasing copper activity are grown as the oxidation proceeds. If equilibrium is established, the successive phases should be, according to the phase diagram (11) (Fig. 1): copper, chalcocite, djurleite, digenite, covellite and sulphur. The reaction occurring at the anode is

$$y\ Cu + H_2S \longrightarrow Cu_yS + 2H^+ + 2e$$

The electrochemical potential of such an electrode (Stokholm convention) is given by the following relationship,

$$E = \varepsilon_o - \frac{RT}{2F} \ln \frac{a_{Cu}^{y}\ a_{H_2S}}{a_{Cu_yS}\ a_{H^+}^{2}} + \eta_s \qquad (3.1)$$

The copper activity at the solid-liquid interface reflects the conditions imposed upon the system and the transport properties of the scale being grown. The sulphide activity is taken as unity. In defined geometric and stirring conditions, under a constant current, the hydrogen sulphide

and hydrogen ion activities are constant in the vicinity of the electrode. In steady-state conditions, the surface overvoltage for a given sulphide is assumed to be a constant. Therefore, the electrode potential variation with time follows the evolution of the copper activity according to the relationship (3.2) derived from Eq. (3.1),

$$\frac{dE}{dt} = -\frac{RT}{2F}\frac{d}{dt}\ln a_{Cu}^{y}$$

$$\frac{dE}{dt} = -y\frac{RT}{2F}\frac{d}{dt}\ln a_{Cu} \quad \text{if } y = \text{constant} \tag{3.2}$$

If the sulphide scale grows uniformly on the electrode surface, the copper activity at the liquid-solid interface can be directly linked to the transport properties of the sulphide layer.

3.2 Theoretical anode model

In the copper sulphides, the sulphur ion mobility is considered negligible in comparison with the copper ion mobility (42). In the case of high temperature phases (αCu_2S, βCu_2S) there is experimental evidence (43,44) to support this. It is also reasonable for the low temperature phases in view of the relatively large size and associated immobility of the anion.

The copper sulphides are electronic conductors. Chalcocite is a p-type semiconductor, its conductivity increasing notably with copper deficiency ($\sigma = 10^{-2} \rightarrow 50\ \Omega^{-1}cm^{-1}$ at room temperature) (23,24). Digenite and covellite are almost metallic in character ($\sigma = 2.10^{4}\ \Omega^{-1}cm^{-1}$ at room temperature (23,25).

The phenomenological equations for diffusion relate the particle flux to the forces responsible for their motion. If the interaction effects are neglected, unidimensional transport in a two component system in the presence of a low strength electric field can be equated by

$$J_{Cu^+} = -M_{Cu^+} \left(\frac{d}{dx} \mu_{Cu^+} + q_{Cu^+} \frac{d}{dx} \phi\right), \tag{3.3}$$

$$J_e = - M_e \left(\frac{d}{dx} \mu_e + q_e \frac{d}{dx} \phi\right) \tag{3.4}$$

The electrical potential gradient can be derived from equation (3.4) and substituted in equation (3.3),

$$J_{Cu^+} - \frac{q_{Cu^+}}{q_e} \frac{M_{Cu^+}}{M_e} J_e = - M_{Cu^+}\left(\frac{d}{dx} \mu_{Cu^+} - \frac{q_{Cu^+}}{q_e} \frac{d}{dx} \mu_e\right) \tag{3.5}$$

Chemical potentials of ion and electron are not experimentally accessible values but are related through the measurable quantity, μ_{Cu},

$$\mu_{Cu} = \mu_{Cu^+} + \mu_e$$

Equation (3.5) is then simplified to

$$J_{Cu^+} + \frac{M_{Cu^+}}{M_e} J_e = - M_{Cu^+} \frac{d}{dx} \mu_{Cu} \tag{3.6}$$

As reported earlier, the copper sulphides are electronic conductors, their electronic conductivity being much larger than their ionic

conductivity, and equation (3.6) can be reduced to

$$J_{Cu^+} = - M_{Cu^+} \frac{d}{dx} \mu_{Cu} \tag{3.7}$$

The Onsager coefficient M_i is directly related to the conductivity, σ_i, mobility, B_i, and diffusivity, D_i, of the particle i.

$$\begin{aligned} M_i &= \sigma_i \, q_i^{-2} \\ M_i &= B_i C_i \\ M_i &= \frac{D_i}{RT} C_i \end{aligned} \tag{3.8}$$

Equation (3.7) can be expressed in terms of any of these four parameters

$$I_{Cu^+} = - \frac{\sigma_{Cu^+}}{F} \frac{d}{dx} \mu_{Cu} \tag{3.9}$$

If the sulphide scale grows uniformly and continuously over the whole electrode surface, the sample thickness at any time is proportional to the number of coulombs passed through the electrolytic cell during that time,

$$x - x_0 = \frac{I_{Cu^+} \, (t - t_0)}{yF} \left(\frac{M}{d}\right)_{Cu_yS} \tag{3.10}$$

Combining equations (3.2), (3.9) and (3.10) yields equation (3.11),

$$I_{Cu^+}^2 \, \frac{1}{2F} \left(\frac{M}{d}\right)_{Cu_yS} = +\sigma_{Cu^+} \frac{dE}{dt} \tag{3.11}$$

which permits the calculation of the ionic conductivity of the sulphide scale, formed under steady state conditions, from the slope of the recording of the electrode potential as a function of time.

3.3 Experimental

The anode was made of copper rod (99.995% purity) 0.905 cm in diameter, mounted in acrylic resin (Koldmount), and polished so that only one plane was in contact with the solution. The solution, 0.2 M in Na_2SO_4 and 0.2 M in H_2SO_4, was saturated by continuously bubbled H_2S. A strong convection pattern was brought about by a magnetic stirrer. The system was held at constant temperature by a regulated water bath. A 21 volt Ni-Cd battery unit provided current to the system through a set of appropriate resistors. The electrode potential was measured versus a saturated calomel electrode by a Keithley 153 voltmeter which fed the signal to a Sargent SRG recorder.

Series of experiments were carried out at temperatures between 30 and 73°C (below the digenite transition temperature) and under selected current densities between 1.9×10^{-4} A cm^{-2} and 1.55×10^{-3} A cm^{-2}.

The sulphide layer showed a uniform thickness over the electrode surface (Fig. 9) which ranged from 50 to 380 μ depending on experimental conditions and the period of oxidation. The reaction products were identified by X-ray diffraction on a powder sample.

The scale structure and morphology could not be investigated by microscopy, electron diffraction or microprobing. The three-sulphide assembly was not in equilibrium and in the absence of an electric

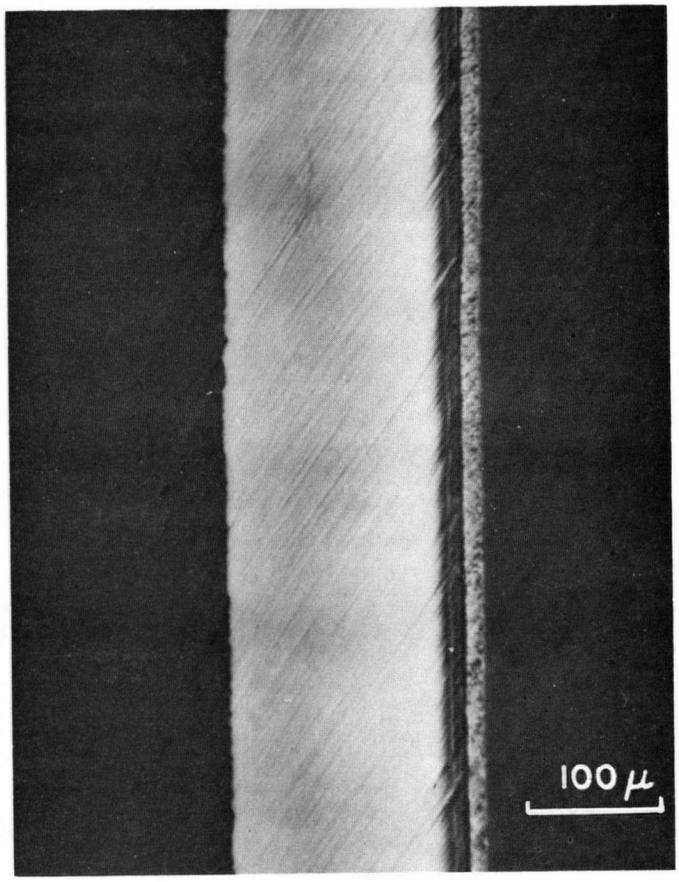

Figure 9. Micrograph of the copper sulphide scale separated from its Cu substratum. The Cu-Cu_2S interface was on the right side of the specimen. Digenite and djurleite are the only two phases to remain present. The band structure results from differences in the scale morphology emphasized by polishing.

current one phase disappeared during the time required for the sample preparation according to the reaction,

$$0.8Cu_2S + 0.2Cu_{1.8}S \longrightarrow Cu_{1.96}S$$

3.4 Results and Discussions

So far, three suphides have been identified, chalcocite, djurleite, and digenite. No evidence, either direct or indirect, for the appearance of covellite was obtained in these experiments.

The sulphide growth model, analysed earlier in this paper, is valid only in steady-state conditions; that is, when the cationic and total electric currents are constant. These conditions are satisfied when the first sulphide layer (Cu_2S) is deposited. The stoichiometry range of low chalcocite is smaller than 0.5% of its copper content (11) and during Cu_2S formation, the ionic current virtually equals the total electric current (Fig. 10).

When a new sulphide starts to grow on the anode, the copper flux reaching the solid-liquid interface is changed according to the Cu^{++} to Cu^{+} ratio in the new phase. If the digenite composition is approximated by $Cu_{1.8}S$, the reaction occurring at the liquid-solid interface at the stage of digenite growth can be represented by Fig. 11, and the correspondingly cationic ($I^b_{Cu}+$) and electronic (I^b_e) currents are equal to 90 and 10%, respectively, of the total current (I). The boundary between two solid phases is characterized by a thermodynamically fixed value of copper activity or electrochemical potential; therefore, the potential drop in each sulphide layer is a constant. Consequently,

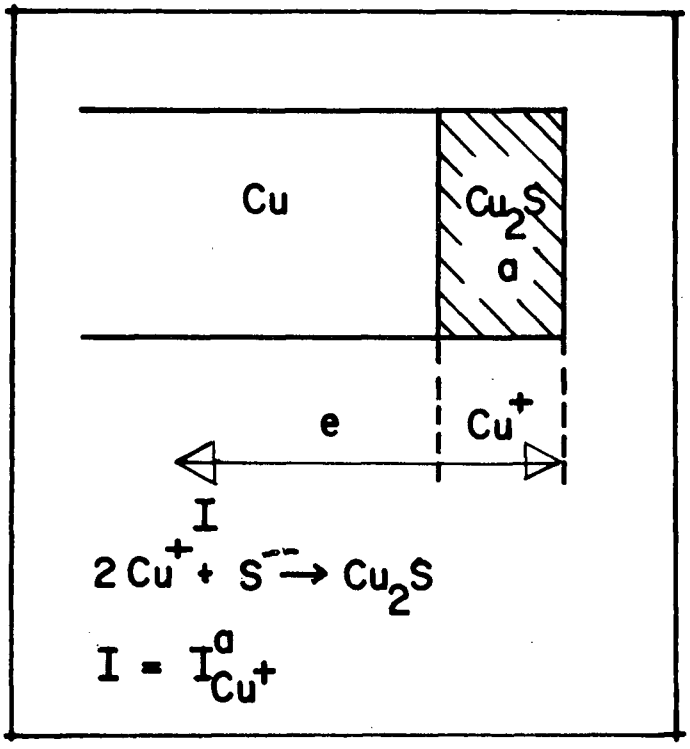

Figure 10. Model of the Cu_2S film growing on the Cu anode.

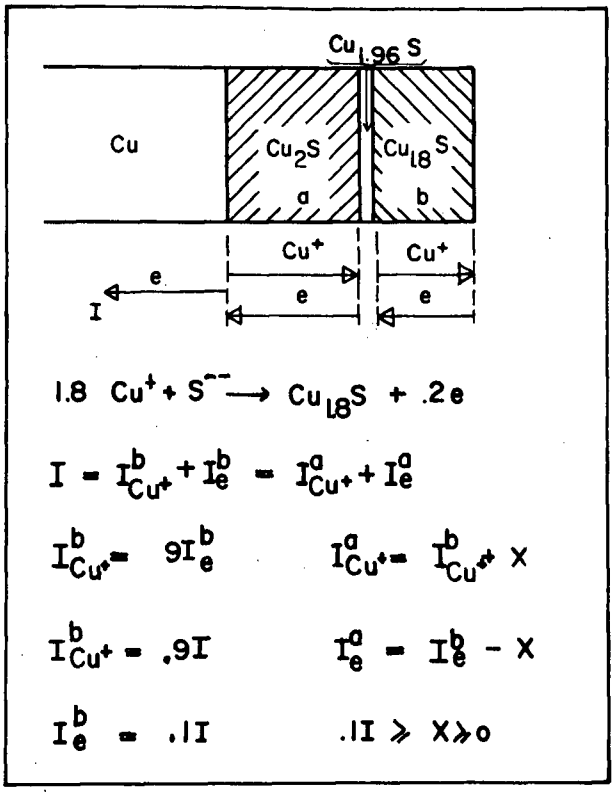

Figure 11. Model of the copper sulphide scale at the stage of $Cu_{1.8}S$ growth.

the abrupt change in cuprous current at the onset of growth of a new phase initiates an unsteady state process during which each sulphide layer adjusts its thickness to the new current conditions. The solid state transformations accompanying the phase boundary motion are believed to generate stresses in the specimen, because the scale always breaks away from the copper before CuS growthis apparent.

So far, the digenite stoichiometry range has been ignored. The digenite composition is reported (11) to extend from $Cu_{1.765}S$ to $Cu_{1.79}S$ at room temperature. Although the Cu poor limit is not affected by temperature, the Cu rich limit changes to $Cu_{1.83}S$ at 83°C where digenite inverts to high digenite. During the digenite layer growth there is a continuous change in the Cu current flowing through the scale, but this variation represents only 1.75% of the total current and is smaller than the experimental accuracy of the method of measurement.

From the set of experimental data, the cationic diffusivity of the chalcocite and digenite in the scale was calculated in the range of temperature from 30 to 73°C (Tables 3 and 4). Though djurleite was present in every sample, the ionic conductivity value could not possibly be derived from the experimental curve. This phase probably did not extend over enough atomic layers to allow a steady state to be established.

The measured ionic conductivity of digenite was independent of the current density used. In the chalcocite case, however, there was a current density value above which the experimental results became inconsistent. This limiting current density increased sharply with temperature. The dependence of the apparent ionic conductivity on the

Table 3

Experimental measurements used in the determination of the cuprous ion diffusion coefficient in low chalcocite $S = 0.644\ cm^2$

T (°C)	i (mA)	E range (mV) Cu_2S/H_2S sat., 0.2 M H_2SO_4-0.2 M Na_2SO_4/S.C.E.(25°C)	Correlation Coefficient r	$-\frac{dE}{dt}$ (mV min^{-1})	σ ($\Omega^{-1}cm^{-1}$)	D (cm^2sec^{-1})
30	0.125	490-410	0.9985	0.0410	0.786×10^{-5}	2.93×10^{-11}
40	0.250	520-465	0.9997	0.0818	1.60×10^{-5}	6.15×10^{-11}
40	0.250	425-390	0.9977	0.0835	1.57×10^{-5}	6.03×10^{-11}
46	0.250	480-425	0.9971	0.0659	1.98×10^{-5}	7.74×10^{-11}
48	0.250	510-475	0.9976	0.0712	1.84×10^{-5}	7.25×10^{-11}
50	0.234	525-485	0.9977	0.0521	2.95×10^{-5}	11.70×10^{-11}
51	0.250	508-450	0.9921	0.0526	2.45×10^{-5}	9.75×10^{-11}
55	0.250	480-445	0.9986	0.0357	3.67×10^{-5}	14.8×10^{-11}
55	0.250	465-430	0.9966	0.0403	3.25×10^{-5}	13.1×10^{-11}
55	0.500	500-456	0.9990	0.140	3.74×10^{-5}	15.1×10^{-11}
58	0.750	510-412	0.9997	0.292	3.97×10^{-5}	16.1×10^{-11}
62	0.750	525-410	0.9980	0.222	5.22×10^{-5}	21.5×10^{-11}
66	0.750	515-458	0.9993	0.241	4.81×10^{-5}	20.0×10^{-11}
70	0.500	500-465	0.9969	0.0738	7.09×10^{-5}	29.9×10^{-11}
70	1.000	505-435	0.9985	0.282	7.43×10^{-5}	31.3×10^{-11}
73	1.000	505-485	0.9989	0.271	7.61×10^{-5}	32.3×10^{-11}

Table 4

Experimental measurements used in the determination of the cuprous ion diffusion coefficient in low digenite $S = 0.644\ cm^2$

T (°C)	i (mA)	E range (mV) $\sim Cu_{1.8}S/H_2S$ sat., 0.2 M H_2SO_4-0.2 M Na_2SO_4/S.C.E.(25°C)	Correlation Coefficient r	$-\frac{dE}{dt}$ (mV min^{-1})	σ ($\Omega^{-1}cm^{-1}$)	D ($cm^2 sec^{-1}$)
30	0.125	235-225	0.9987	0.0137	1.76×10^{-5}	0.683×10^{-10}
40	0.250	251-240	0.9936	0.0280	3.50×10^{-5}	1.40×10^{-10}
40	0.500	235-200	0.9989	0.110	3.56×10^{-5}	1.42×10^{-10}
40	0.500	281-255	0.9976	0.123	3.17×10^{-5}	1.27×10^{-10}
40	0.500	275-243	0.9990	0.112	3.50×10^{-5}	1.40×10^{-10}
40	0.750	250-225	0.9999	0.292	3.09×10^{-5}	1.23×10^{-10}
40	0.750	240-210	0.9998	0.253	3.48×10^{-5}	1.39×10^{-10}
46	0.250	251-225	0.9968	0.0239	4.08×10^{-5}	1.66×10^{-10}
48	0.250	270-260	0.9888	0.0221	4.43×10^{-5}	1.81×10^{-10}
51	0.250	268-245	0.9964	0.0168	5.74×10^{-5}	2.38×10^{-10}
55	0.500	250-225	0.9973	0.0522	7.50×10^{-5}	3.14×10^{-10}
55	0.750	251-225	0.9987	0.107	8.24×10^{-5}	3.45×10^{-10}
55	0.250	255-240	0.9815	0.0143	6.85×10^{-5}	2.87×10^{-10}
58	0.750	262-238	0.9976	0.0967	8.96×10^{-5}	3.81×10^{-10}
62	0.750	255-235	1.0000	0.0833	10.6×10^{-5}	4.53×10^{-10}
66	0.750	250-225	0.9966	0.0799	10.9×10^{-5}	4.74×10^{-10}
70	0.500	245-230	0.9865	0.0264	14.8×10^{-5}	6.47×10^{-10}
70	1.000	247-234	0.9965	0.0833	18.8×10^{-5}	8.22×10^{-10}
73	1.000	250-230	0.9940	0.0711	21.7×10^{-5}	9.62×10^{-10}

current density raises the problem of the morphology of the sulphides grown electrolytically.

It is usual practice to classify anodic films as continuous or non continuous films. In most of the cases reported in the literature, the distinction between continuous and non continuous films is based on the nature of the resistance of the film to the current flow. It is characteristic of non continuous film to exhibit an approximately constant and low resistance (a few ohms) to the current flow during the growth of the scale (45). The smooth copper anode and the one plane electrode surface prevented introducing stresses which might have lead to the cracking of the film. There was no solid state transformation when the useful measurements were made, i.e., when steady-state conditions prevailed. The film growth was kinetically controlled by the copper ion diffusion through the solid, which mechanism favoured the formation of a continuous uniform scale. A decrease of the ionic strength of the solution (0.1 Na_2SO_4, 0.1 H_2SO_4) did not affect the experimental results.

The measured diffusion coefficient of cuprous ion in low chalcocite was found to be (Fig. 12)

$$D_{Cu^+} = 8.1 \times 10^{-3} \exp. - \frac{5,870}{T} \qquad cm^2 sec^{-1}$$

$$D_{Cu^+} = 1.1 \times 10^{-10} \qquad cm^2 sec^{-1} \text{ at } 50°C.$$

The measured diffusion coefficient of cuprous ion in low digenite was found to be (Fig. 13)

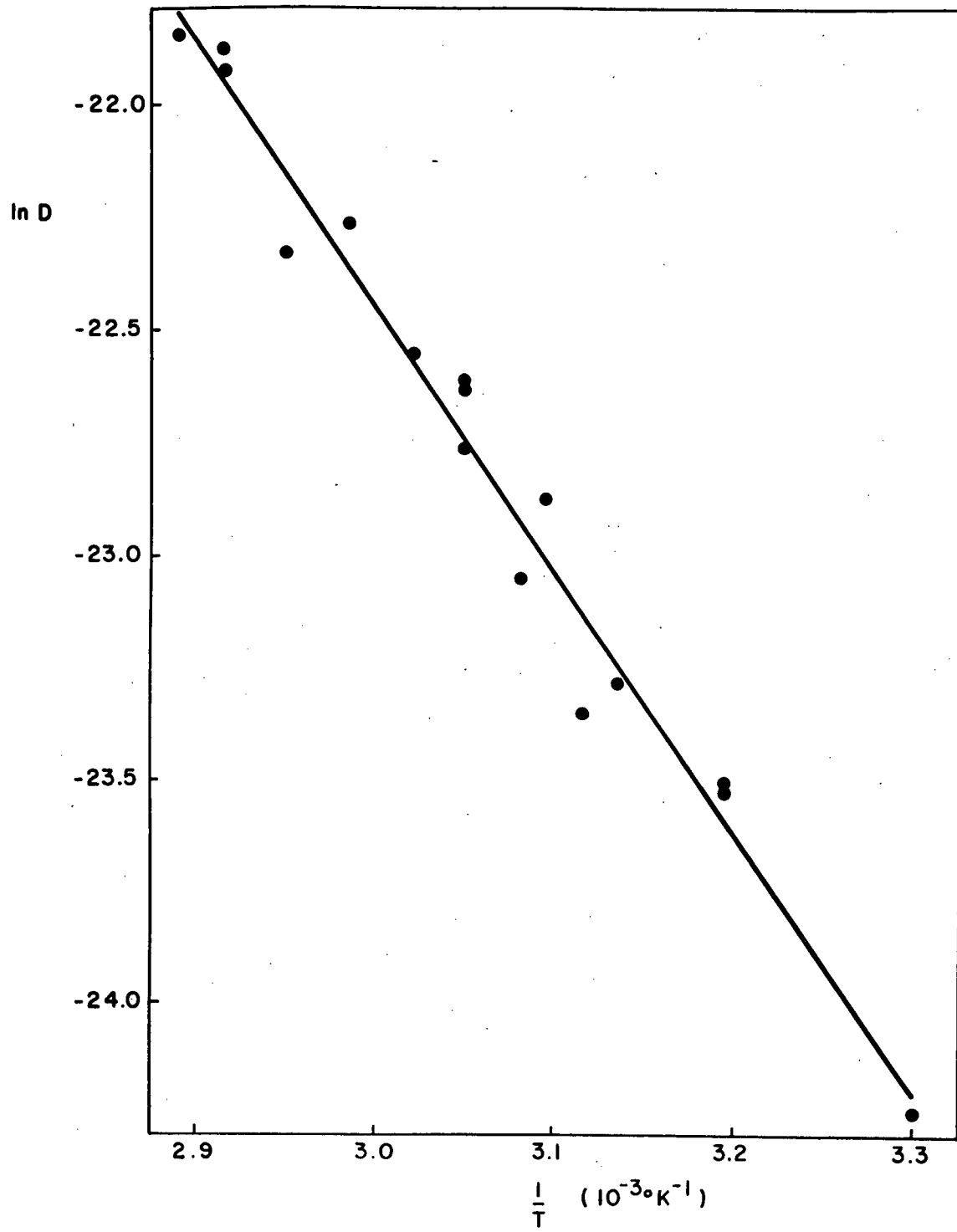

Figure 12. Temperature dependence of the cuprous ion diffusion coefficient in low chalcocite.

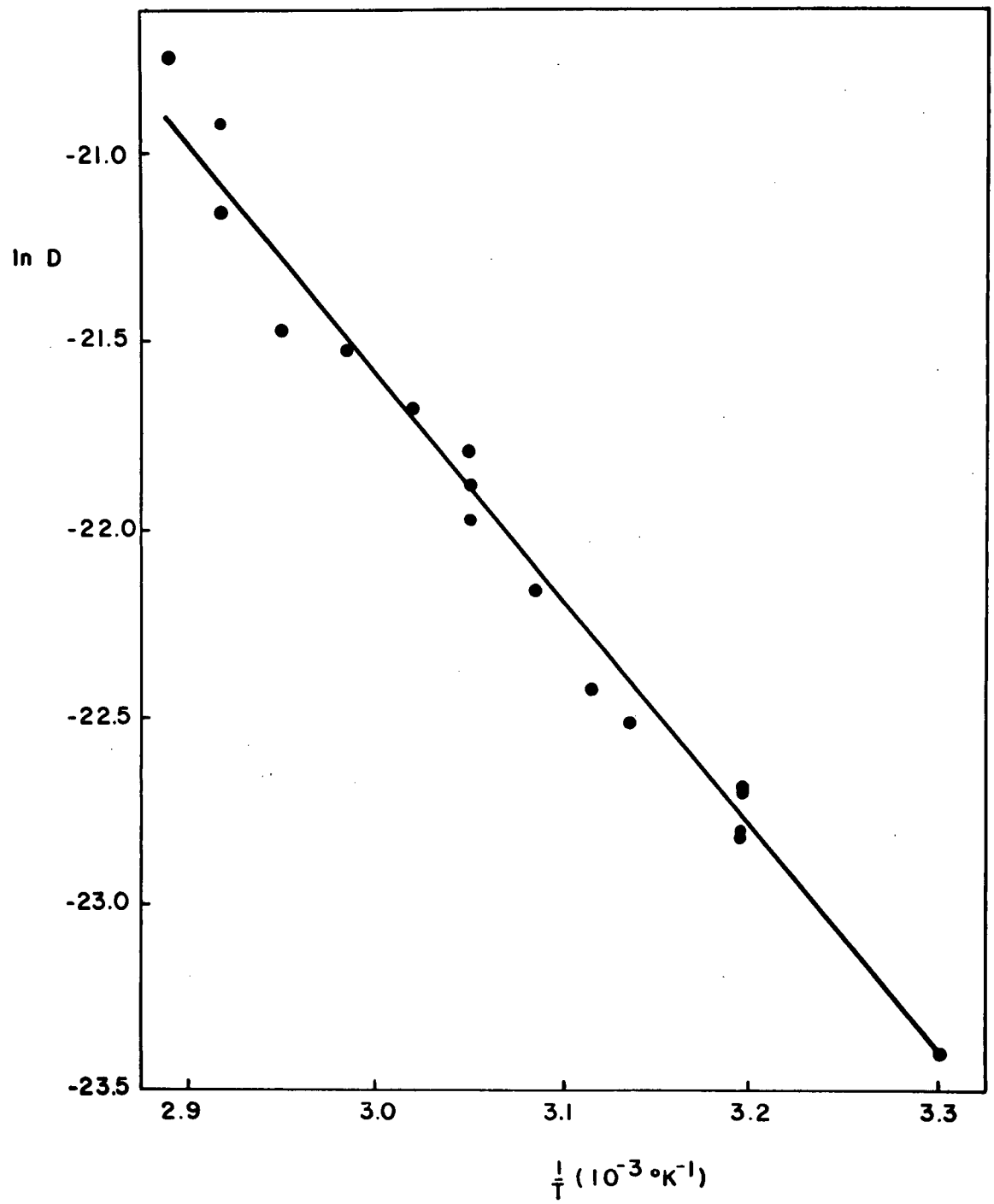

Figure 13. Temperature dependence of the cuprous ion diffusion coefficient in low digenite.

$$D_{Cu^+} = 3.6 \times 10^{-2} \exp. - \frac{6{,}100}{T} \qquad cm^2 sec^{-1}$$

$$D_{Cu^+} = 2.4 \times 10^{-10} \ cm^2 sec^{-1} \text{ at } 50°C.$$

In the temperature range studied, cuprous ions diffuse about twice as fast in digenite as in chalcocite. The activation energy for diffusion (ΔH) is 11.7 ± 1* kcal $mole^{-1}$ for chalcocite, and 12.1 ± 0.8* kcal $mole^{-1}$ for digenite.

If an activation entropy for diffusion is to be calculated, the nature and concentration of diffusing defects must be known. The diffusion in ionic type crystals is often associated with the migration of Schottky or Frenkel type defects. X-ray investigations have suggested that in some ionic type crystals metallic ions were distributed virtually at random among a large number of nearly equivalent lattice sites (αAg_2S (46), αAgI (47), αCu_2S (44)). In the case of low chalcocite and digenite which have relatively ordered copper lattices, an interstitialcy mechanism (the cations being equally mobile) may account for the cuprous ion diffusion. This is supported by the experimental observation that no significant variation of the diffusion coefficient has been observed with deviation from stoichiometry. Therefore, the equation of zeolitic diffusion should be applicable (48),

$$D = \lambda^2 \frac{kT}{h} \exp. \frac{\Delta S}{T} \exp. - \frac{\Delta H}{RT},$$

where λ is the average distance travelled by the diffusing particle in one jump ($\lambda \simeq 2 \times 10^{-8}$ cm)

---

* The limits of confidence for the calculated activation energies are estimated for a probability of 95%.

k is the Boltzmann constant, 1.380×10^{-16} erg. molecule^{-1} °K^{-1}

h is the Planck constant, 6.62×10^{-27} erg. sec.

The activation entropy for diffusion (ΔS) is then 1.9 e.u. for chalcocite and 1.3 e.u. for digenite, respectively. These low values are consistent with a mechanism which introduces little disordering in the lattice.

CHAPTER 4.

ELECTROLYTIC DISSOLUTION OF ROTATING DISKS OF COPPER SULPHIDES

A. GENERALITIES ON ELECTRODE KINETICS

4.1 Various types of overvoltage

An electrode reaction rate, according to Faraday's law, is proportional to the current density, I. The dependence of current density upon electrode potential, concentrations of reactants, and other variables such as stirring and temperature, must be established in order to determine the electrode reaction rate - functions, and to explain the sequence of partial reactions constituting the overall electrode reaction, which is observed by means of chemical analysis. The resistive partial reactions govern the type and magnitude of the overvoltage,

$$\eta = E - E_o$$

where E is the electrode potential when current flows and E_o is the potential in the absence of current, i.e., the equilibrium potential if there is only one reaction taking place at the electrode.

The following distinction between the various types of overvoltage, which correspond to the four possible types of rate-control, was introduced by Bonhoeffer, Gerisher and Vetter (1950) and is developed in Vetter's "Electrochemical Kinetics" (49):

- A charge-transfer overvoltage, η_t, prevails if only the transport

of charge carriers across the electrical double layer existing at the phase boundary is hindered.

- If a chemical reaction is hindered, the rate constant of which is, by definition, independent of the potential, the current flow produces a reaction overvoltage, η_r.

- Diffusion overvoltage, η_D, is encountered when mass transport by diffusion to and from the electrode surface is rate-determining during current flow.

- Hindrance of the process by which atoms are incorporated into or removed from the crystal lattice leads to crystallization overvoltage, η_C.

The various overvoltage types have been analysed individually on a theoretical basis so that the current density versus overvoltage relationship has received a general mathematical expression in several cases.

If several of the partial reactions have low rates of similar order of magnitude, the corresponding overvoltages are superimposed to form the total overvoltage. Since the various overvoltages are interrelated, Vetter (49) proposed a definition for the division of the measured overvoltage in its diffusion, reaction, crystallization and charge-transfer components, which is based on the requirement that upon the disappearance of all overvoltage types but one, the residual overvoltage must agree with the definition for the single remaining overvoltage type (Appendix 2). The components of the measured overvoltage can, then, be sorted out on the basis of the theoretical relationships obeyed by the various overvoltage types, provided only

one overall electrode reaction occurs.

The experimental investigation of electrode kinetics requires a careful design of the experimental conditions in order to eliminate or calculate the ohmic drops and the mass transport limitations. The rotating disk electrode provides a system where these calculations are possible in the steady-state conditions.

B. THE ROTATING DISK ELECTRODE TECHNIQUE

4.2 Equation of transport at the disk surface

The calculation of the maximum rate at which a substance can be transported towards or from an electrode, J_{lim}, is in general an intractable problem. Transport may be effected by diffusion, convection and electrical migration. The situation is still more complex if one of the species takes part in a homogeneous reaction since the chemical reaction rate has to be taken into account in the calculation.

A rotating disk of infinite diameter, in a non-turbulent, stationary regime, is one of the few systems where the velocity distribution throughout the body of the viscous fluid can be calculated (51). Figure 14 illustrates the pattern of streamlines at the surface of a rotating disk.

Using this model, Levich (51) solved explicitly the steady-state convective diffusion equation, assuming constant physical properties, in some cases: transport of uncharged particles, transport in a binary electrolyte, transport of an ionic species in the presence of an excess of indifferent electrolyte (3 ions). As the Schmidt number,

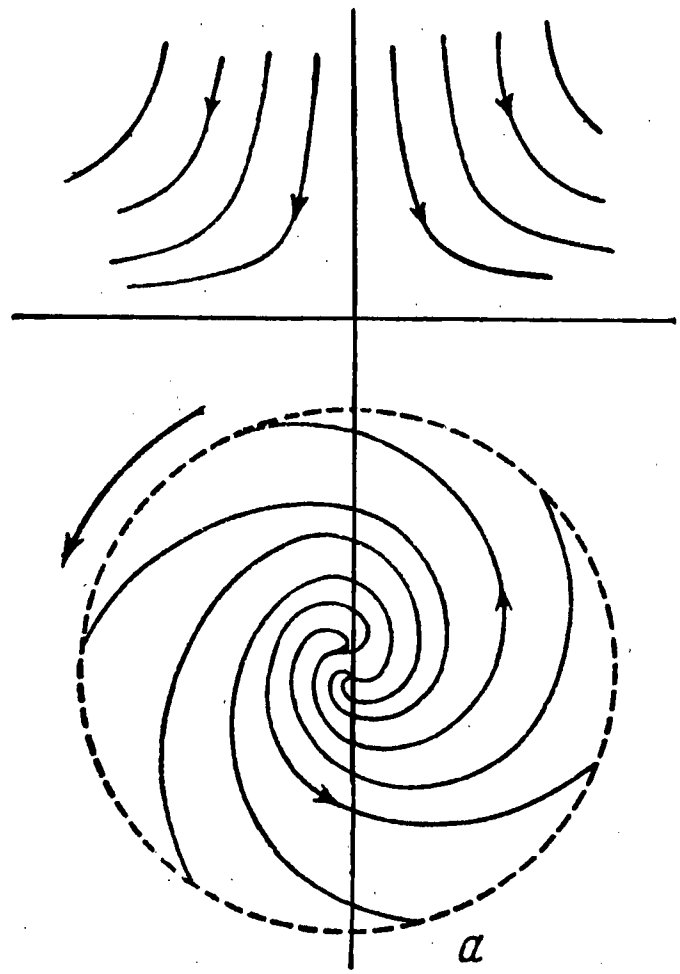

Figure 14. Pattern of streamlines at the surface of a rotating disk (51).

$Sc = \frac{\nu}{D}$, approaches ∞, Levich's solution takes the form

$$J_i = \pm \frac{0.620\ D_i^{2/3}\ \nu^{-1/6}\ \omega^{1/2}(C_i - \bar{C}_i)}{1 - t} \qquad (4.1)$$

where t is the transport number of species i in a binary electrolyte, t = 0 for uncharged species or for a charged species in the presence of an excess of indifferent electrolyte, ν is the kinematic viscosity of the solution, ω is the angular velocity of the disk.

The diffusion boundary layer is defined as a region of rapidly changing concentration in the immediate vicinity of the electrode surface, the thickness, δ, of which is defined as

$$\delta = \frac{1}{0.620} D_i^{1/3}\ \nu^{1/6}\ \omega^{-1/2},$$

and appears to be constant over the entire surface of the disk. Thus, from the diffusion point of view, the rotating disk electrode (R.D.E.) offers a uniformly accessible reaction site.

The diffusion overvoltage can be calculated with the Nernst equation and Eq. (4.1), if the physical properties of the solution are known or if the limiting current density has been determined.

The sum of experimental studies intended to verify the validity of equation (4.1) leaves no doubt that Levich's theory is correct (52). The correction suggested by Gregory and Riddiford (53) to take into account the finite value of the Schmidt number, $Sc = \frac{\nu}{D}$, ($100 < Sc. < 5000$ in aqueous solutions) is only significant in the cases of very accurate experimental measurements (54) (experimental error $\simeq$ 1%).

The assumption of constant transport properties (D,ν) restricts the application of equation (4.1) to dilute solutions; Newman and Hsueh developed a numerical solution to compute the limiting current in the case of variable physical properties (54).

4.3 Ohmic drop in solution

Newman studied theoretically the effect of the solution resistance to the current flow, below the limiting current density (55).

In the absence of electrode overvoltages, the current distribution is completely determined by the ohmic drop in solution. A calculation shows that the primary current density is infinite at the edge of the disk and half of the average value at the center.

Newman assessed the degree of non-uniformity of the current distribution, in the case of kinetic control by mass transport in the solution and charge-transfer at the electrode, against the physical and electrochemical parameters of the system. The predicted current distribution was verified experimentally by measuring the variations in the thickness of a copper deposit in 0.1 M $CuSO_4$-0.1 M H_2SO_4 solution (56).

A uniform current density can be expected at a R.D.E. if the ohmic drop in solution is small compared with the electrode overvoltage.

Newman established, in the case of the primary current distribution, the following formula to calculate the ohmic drop between the electrode and a point situated in the electrode plane, outside the rim ($r > r_o$), at a distance, r, from the center (57,58).

$$\eta_\Omega = \frac{r_o I}{2\sigma} \tan^{-1}\left[\left(\frac{r}{r_s}\right)^2 - 1\right]^{1/2}, \qquad (4.2)$$

where σ is the conductivity of the bulk solution.

4.4. Design of practical R.D.E.

Riddiford, in his review of the rotating disk electrode technique (52), discussed the design of a practical electrode which conforms as closely as possible to the theoretical requirements.

A disk of finite radius will meet the liquid flow requirements provided the radius, r_o, is very much greater than the thickness of the momentum boundary layer, i.e.,

$$\frac{2.8}{r_o} \left(\frac{\nu}{\omega}\right)^{1/2} \simeq 0,$$

and provided the Reynolds number, $Re = r_o^2 \frac{\omega}{\nu}$, is less than the critical value for the onset of turbulence. Experimental studies of the critical Re number at a rotating disk indicate that for a practical R.D.E., the Re number should not exceed 2×10^5 at the edge of the disk. On the other hand, the rotational speed of the disk must be large enough to exclude any significant contribution from natural convection.

The shape and dimensions of an electrode of finite span must be carefully designed and checked to introduce no disturbing edge effect. In that respect, the best design is a conical electrode, the base of which is active for $0 < r < r_o$, the region r_o to r_1 being inactive. Riddiford pointed out that cylindrical electrodes should be avoided since it was shown experimentally that, in this case, the fluid flow was turbulent even for very small Re numbers.

A further requirement is that the disk surface is the only effective bounding surface in the system. The liquid-gas boundary, the walls of the containing vessel, the counter-electrode, the Luggin capillary, etc. should not interfere with the flow pattern brought about by the spinning disk. Gregory and Riddiford (52), using disks 5.3 cm in diameter, rotating at 146 r.p.m. in beakers of different sizes, checked that this requirement was satisfied when the solution-air interface and the bottom and side walls of the beaker were all more than 0.5 cm away from the disk. In a practical R.D.E., the Luggin capillary may be located in the lower half of the system projecting up close to the center of the disk along the axis $r = 0$. More often, it is located in the upper half of the system with the tip reaching the plane of the disk ($y = 0$). Flows in the upper and lower part do not interact in this system.

Finally the disk must be horizontal, of minimum eccentricity (eccentricity of 0.025 mm is quoted by a number of workers) and smooth to the extent that the surface irregularities are much smaller than the diffusion boundary layer.

Experimentally, the R.D.E. system has been mainly used to determine diffusion coefficients in liquids and to study the kinetics of moderately fast electrode processes.

C. POLARIZATION OF ROTATING DISKS OF COPPER SULPHIDES

Polarization of digenite and covellite rotating disk anodes was investigated, at 55°C, in acidified copper sulphate solution (0.1 M $CuSO_4$, 0.1 M H_2SO_4) by a galvanostatic method.

4.5 Experimental

The rotating disk electrode is shown on Figure 15. The hollow shaft was of acetal plastic (0.62 cm in diameter). The specimen was imbedded in an acrylic resin (Koldmount) mount machined in the shape of a cone. The active surface exposed to the solution was 1.3 cm in diameter.

Electrical connections were made through mercury contained in the hollow shaft and separated from the specimen by a platinum foil. Mercury reacted readily with copper sulphides and so direct contact should be avoided.

Figure 16 describes the mechanical arrangement of the shaft in the stainless steel cell head.

Figure 17 and 18 show the arrangement of the cell. A porous porcelain diaphragm separated the anodic compartement, in the center, from the cathodic compartment. A two-compartment cell was, indeed, necessary because cuprous ions in the solution reacted with the copper sulphides and were regenerated by metallic copper immersed in the same solution. As a matter of fact, covellite and digenite were found, at 40°C, to be transformed into chalcocite, in a few days, in cupric sulphate solutions containing metallic copper. The effect was a shortcircuit in the cell, which was equivalent to a slight electronic conductivity in the electrolyte.

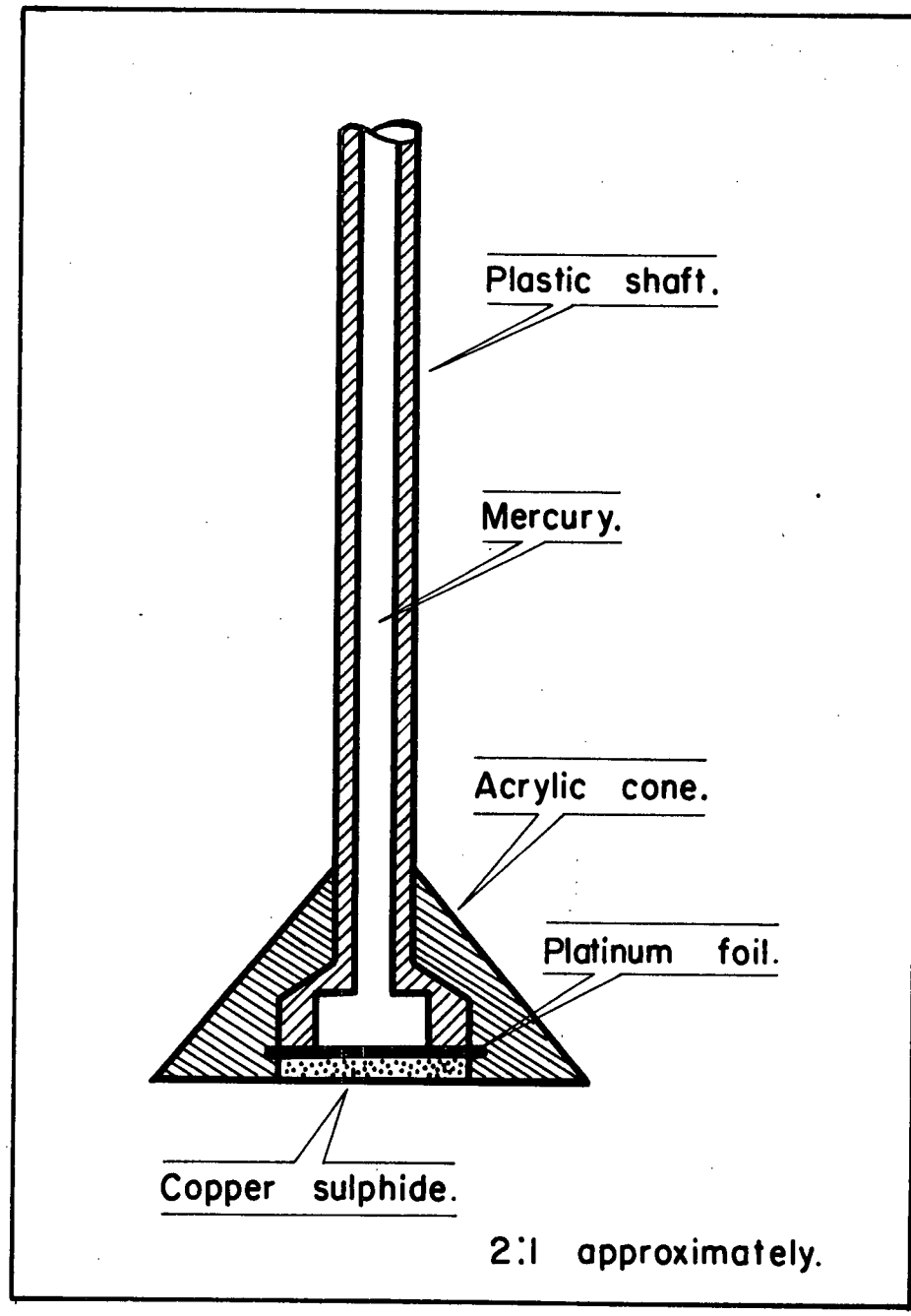

Figure 15. Design of the rotating disk electrode.

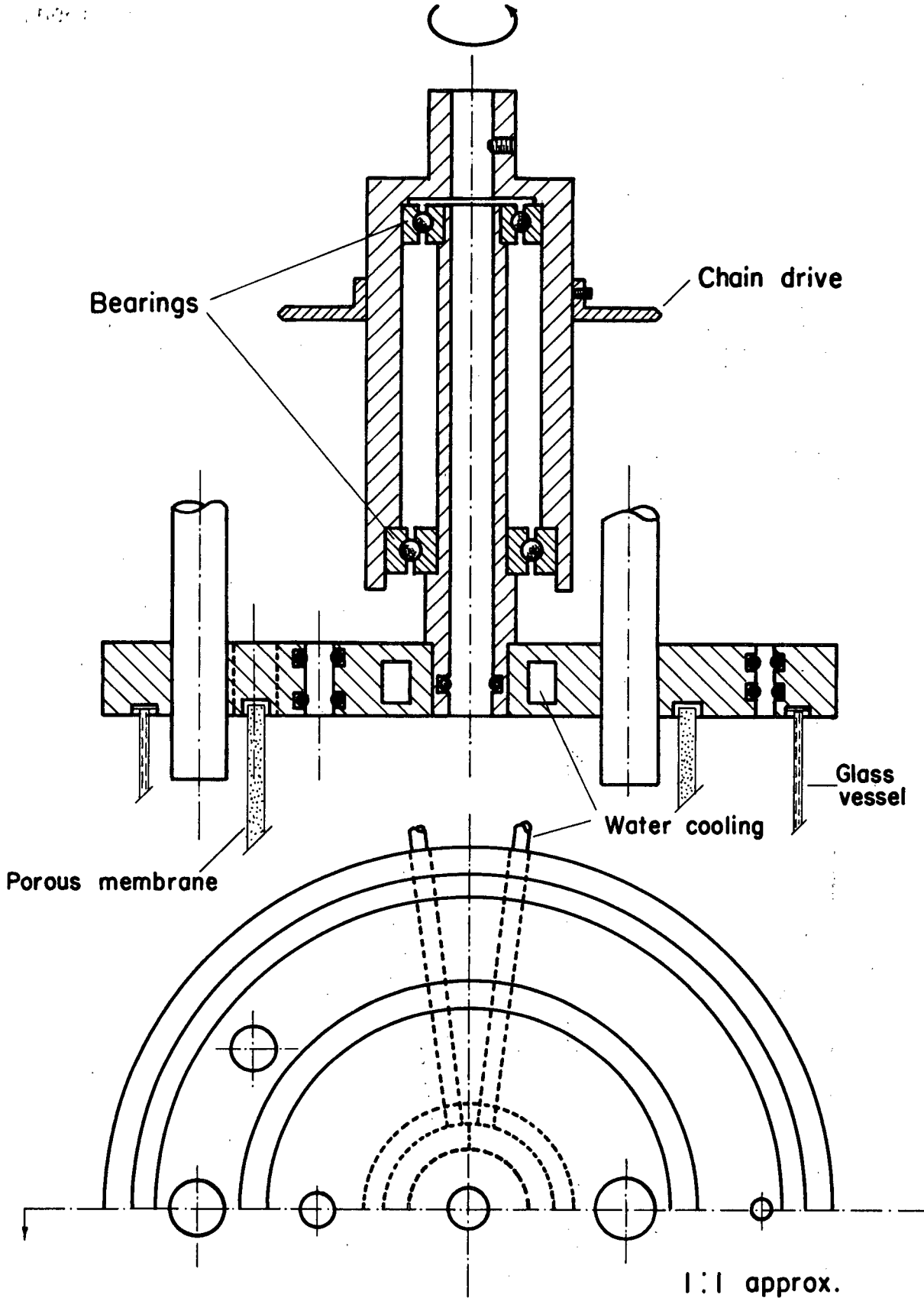

Figure 16. Design of the stainless steel head.

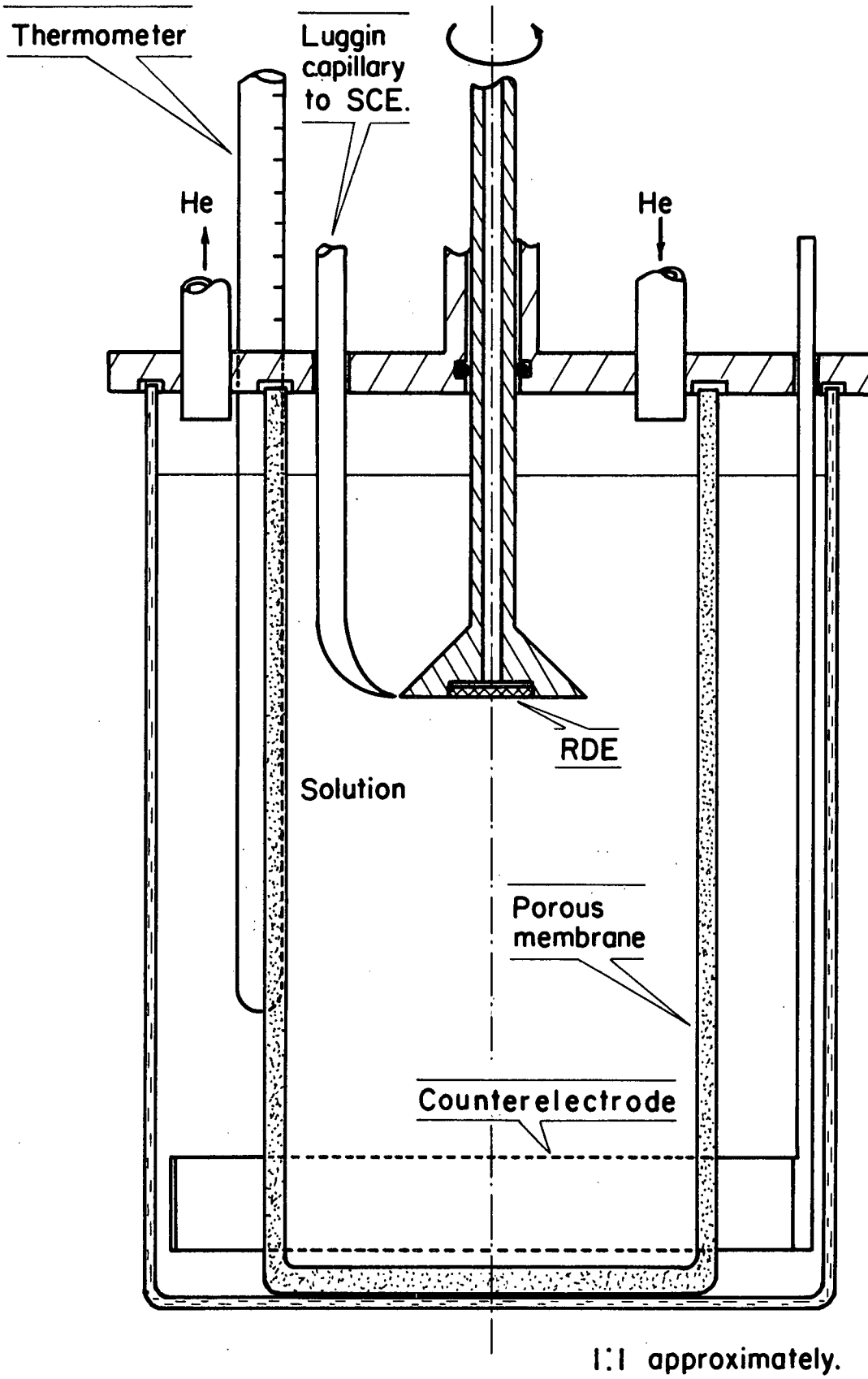

Figure 17. Electrolytic cell.

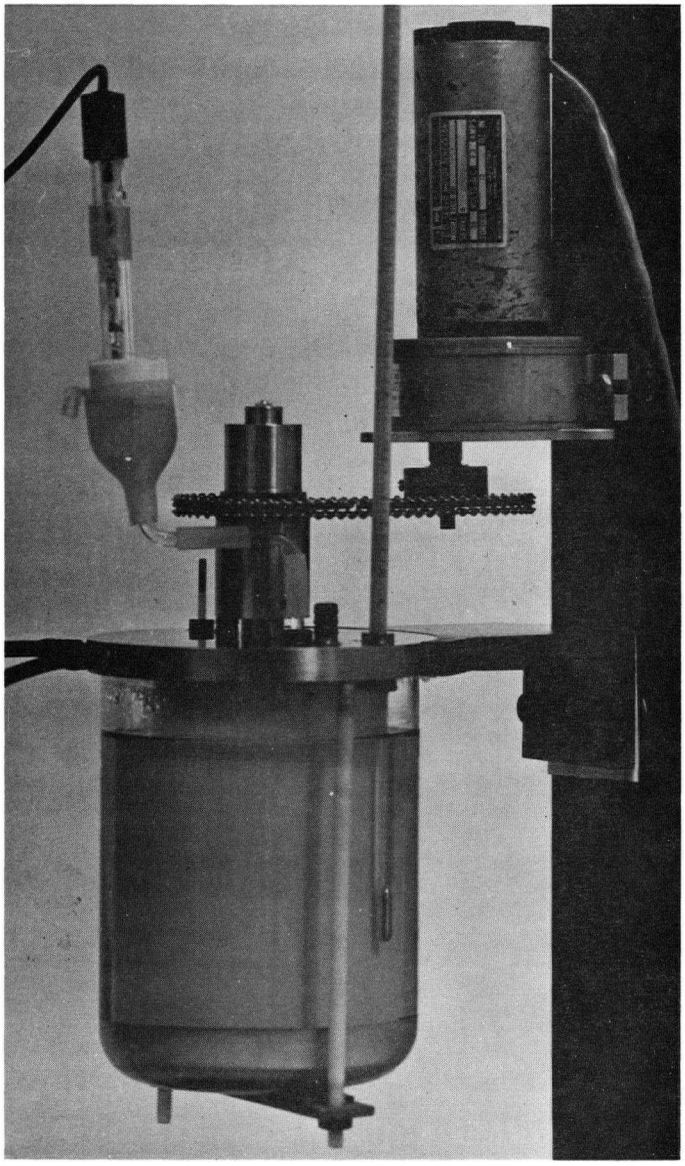

Figure 18. Electrolytic cell arrangement.

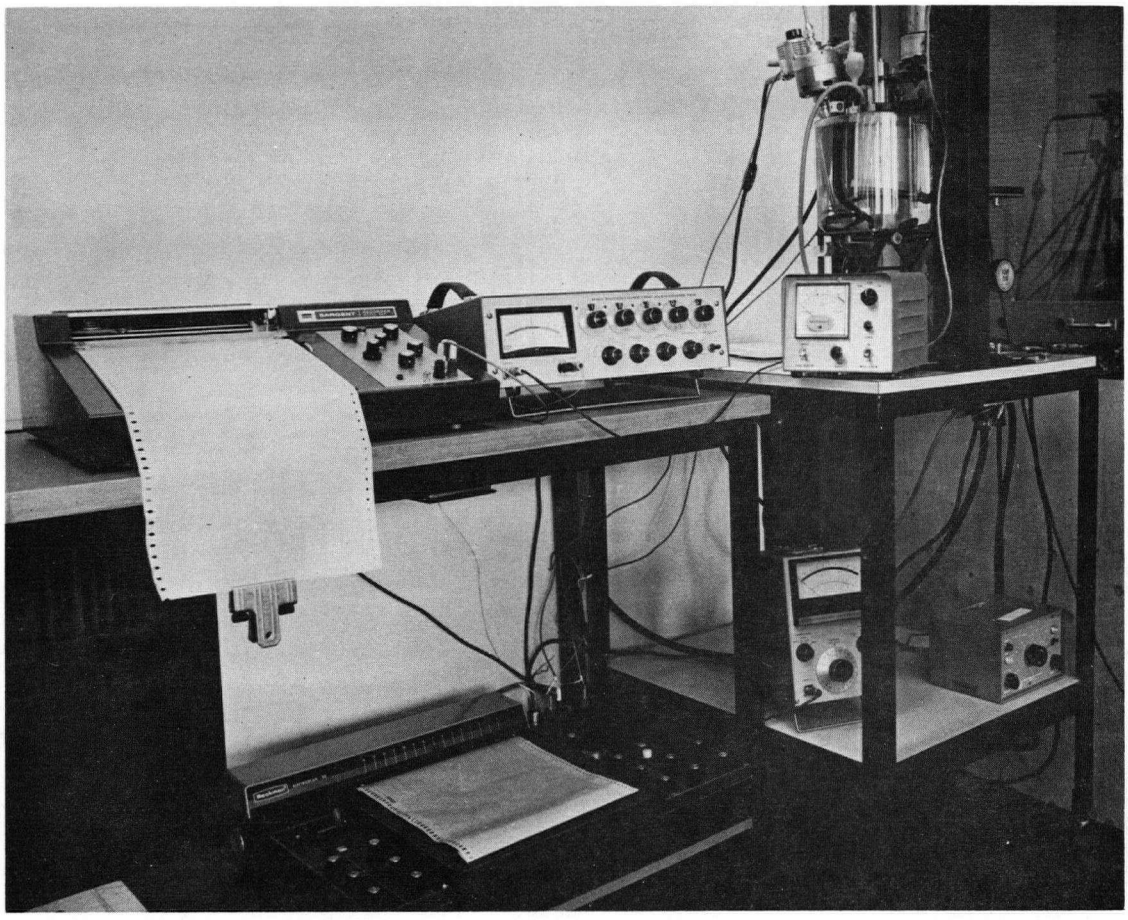

Figure 19. Experimental apparatus.

The area of the copper ring cathode was 80 times larger than that of the active surface of the anode.

The instruments associated with the present experiment are shown on Figure 19. Included were a D.C. servomotor (E.C. Motomatic E 550 MGHD) linked to a motor speed control unit (E.C. Motomatic E 550) which controlled the r.p.m. of the electrode within 1.5% of the set value, an Electroscan, Beckman Model 30, as a constant current source, a Keithley Model 153 microvoltammeter measuring the current to ±2% of full scale, and a Keithley Model 630 potentiometric electrometer measuring and amplifying the voltage signal fed to a Sargent Model S.R.G. recorder.

The cell was immersed in a thermostat-regulated water bath. Experiments were done in a helium atmosphere with deaerated 0.1 M $CuSO_4$-0.1 M H_2SO_4 solutions.

The measuring circuit was kept ungrounded. All potential measurements were made with respect to a saturated calomel electrode at 25°C.

The angular velocity of the disk was set at 250 r.p.m. yielding at the edge of the disk a Reynolds number of

$$R_e = r^2 \frac{\omega}{\nu} = 6.25 \times 10^3$$

which was characteristic of a laminar flow regime for that kind of geometric arrangement (see 4.4).

Preparation of the copper sulphides

Digenite was synthesized at 600°C in an evacuated quartz tube from 0.99999 pure copper and sulphur, purified according to the method of

Bacon and Fanelli (31), in the molar ratio, 1.78:1.

Covellite was synthesized at 450°C in an evacuated quartz tube from 0.99999 pure copper in the presence of an excess of purified sulphur. A temperature gradient prevailing along the reaction tube prevented the sulphur from condensing on the covellite during the cooling period.

The copper sulphides were ground under helium in an alumina ball mill and then cold-pressed under vacuum into disks (1.3 cm in diameter, approximately 2 mm thick) in a Perkin Elmer evacuable die. The digenite disks, compacted under a pressure of 8100 kg cm^{-2}, had 93% of their theoretical density. The covellite disks, shaped under a pressure of 2700 kg cm^{-2}, were sintered in the presence of sulphur vapour; their final density was 86% of the theoretical value.

The electrodes were lightly polished. The total internal resistance of each electrode was measured with a Keithley, model 503, milliohmeter and found to be approximately 0.1 Ω for digenite and 0.05 Ω for covellite electrodes.

4.6 Polarization of digenite anodes

4.6.1 Results

Digenite anodes were studied at 55°C by a galvanostatic polarization method using current densities between 7.5 and 75 mA cm^{-2}. The information obtained by this study is summed up in Table 5.

A typical potential-time curve is shown on Figure 20. These curves were characterized by a region in which the potential slowly rose as a function of time, ending in a potential discontinuity in a transition

Table 5

Polarization of digenite anodes

S.C.E. (25°C)/0.1 M $CuSO_4$-0.1 M H_2SO_4/~$Cu_{1.8}S$

I mA cm^{-2}	E_o mV	E_i mV	$\eta_{\Omega,sol.}$ mV	$\eta_{\Omega,el.}$ mV	η_D mV	E_s mV	E_τ mV	$E_\tau - E_i$ mV	τ sec
3.77	248	280	21	-	-	259			
7.5	236	298	42	-	1.1	255	760	462	124,800
11.3	245	355	64	1.5	1.6	288	725	370	39,060
15.1	237	350	85	1.5	2.1	261	515	165	10,950
18.8	245	405	104	2	2.5	296.5	575	170	8,670
18.8	244	409	106	2	2.5	298.5	604	195	7,500
37.7	241	526	209	4	4.7	308.5	678	152	1,950
45.2	243	659	252	5.5	5.2	396	818	159	1,110
56.5	238	768	316.5	6	6.5	439	978	210	720
56.5	244	765	312	6	6.5	438.5	1004	239	912
75.3	244	914	423	8	8.5	474.5	1123	209	420

E_o, E_i, E_τ are the o current, initial and transition potentials, respectively as defined in Fig. 20.

$\eta_{\Omega,sol.}$ is the ohmic drop in solution, calculated from Eq. (4.2)

$\eta_{\Omega,el.}$ is the ohmic drop inside the electrode

η_D is the concentration overvoltage due to diffusion in the electrode boundary layer (Appendix 4)

$E_s = E_i - \eta_{\Omega,sol.} - \eta_{\Omega,el.} - \eta_D$.

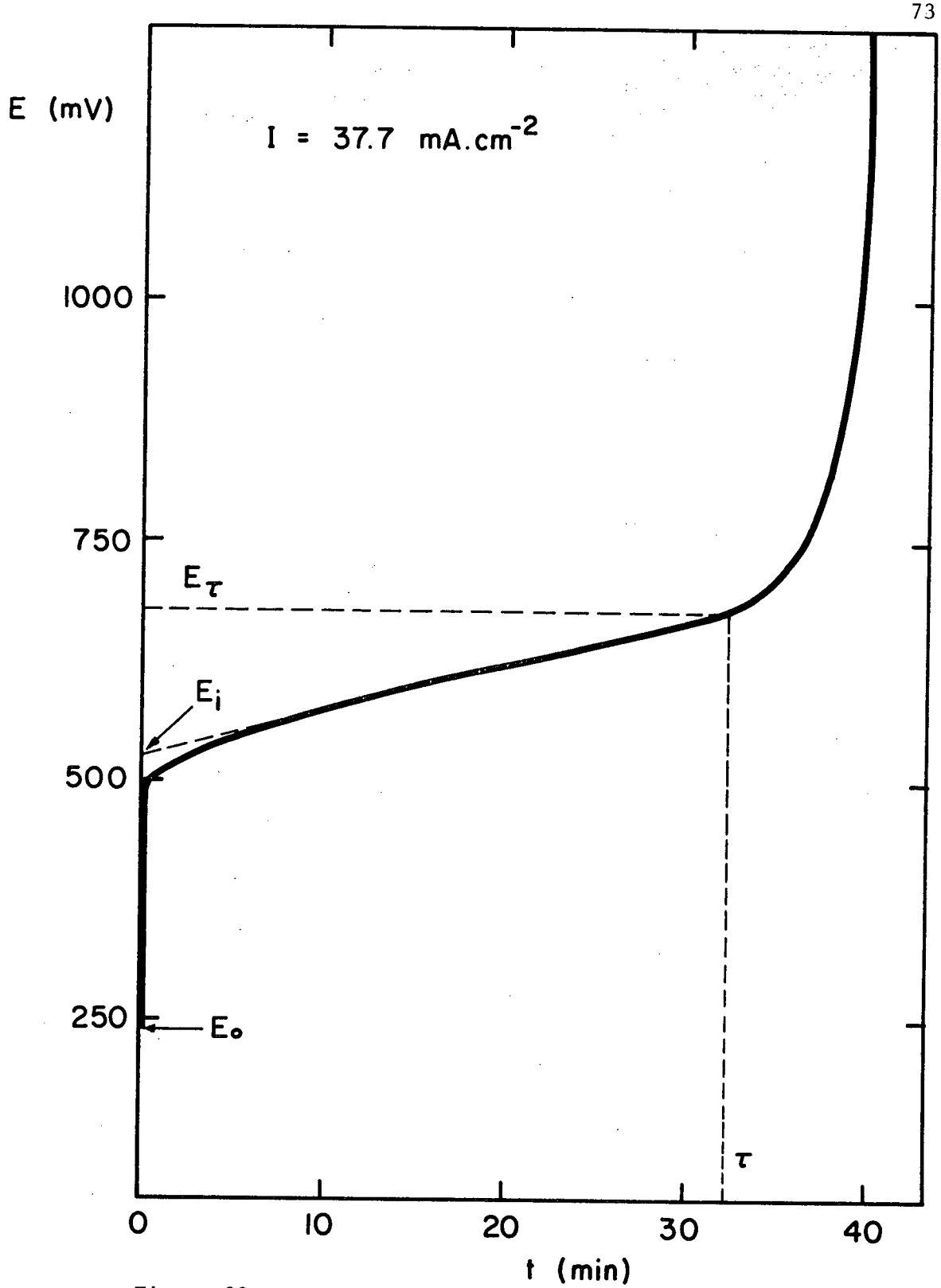

Figure 20. Potential-time curve recorded during the galvanostatic oxidation of a digenite anode at 55°C. S.C.E.(25°C) | 0.1 M $CuSO_4$-0.1 M H_2SO_4 | $Cu_{1.78}S$.

time τ, beyond which the potential was much higher (> 1.5 V) and poorly reproducible.

The first part of the curve up to the transition time corresponded to the overall electrode reaction

$$Cu_{1.78}S \longrightarrow CuS + 0.78\ Cu^{++} + 1.56\ e, \qquad (4.3)$$

which was found in a previous study (Chapter 2) to control the rest potential of a digenite-covellite electrode. In fact, covellite was identified by X-ray diffraction in the porous, loosely coherent solid separated from the surface of a specimen. No variation of the copper content of the solution could be detected after 35 hours of electrolysis under a current density of 7.5 mA cm^{-2}.

The sharp increase in potential after the transition time indicated the appearance of a highly resistive electrode reaction consisting probably of oxygen discharge and sulphur formation and possibly sulphate formation (15).

At the transition time, the digenite was far from being completely transformed into covellite but reaction (4.3) was not capable of maintaining a constant rate. As the reaction proceeded, the covellite-digenite interface receded from the original surface, and copper ions should diffuse through the CuS layer to enter the electrolyte.

It was observed experimentally that the current density was proportional to the inverse of the square root of the transition time (Figure 21) and this led to the relationship (I > 7.5 mA cm^{-2}).

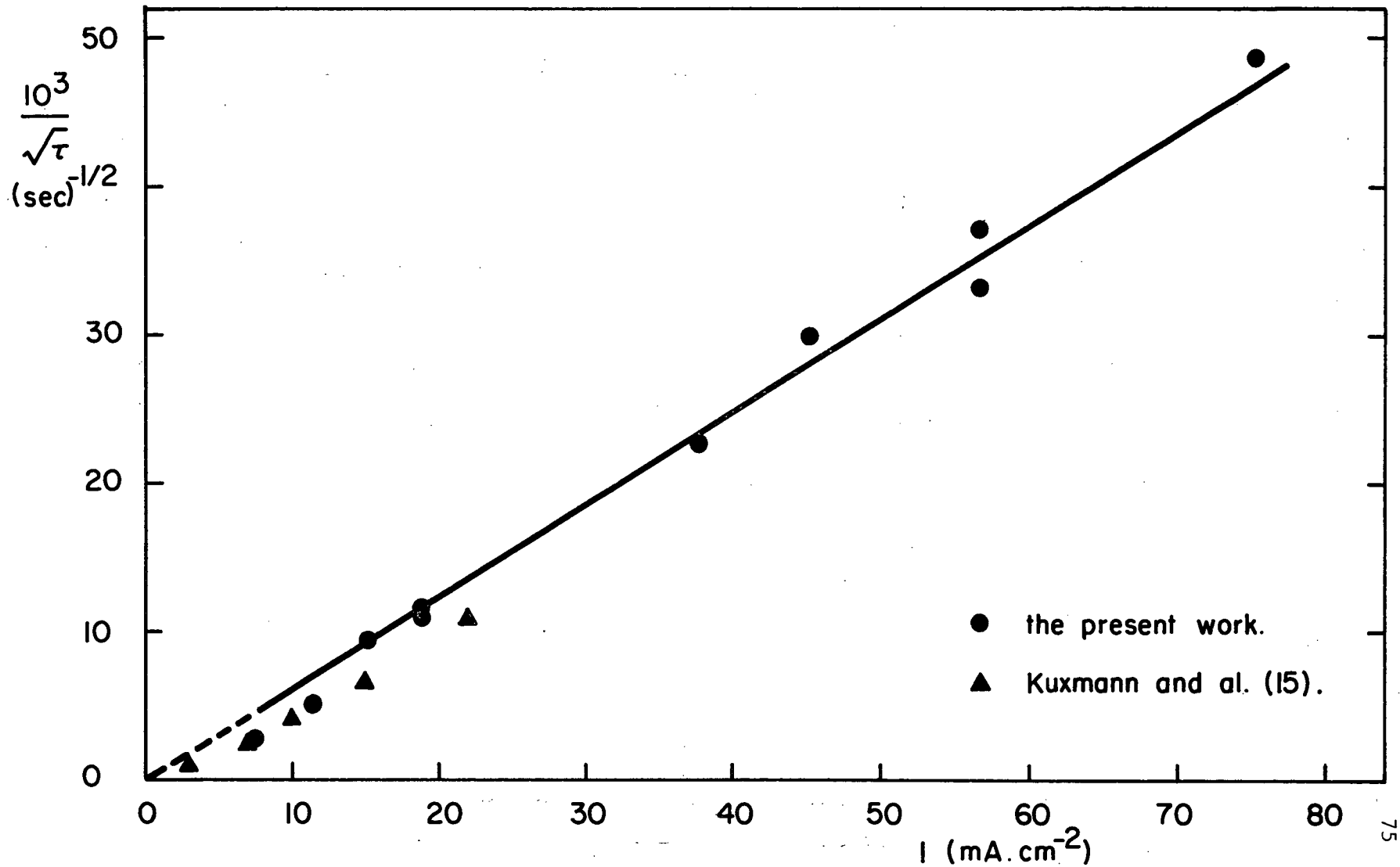

Figure 21. Relationship between the current density and the transition time observed during the galvanostatic oxidation of digenite anodes at 55°C. (▲ were estimated from Kuxman's results by the author).

$$I^2\tau = 2.5 \quad A^2cm^4sec^{-1} \tag{4.4}$$

The depth of penetration of the digenite-covellite interface, ℓ, provided it progresses uniformly, is directly proportional to the number of coulombs passed through the electrode during the time considered

$$\ell = \left(\frac{M}{d}\right)_D \frac{I\tau}{1.56F} = 1.81 \times 10^{-4} I\tau, \tag{4.5}$$

where $\left(\frac{M}{d}\right)_D = \frac{25.4}{0.93}$ is the actual molar volume of the initial digenite phase.

Given the I-τ dependence, the dissolution constant relevant to the covellite layer, k_c, can be defined by the relation

$$I = \frac{2F\, k_c}{\ell} \tag{4.6}$$

The dissolution constant describes the steady-state transport of copper ions across the porous covellite layer resulting from the digenite oxidation, $k_c = 2.35 \times 10^{-9}$ mole $cm^{-1}sec^{-1}$ in the present experimental conditions (T = 55°C, 0.1 M $CuSO_4$-0.1 M H_2SO_4 solution, $d_D = 0.93\, d_{th}$)

4.6.2 Discussion of the mode of transport of copper ions through the covellite layer

The covellite layer was porous; as a matter of fact, the molar volume of digenite and covellite is 25.4 and 20.4 cm^3mole^{-1}, respectively (59) and the digenite-covellite transformation develops 19.7% of additional porosity if the original solid volume is retained. The

copper ion transport may be effectuated by bulk diffusion through the solid sulphide, by surface diffusion along grains or by diffusion in the solution filling the pores.

a. Solid state diffusion

In the case of solid state diffusion, the copper flux through CuS is given by the integrated form of equation (3.7), which is valid regardless of the actual state of the diffusing species (cupric or cuprous ions),

$$J_{Cu} = - M_{Cu} \frac{\Delta\mu_{Cu}}{\ell} \quad . \tag{4.7}$$

When the transition occurs, the difference of copper electrochemical potential across the CuS layer ($\Delta\mu_{Cu}$), which can be expressed in terms of electrode potentials ($2F\Delta E = - \Delta\mu_{Cu}$), corresponds to the stability limits of CuS. It can be calculated from the thermodynamic data on the stable, stoichiometric CuS that ΔE is equal to approximately 75 mV at 55°C (Chapter 2). During polarization of a digenite anode, an average potential rise ($E_\tau - E_i$) of 187 mV was encountered during the quasi-linear potential increase preceding the transition (Table 5). If some unstable, non-stoichiometric covellite was formed, the entire potential difference measured might be available to drive the solid state diffusion process. The Onsager coefficient, M_{Cu}, capable of accounting for the experimental results can be calculated from equations (4.7) and (4.6).

$$k_C = 0.745 \times 2F\, M_{Cu}\, \Delta E. \qquad (4.8)$$

The factor 0.745 takes into account the porosity of the covellite layer: initially, the digenite had 7% of porosity, and the transformation developed an extra 19.7% of porosity. The ionic conductivity, which is related to the Onsager coefficient by equation (3.8), can then be calculated to be $3.3 \times 10^{-3}\ \Omega^{-1}cm^{-1}$ if the cupric ions are the diffusing species and $8 \times 10^{-4}\ \Omega^{-1}cm^{-1}$ if the cuprous ions are the diffusing species. This latter value is 23 and 11 times larger than the cuprous ion conductivity measured in chalcocite and digenite, respectively at 55°C (Chapter 3). As these two sulphides seem to display a relatively high ionic conductivity, and there is no evidence for this in CuS, it appears reasonable to consider that the solid state diffusion through covellite is not able to account for the observed rate of transport of copper towards the solution.

b. Diffusion in the solution filling the pores

If the aqueous electrolyte occupies 19.7% or more (owing to the initial porosity) of the cross section, the most likely mechanism for the transport of cupric ion is by diffusion through the electrolyte that invades the pores as they form. Eventually, the pores get so deep that the concentration gradients necessary to transport cupric ions as fast as they are forced into solution leads to saturation of the electrolyte by a cupric salt at the digenite-covellite interface. At this stage, the reaction (4.3) clogs the pores progressively, forcing the potential to rise abruptly and impeding the current flow. Part of

the current is, then, used to charge the electrical double layer and other electrode reactions, involving decomposition, rather than formation of covellite occur.

The constancy of the product $I^2\tau$ can be demonstrated for a binary $CuSO_4$ electrolyte, which approximates the actual solution existing in the pores.

It should first be noted that the accumulation rate of copper in the pores, A, represents a negligible fraction of the total copper flux, JS. A can be approximated by

$$A = C_{Cu} fS \frac{dx}{dt},$$

where $-C_{Cu}$ is the copper concentration at the digenite-covellite interface. At the maximum, C_{Cu} = 2.2 M, which corresponds to the saturation in $CuSO_4 \cdot 5H_2O$ at 55°C (60),

- fS is the actual cross section of pores $fS < 0.2\ S$,
- $-\frac{dx}{dt} = \frac{1}{0.78} \left(\frac{M}{d}\right)_D J$, the interface velocity.

The accumulation rate of copper in the pores was calculated to remain lower than 1.4% of the total copper flux.

Cupric sulphate dissolved in water is only partially ionized. Investigation of the U.V. spectra of these solutions revealed the existence of a complex which was believed to be $CuSO_4$; its stability constant was estimated to be 125 (61). On the basis of this value, it can be calculated that approximately 73% of the copper is in the complex form in 0.1 M $CuSO_4$ solution at ambient temperature. This value is approximate since a more accurate estimation requires the

appropriate activity coefficients to be taken into account. However it is apparent that a relatively important fraction of $CuSO_4$ remains undissociated in 0.1 M $CuSO_4$ solution. Furthermore, the diffusivity of the $CuSO_4$ complex will be assumed equal to the diffusivity quoted in the literature for the cupric ions. In fact, the copper ion diffusion coefficients measured by Newman and al. (54,62) with the R.D.E. technique in $CuSO_4$ solutions are aggregate values taking into account diffusion of both cupric ions and neutral complex.

If $CuSO_4$, Cu^{++}, and SO_4^{--} are noted, 1, 2, 3, respectively, the unidimensional diffusion equations can be written (convection term is negligible*)

$$J_1 = - D_1 \frac{\partial C_1}{\partial x}$$

$$J_2 = - D_2 \frac{\partial C_2}{\partial x} - D_2 \frac{2F}{RT} C_2 \frac{\partial \phi}{\partial x} \qquad (4.9)$$

$$J_3 = - D_3 \frac{\partial C_3}{\partial x} + D_3 \frac{2F}{RT} C_3 \frac{\partial \phi}{\partial x}$$

along with the electroneutrality condition $C_2 = C_3$,

the flow requirements $J_1 + J_2 = \frac{J}{f}$ **

$J_1 = -J_3$

---

* Convection term = $\bar{C}$ f S $\frac{dx}{dt}$, where $\bar{C}$ is the concentration in the bulk solution, and is less than 7×10^{-2} % of the total flux JS.

** J represents the apparent flow normal to the geometric electrode area. f. (< 0.2) is a correction factor to take into account that only a fraction of the cross section, occupied by the pores, is available for the transport of copper.

and the chemical equilibrium statement $C_1 = KC_2^2$.

It follows after rearrangement of these equations

$$\frac{J}{f} = -(D_1 + D_1 \frac{D_2}{D_3}) \frac{\partial C_1}{\partial x} - 2D_2 \frac{\partial C_2}{\partial x}, \qquad (4.10)$$

Integration of Eq. (4.10) over the thickness of the covellite layer yields

$$I\ell = f\ 2F \quad [(D_1 + D_1 \frac{D_2}{D_3})(C_1 - \bar{C}_1) + 2D_2 (C_2 - \bar{C}_2)].$$

At the transition, i.e., when saturation is achieved in the bottom of the pores, every term on the right hand side is a constant and it follows from Eq. (4.5)

$$I^2\tau = \text{cst.}$$

4.6.3. Discussion of the potential increase taking place before the transition

a. Diffusion overvoltage and potential drop in the pores

If the copper is transported in the solution filling the cracks and pores of the covellite layer, the potential rise ($E_\tau - E_i$) observed during the pseudo linear portion of the potential-time curve (Fig. 20) is the sum of the diffusion overvoltage and resistance polarization (ohmic drop + liquid junction potential) in the pores. The average potential difference measured amounts to 187 mV ($I > 15$ mA cm^{-2}). The experimental values lie in a band between 152 and 239 mV (Table 5) and

seem to be randomly distributed with respect to measured transition time, around the mean values stated by equation (4.4).

The diffusion overvoltage can be calculated with the Nernst equation

$$\eta_D = \frac{RT}{2F}\left[\ln a_{Cu^{++}} \text{ (in satd. } CuSO_4 \text{ soln.)} - \ln a_{Cu^{++}} \text{(in 0.1 M } CuSO_4, \text{ 0.1 M } H_2SO_4)\right].$$

The activity of the cupric ions in a saturated cupric sulphate solution may be set equal to the square root of the activity of the saturated copper sulphate electrolyte. The latter is equal to exp. $(-\frac{\Delta F^\circ}{RT})$ where ΔF° is the standard free enthalpy of solution of copper sulphate according to the equation

$$CuSO_4 \cdot 5H_2O(s) \longrightarrow Cu^{++} + SO_4^{--} + 5H_2O$$

$$\Delta F^\circ = 1350 + 9.3\ T \quad (2).$$

However, experimental data on the saturated copper sulphate electrode are available ($0.296 < E_o < 0.317$ V at 25°C) (32). The average value of 0.306 V is retained along with the experimental thermal temperature coefficient of 0.93 mV $°C^{-1}$ (32). The potential of the 0.1 M cupric sulphate-sulphuric acid, copper electrode was measured (Chapter 2) to be 0.312 V at 55°C with respect to the standard hydrogen electrode. The diffusion overvoltage is then estimated to amount to approximately 22 mV.

The resistance polarization in the pores should then be able to account for the remaining 165 mV. It is shown in Appendix 3 that, in the case of a weak electrolyte, the potential drop in a diffusion layer depends on the magnitude of the complex stability constant and may be much higher than the diffusion overvoltage in contrast with the case of a fully ionized electrolyte.

b. Interface overvoltage

The digenite-covellite interface is associated with a dynamic potential, which should be attained almost instantaneously (the response time of the measuring circuit is approximately 2.5 sec) after the current is switched on, before the interface begins its migration into the specimen.* The digenite composition at the surface has been calculated to reach the value $Cu_{1.765}S$ in 1.25 10^{-3} sec at a current density of 10 mA cm^{-2}. In fact, the most reproducible initial potentials (E_i) are obtained by extrapolating to zero time a tangent to the quasi-straight initial part of the potential-time curve (Fig. 20).

These measured potentials contain an ohmic component which can be calculated with the help of equation (4.2) and a concentration overvoltage due to the diffusion in the electrode boundary layer. The diffusion overvoltage was estimated with the Nernst equation and Eq. (4.1), using the physical parameters measured by Newman et al. (62) in 0.1 M $CuSO_4$-0.1 M H_2SO_4 solution, (Appendix 4). It was found to be

* Provided nucleation resistances do not impede covellite formation

8.5 mV at 75 mA cm^{-2}; at lower current densities it was proportionally smaller and might be effectively neglected. The corrected interface potential, E_s, versus S.C.E. (25°C) is plotted against the logarithm of the current density on figure 22.

For small current densities, the electrode retains a potential very close to the equilibrium value reported in Chapter 2 (252 mV at 55°C). A linear relationship appears to satisfy the experimental data in the higher current density range. Such a Tafel relationship presupposes that a charge-transfer process is rate determining, but the scatter of the experimental data does not permit exclusion of a mechanism in which the interface overvoltage is due to recrystallization. The most irreversible part of the recrystallization process is the diffusionless structural change of sulphur anions from the lattice form of digenite to that of covellite (12).

4.7 Polarization of covellite anodes

4.7.1. Results

a. Electrode potential measurements

Covellite anodes were studied at 55°C by galvanostatic polarization methods with current densities between 0.075 and 2.26 mA cm^{-2}. This was a much lower range than used in the digenite studies and both ohmic drop and concentration overvoltage due to diffusion in the electrode boundary layer were negligible . The results obtained during these experiments are reported in Table 6.

The potential-time curves obtained with covellite were of two types, depending on the current densities. Figure 23 shows a curve

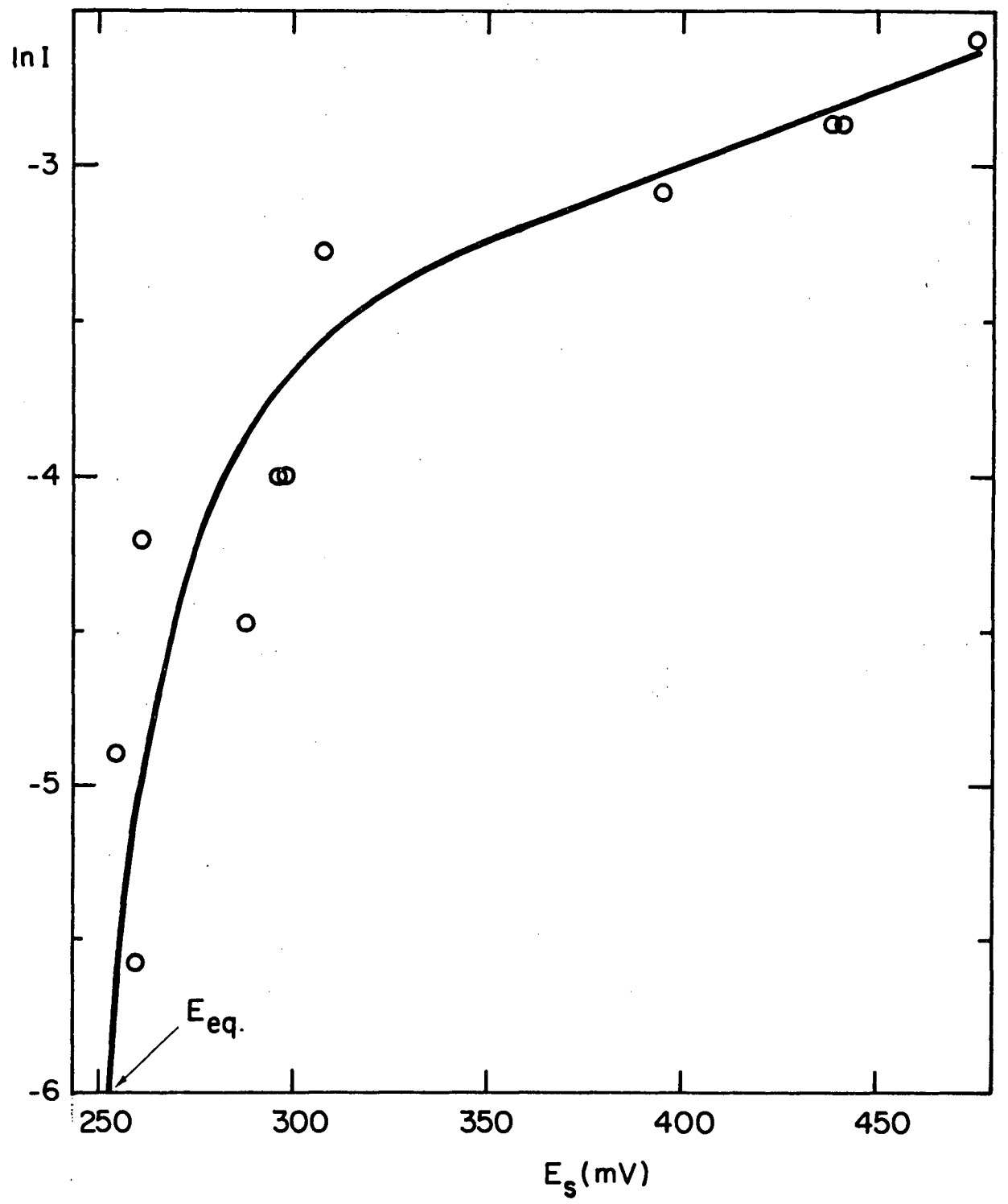

Figure 22. Relationship between the logarithm of the current density and the surface potential, observed during the galvanostatic oxidation of digenite anodes at 55°C.
S.C.E. (25°C) | 0.1 M $CuSO_4$, 0.1 M H_2SO_4 | $Cu_{1.78}S$.

Table 6

Polarization of covellite anodes

S.C.E. (25°C)/0.1 M $CuSO_4$-0.1 M H_2SO_4/CuS

I	E_o	E_N	E_{min}	E_s	E_f
mA cm^{-2}	mV	mV	mV	mV	mV
0.075	323	557	395	395	
0.23	337	592	448.4	448.4	
0.38	336	587	498	498	
0.57	350	603	496	496	
0.75	335	779	568	568	
	341	626	498	498	
1.13	343	690	518	518	
1.36	338	670	538		615
1.51	302	802		1.532	
1.88	338	774	612	1.526	
2.26	338	808	654	1.568	

E_o = 0 current potential

E_N = maximum of potential obtained shortly after the current is switched on.

E_{min} = the minimum of potential measured during the experiment (see Fig. 24).

E_s = steady-state potential.

E_f = final value of the potential recorded after 6 days of electrolysis.

typical of low current densities (< 1 mA cm^{-2}) while Figure 24 shows a curve found for higher currents (> 2 mA cm^{-2}). In both cases, there was a gradual decline in the potential during the first several hours. In the case of the lower current densities, it gradually levelled off at

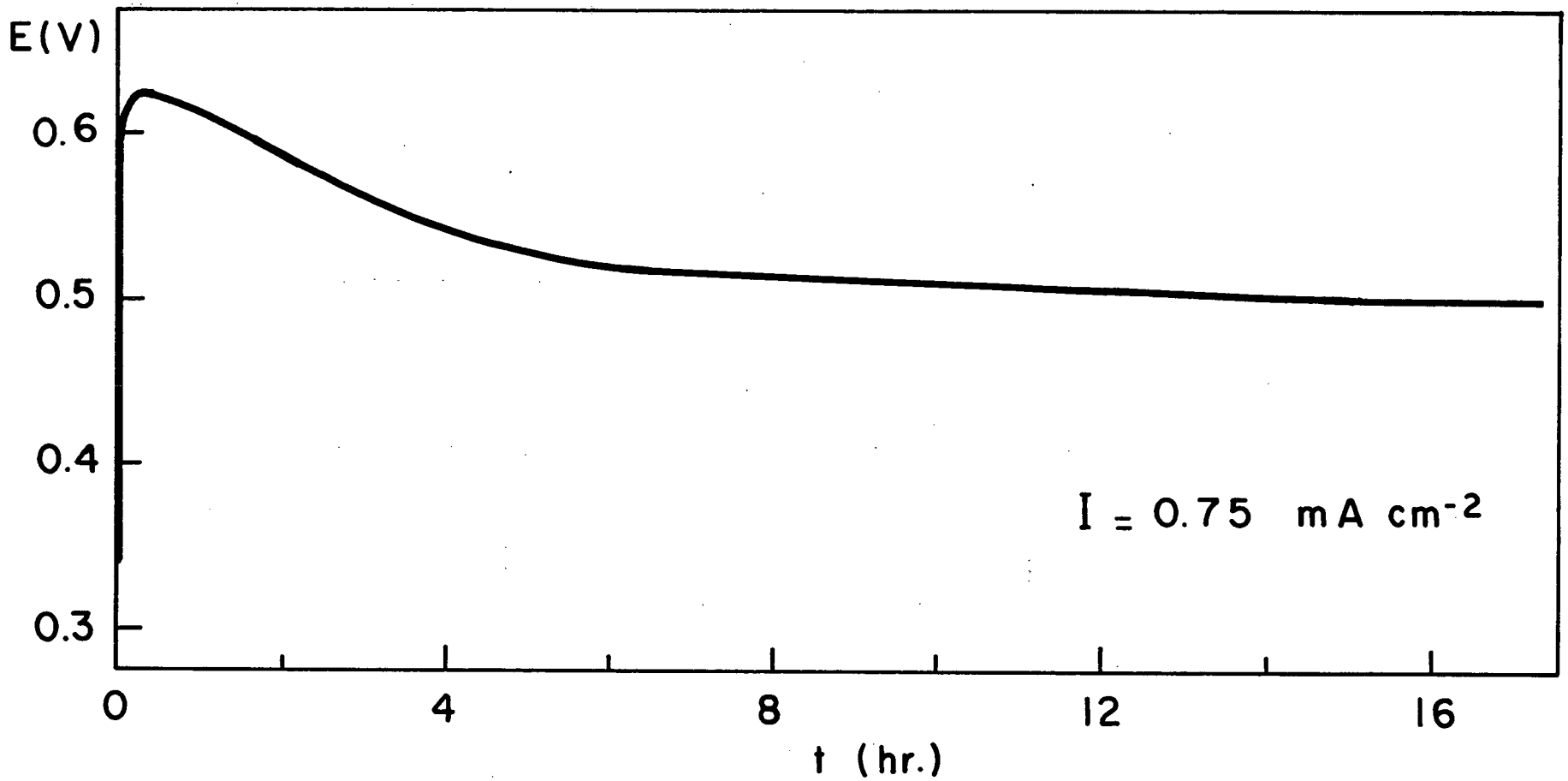

Figure 23. Potential-time curve recorded during the galvanostatic oxidation of a covellite anode at 55°C.
S.C.E. (25°C) | 0.1 M $CuSO_4$-0.1 M H_2SO_4 | CuS.

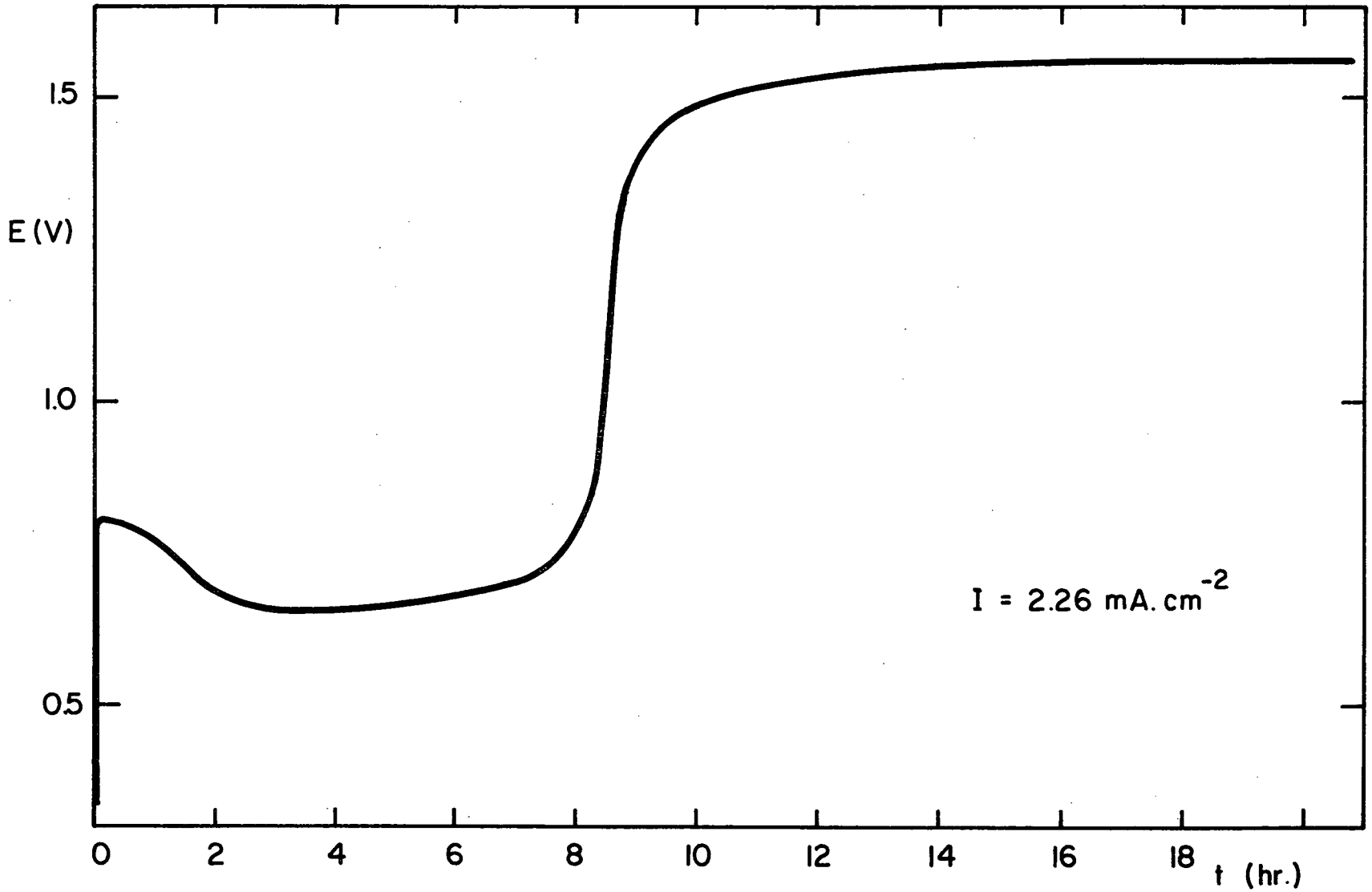

Figure 24. Potential-time curve recorded during the galvanostatic oxidation of a covellite anode at 55°C.
S.C.E. (25°C) | 0.1 M $CuSO_4$-0.1 M H_2SO_4 | CuS.

a steady value while in the case of the higher current densities, the potential, undergoing a discontinuity rose abruptly to a very high value. In the latter case, the final potential was about half a volt above the resversible oxygen electrode, where most insoluble electrodes discharge oxygen.

The apparent current densities are plotted against the covellite electrode potential versus S.C.E. (25°C) on Figure 25. The two curves drawn in solid line represent the steady-state potentials observed during the electrolysis of covellite. The dashed line extending the first curve toward the higher current densities represents the minimum potential measured on the potential-time recording. It appears on that graph that current densities higher than 1.35 mA cm^{-2} cause a change of the overall reaction leading to very high electrode potential.

The dotted line joining the two curves pictures the behaviour of covellite electrode in the intermediate current range (1.35 mA m^{-2} < I < 1.5 mA m^{-2}). The potential of such electrodes increased very slowly during prolonged period of time (1 week), eventually leading to the final value reported on the dotted line.

b. Electrode reactions

To assess the overall electrode reaction corresponding to the two potential regions, chemical analysis was carried out on the reaction products.

An experiment conducted for six days in a 0.01 M $CuSO_4$-0.01 M H_2SO_4 solution at 0.75 mA cm^{-2} revealed no variation of the average copper content in the electrolytes, indicating that the anode and cathode

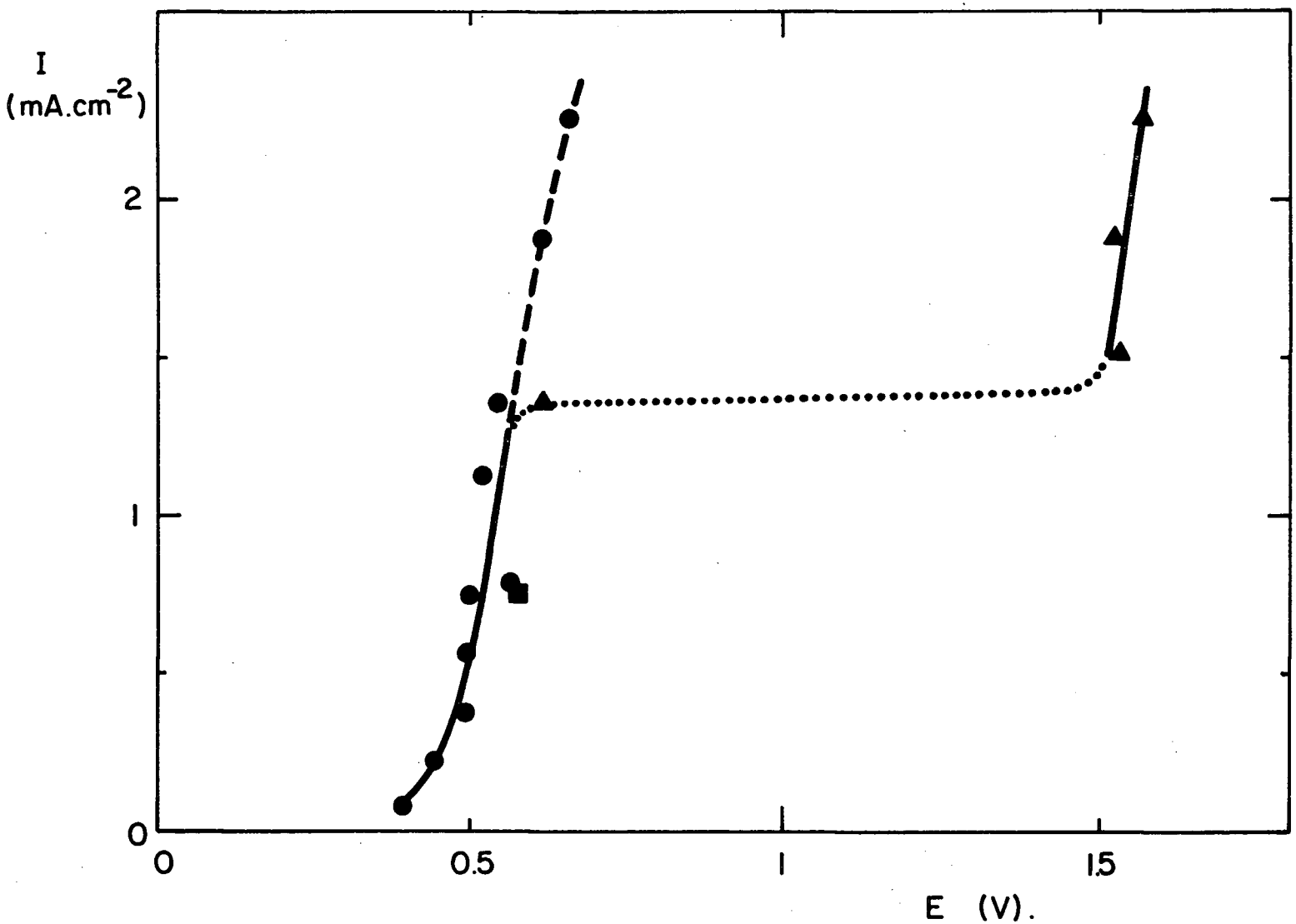

Figure 25. Polarization curve obtained during the galvanostatic oxidation of covellite anodes at 55°C.
S.C.E. (25°C) | 0.1 M H_2SO_4-0.1 M $CuSO_4$ | CuS.
(■ corresponds to 0.01 M $CuSO_4$-0.01 M H_2SO_4 solution)

reactions were of equal current efficiency, approximately 100%*. A similar experiment performed at 2.26 mA cm^{-2} depleted the copper in the electrolytes to an extent that would indicate an average current efficiency of 39% for the anodic process. The porous porcelain diaphragm appeared to have been exchanging ions with the solution and prevented any reasonable determination of the H^+ content of the solution. The quantity of SO_4^{--}, if any, put into solution was too small to be detected.**

Both covellite and orthorhombic sulphur were identified by an X-ray diffraction study of surface residues.

On the basis of these investigations, the covellite anodic reaction at lower potentials conforms to:

$$CuS \longrightarrow Cu^{++} + S^\circ + 2e \qquad (4.11)$$

The copper is dissolved and sulphur is left behind as an anode slime. When the sulphur structure forms there is a 24% shrinkage in volume (the molar volume of covellite and of sulphur being 20.4 and 15.5 cm^3 $mole^{-1}$, respectively (59)), thus the elemental sulphur is associated with cracks and pores that permit the electrolyte to retain access to the interface between covellite and elemental sulphur. Cupric ions are

---

* No bubbling was ever detected at the Cu cathode at any of the current densities used. The limiting current density at the Cu cathode in 0.1 M $CuSO_4$ is reported to be about 15 mA cm^{-2} at 25°C in free convection conditions (51), a value which was never approached in these experiments.

** The total dissolution of 1 g CuS specimen, leads to only 10^{-2} mole of sulphur species in approximately 1 ℓ of solution.

transported from this interface by diffusion in the solution invading the cracks. Thus, as in the digenite case, when the pores get sufficiently long, diffusion of cupric ions can no longer support the applied current and supplementary electrode reactions involving much higher potentials must support the excess current density.

c. Microscopic examination of the reacted electrode

An examination of covellite after electrolysis revealed that even when 40% of the copper was dissolved, the disk retained its shape and cohesion. The surface of the disk presented unreacted particles of covellite suspended in sulphur as seen on the micrograph (Fig. 26). A perpendicular section of the disk shows sulphur penetrating deeply into the specimen and in fact going through it (Fig. 27). At higher magnification, the sulphur matrix shows a fine network of lines that may represent shrinkage pores and cracks (Fig. 28). Micrographs taken with the scanning electron microscope show the high relief surface (Fig. 29 and 30).

An examination of the reacted disk with the electron microprobe was very inconclusive (Fig. 31,32,33). Even very light polishing tore sulphur particles away from the specimen surface, leaving sulphur depressions and covellite hills; the microprobe readings reflected the topography of the hilly surface more than the composition of the phases.

4.7.2 Discussion

The initial rise of the electrode potential to a maximum during the first 15 minutes, or so, of current flow (see Fig. 23,24) are most

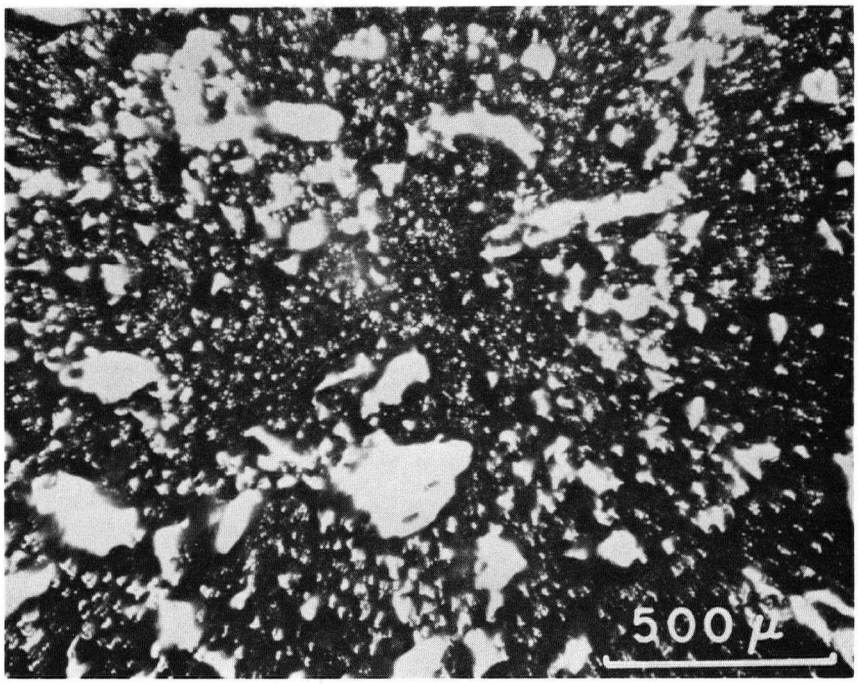

Figure 26. Micrograph of the surface of an oxidized covellite disk (unreacted covellite appears white).

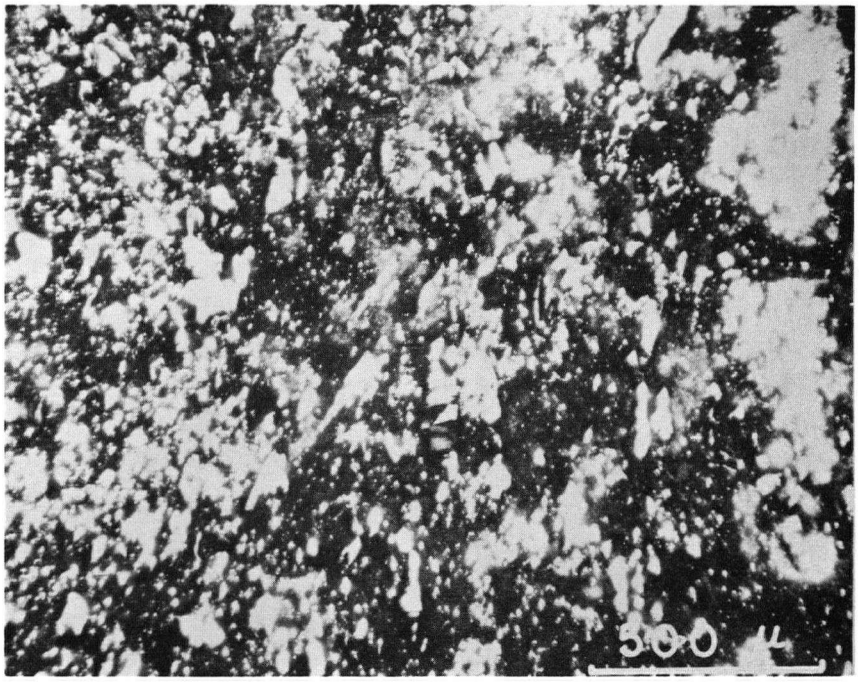

Figure 27. Micrograph of a section of an oxidized covellite disk, perpendicular to the surface.

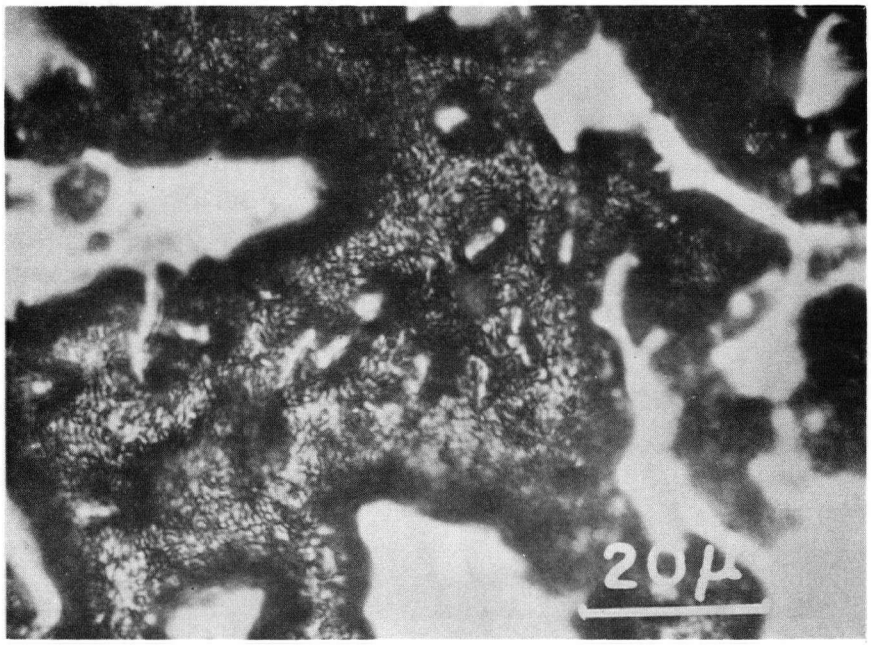

Figure 28. Optical micrograph of an oxidized covellite disk.

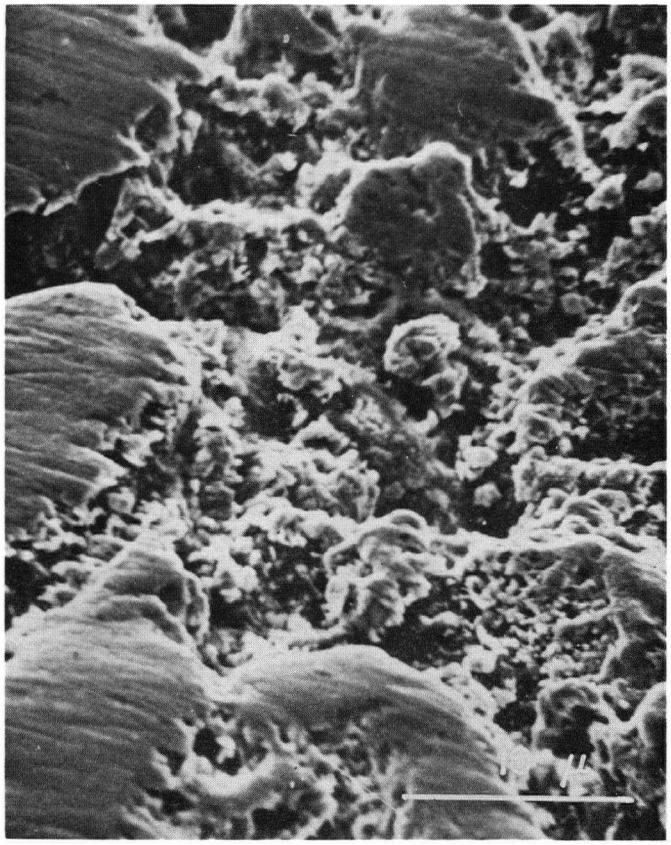

Figure 29. Scanning electron micrograph of an oxidized covellite disk.

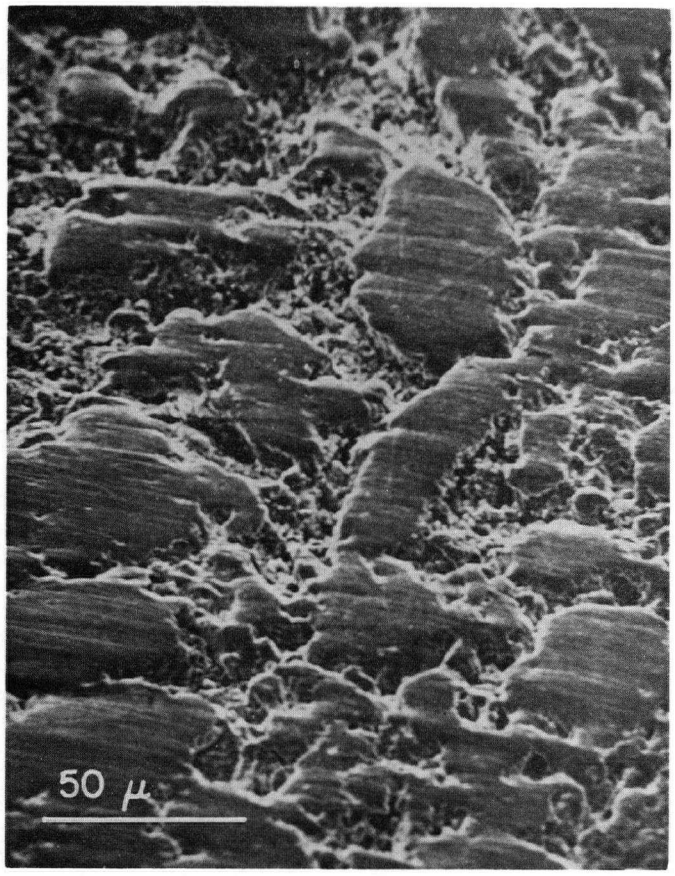

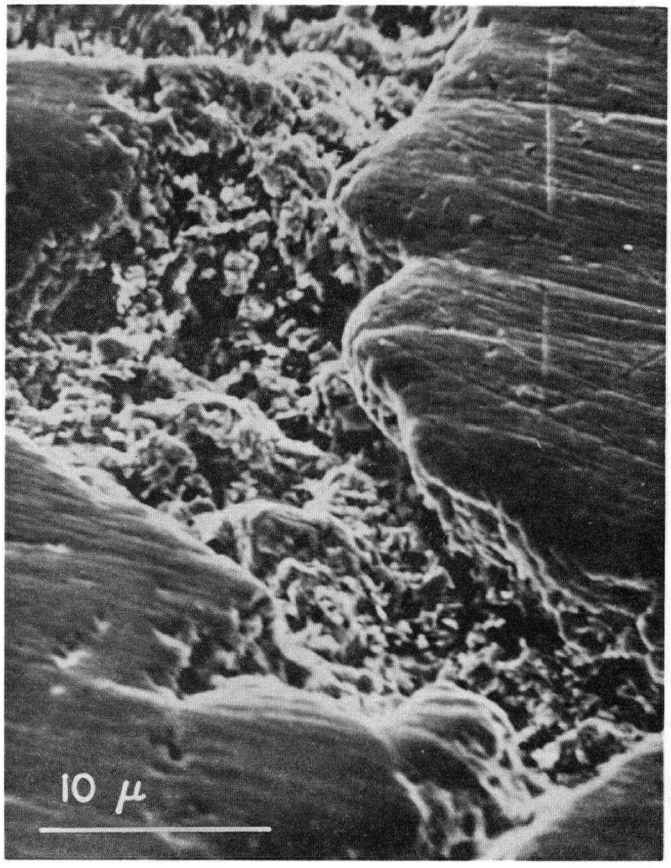

Figure 30. Scanning electron micrograph of an oxidized covellite disk.

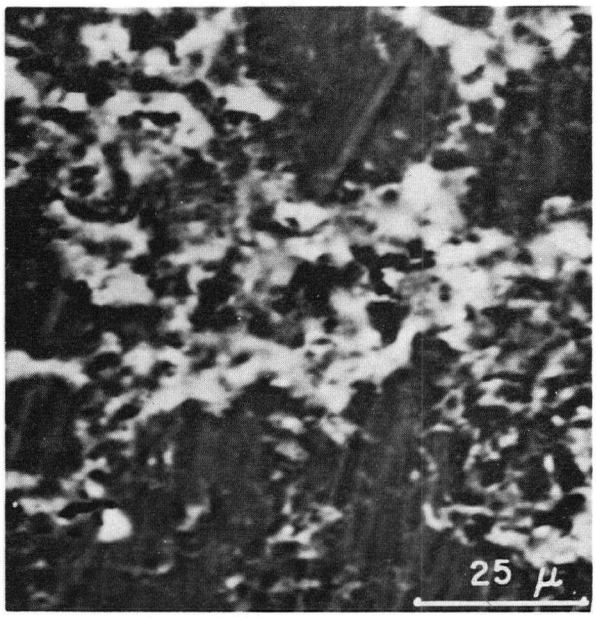

Figure 31. Absorbed electrons.

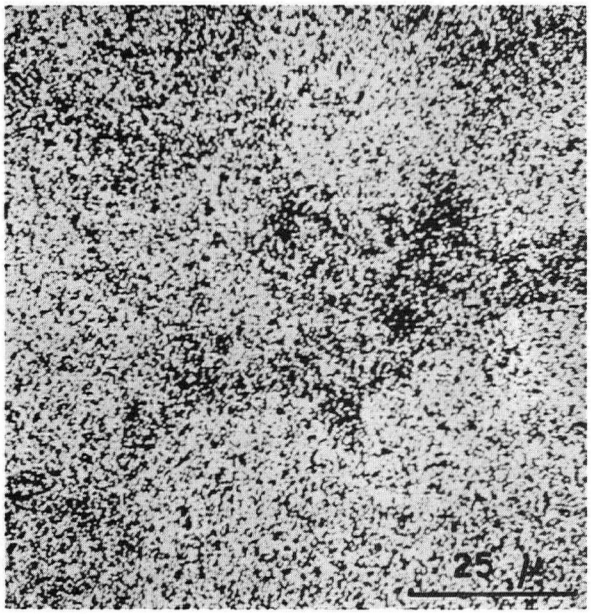

Figure 32. Cu emission.

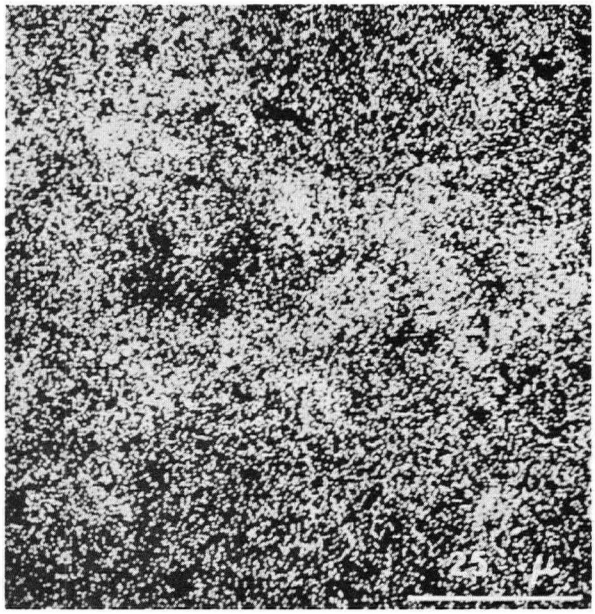

Figure 33. S emission.

Microprobe pictures of an oxidized covellite disk.

probably due to supersaturation and finally nucleation of orthorhombic sulphur in the covellite phase. It may be postulated that the decline in potential is due to the rapid increase in the covellite-sulphur interface area, which decreases the effective local current density and the associated overvoltage. In a reacted disk, the interface area between unreacted covellite and the sulphur product is very large compared with the exposed geometric surface area of the specimen as it appears on the various micrographs.

The scatter of the experimental points on the polarization curve (Fig. 25) could, in fact, reflect the uncertainty on the microscopic current density.

The appearance of a new electrode reaction (probably oxygen evolution) for current densities larger than 1.35 mA cm^{-2} cannot be rationalized only in terms of a limited diffusion rate of copper ions in the solution filling the pores resulting from the crystallization of sulphur, as was the case in digenite electrodes, because the active interfacial area and its variation with time are completely unknown.

The minimum value of current density leading to changes in the original electrode process is likely to depend upon a number of parameters, the preparation and history of the covellite being probably one of them (initial porosity, grain size,...). The experimental polarization curve (Fig. 25) should, however, be able to describe, to a first approximation, the behaviour of covellite during current flow.

CHAPTER 5.

DISCUSSION OF THE MECHANISMS OF DISSOLUTION OF THE COPPER SULPHIDES

The study of the galvanostatic polarization of rotating disk anodes of digenite and covellite at 55°C (Chapter 4) suggests the following models for the oxidation of these sulphides in acid medium:

- The reaction taking place at the digenite-covellite interface seems to present a relatively small resistance.

- The digenite oxidation rate appears to be controlled by the transport of the copper ions released by the reaction (4.3) through the porous covellite layer; the main transport component is likely diffusion in the solution filling the shrinkage pores of the covellite.

- After nucleation of elemental sulphur, the oxidation rate of covellite might be controlled simultaneously by the reaction (4.11) at the covellite-sulphur interface and diffusion of cupric ions in the solution filling the pores and cracks resulting from the crystallization of the sulphur. The peculiar way in which the sulphur grows in the covellite anode excludes, so far, any discussion of the relative influence of these two resistances on the overall reaction. However, during oxidation, covellite appears to exhibit a limiting current of dissolution similar to diffusion controlled reactions.

In the following discussion, a model, which is derived from the present work and from Kuxmann and al.'s experimental observations (15), is proposed to describe the electrolytic dissolution of chalcocite.

These models will then be used to try to account for the actual leaching behaviour of the copper sulphides using acidic ferric solutions.

5.1 Electrolytic dissolution of chalcocite: constant current oxidation

Kuxmann and Biallass (15) studied the galvanostatic polarization of chalcocite anodes in cupric sulphate solutions, with current densities in the range between 3 and 22.5 mA cm^{-2}. The potential-time curves were characterized by an abrupt potential discontinuity occurring after a transition time, similar to that encountered in the present study of digenite anodes. The copper content of the electrolyte remained unchanged up to the transition, then it decreased linearly with time. Covellite (and sulphur in some cases) was clearly recognizable in the surface layer of the electrode.

The transition times observed at 55°C in that work were back-calculated from the graphs reported in the paper - certainly, with a substantial loss of precision - and compared with the present data in Figure 21. The transition times measured in both works appear to be similar in values and to obey the same type of relationship, i.e., $I^2\tau=cst$.

In contrast to the present results, Kuxmann and Biallass observed that, before the transition, the anode potential remained approximately constant. This observation should rule out the possibility of a substantial transport of copper ions through the solid covellite. On the other hand, the potential drop resulting from the transport of the current through the solution filling the pores should remain very small in this case since there was an excess of sulphuric acid in the electrolyte (30 g/l $CuSO_4$-250 g/l H_2SO_4). The conductivity of a 5 N H_2SO_4 solution is 0.673 $\Omega^{-1}cm^{-1}$ at 25°C (63) as compared to a conductivity of 0.051 $\Omega^{-1}cm^{-1}$ for 0.1 M $CUSO_4$-0.1 M H_2SO_4 solution at the same temperature (64). The concentration overvoltage corresponding

to the saturation of the solution with a cupric salt is small ($\simeq$ 10 mV).

The constancy of the product $I^2\tau$ can be supported by the same arguments that were proposed for the digenite case (4.6.2) i.e., transition of the electrode process resulting from the saturation of the electrolyte with a cupric salt at the digenite-covellite interface and reaction interface moving at a constant rate. In the case of an excess of indifferent electrolyte, the diffusion equations are considerably simplified since the effect of the electric field can be neglected, and in the aggregate, the flux of copper can be described by

$$J_{Cu} = -D_{Cu}\, f\, \frac{\partial C_{Cu}}{\partial x}$$

where f is the effective fraction of the cross section occupied by pores. (If the initial chalcocite is fully dense, $f < 0.255$). It follows after integration between the limits of the covellite layer that

$$I\ell = 2F\, D_{Cu}\, f\, (C_{Cu,sat.} - \bar{C}_{Cu}),$$

where D_{Cu} is an average diffusion coefficient for the range of concentrations considered. This last relationship is equivalent to $I^2\tau =$ constant provided the covellite layer thickness increases linearly with time.

The oxidation of chalcocite to covellite implies the formation of the intermediate djurleite and digenite phases. Kuxmann's results, along with the observations reported in Chapters 2, 3 and 4 seems to indicate that these interface reactions are relatively non resistive, and that the overall oxidation rate is controlled by the transport of

copper ions through the reaction products.

The anode morphology resulting from the oxidation of chalcocite at constant current can be analysed theoretically: the problem consists in calculating the thickness of the various sulphide layers with respect to time, when the overall oxidation is controlled by diffusion through the reaction products.

Theoretical model: constant current multiplelayer oxidation (Fig. 34)

The djurleite will be considered undistinguishable from the chalcocite. This assumption is based on the facts that the composition and physical properties of the two phases are very similar. On the other hand, the standard electrode potentials reported for cast or mineral chalcocite (15,28,29) are very close to the standard potential of a djurleite-digenite electrode derived from the measurements reported in Chapter 2 (ε_o = 503 mV at 25°C). The digenite composition is averaged to $Cu_{1.78}S$ while the secondary effects due its stoichiometry range are neglected.

If the origin of times is taken when the anodic current is applied, a layer of digenite starts to form at t = 0, and its thickness is given at time, t, by the relationship

$$x_1 = Jt\,\alpha_1 \qquad \alpha_1 = \left(\frac{M}{d}\right)_{Ch} \frac{1}{0.22}$$

$$Cu_2S \rightarrow Cu_{1.78}S + 0.22Cu^{++} + 0.44e$$

which translates a simple material balance between the flux of copper, J, and the amount of chalcocite reacted.

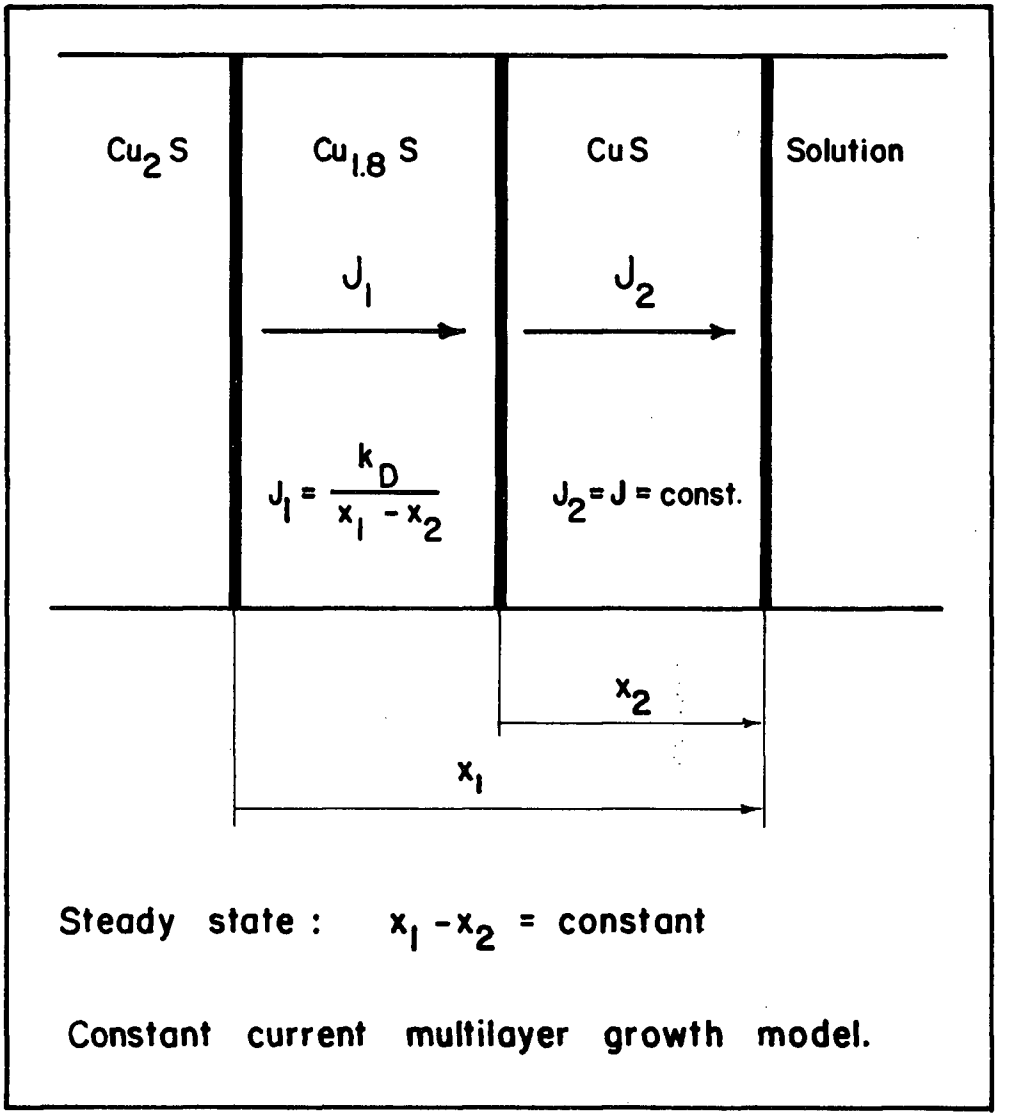
Cu2 S
Cu1.8 S
Cu S
Solution
J1
J2
J1 = kD / (x1 - x2)
J2 = J = const.
x2
x1
Steady state : x1 - x2 = constant
Constant current multilayer growth model.

Figure 34

The mechanism of transport of copper ions through the digenite layer is subject to a discussion similar to that conducted in section (4.6.2) for covellite. The transformation of chalcocite into digenite, without volume change, introduces 7% of porosity in the digenite layer. No data are available to assess the effect of this porosity on the transport properties of the digenite layer. Covellite forms when the electrode potential at the outside surface of the digenite has reached the equilibrium potential of a digenite-covellite electrode or when saturation of the solution filling the pores with a cupric salt is reached. At the onset of growth of covellite ($t = t_D$), the thickness of the digenite layer (x_D) is given, in both cases, by (see section 4.6.2)

$$J = \frac{k_D}{x_D}, \qquad x_D = J\alpha_1 t_D, \tag{5.1}$$

where k_D is the constant of dissolution through digenite.

The simultaneous growth of digenite and covellite is governed by the two first order differential equations which relate the rate of progression of the interfaces to the copper flux,

$$\frac{dx_1}{dt} = \frac{k_D\alpha_1}{x_1-x_2}$$

$$\frac{dx_2}{dt} = J\alpha_2 - \frac{k_D\alpha_2}{x_1-x_2} \qquad \alpha_2 = \left(\frac{M}{d}\right)_{Ch} \frac{1}{0.78}$$

$$Cu_{1.78}S \longrightarrow CuS + 0.78Cu^{++} + 1.56e$$

where x_1 is the total thickness of the reaction products, x_2 is the thickness of the covellite layer (see Fig. 34). These can be transformed

in the following system of equations,

$$\frac{\alpha_2}{\alpha_1}\frac{dx_1}{dt} + \frac{dx_2}{dt} = J\alpha_2 \tag{5.2}$$

$$\frac{d(x_1-x_2)}{dt} = \frac{k_1(\alpha_1+\alpha_2)}{x_1-x_2} - J\alpha_2 , \tag{5.3}$$

which can be integrated to give the following solutions (Appendix 5),

$$\frac{x_1-x_D}{\alpha_1} + \frac{x_2}{\alpha_2} = J(t-t_D) \tag{5.4}$$

$$-\frac{x_1-x_2-x_D}{J\alpha_2} - \frac{k_D(\alpha_1+\alpha_2)}{J^2\alpha_2^2}\ln\frac{k_D(\alpha_1+\alpha_2) - J\alpha_2(x_1-x_2)}{k_D(\alpha_1+\alpha_2) - J\alpha_2 x_D} = t-t_D \tag{5.5}$$

It appears in equation (5.5) that the logarithm becomes infinite for

$$k_D(\alpha_1+\alpha_2) = J\alpha_2(x_1-x_2) \quad \text{or} \quad x_1-x_2 = \frac{\alpha_1+\alpha_2}{\alpha_2}x_D \tag{5.6}$$

When time increases, the distance between the two interfaces converges, therefore, towards a constant value ($4.545\ x_D$), and the two phases penetrate the anode at the same constant rate

$$\frac{dx_1}{dt} = \frac{dx_2}{dt} = J\frac{\alpha_1\alpha_2}{\alpha_1+\alpha_2} = \left(\frac{M}{d}\right)_{Ch} J \tag{5.7}$$

The set of equations (5.4) and (5.5) was solved for x_1 and x_2 taking a value of k_D which corresponds to the solid state diffusion of copper ions in digenite. The integration of equation (3.9) with respect to the thickness of the digenite layer at the onset of growth of

covellite yields

$$Jx_D = - \frac{\sigma_{Cu^+}}{F^2} \Delta\mu_{Cu} , \qquad (5.8)$$

where $\Delta\mu_{Cu} = -2F\Delta E$ corresponds to the range of stability of digenite, which was measured to be 20 mV at 55°C (Chapter 2), and σ_{Cu^+} is the copper ionic conductivity of digenite, measured to be approximately $7.5\ 10^{-5}\ \Omega^{-1}cm^{-1}$ at 55°C (Chapter 3). It follows from equations (5.1) and (5.8) that

$$k_D = 2 \frac{\sigma_{Cu^+}}{F} \Delta E = 3.1\ 10^{-11} \quad \text{mole cm}^{-1}\text{sec}^{-1}$$

The depth of penetration of the two interfaces are plotted as a function of time on figures 35 and 36. It appears from the calculations that the interfaces assume their steady motion for time longer than $90\ t_D$ and that the thickness of the covellite layer is then adequately described by

$$x_2 = J\left(\frac{M}{d}\right)_{Ch} (t - 4.545\ t_D) \qquad (5.9)$$

Since it was observed that a layer of covellite formed on the chalcocite sample subjected to oxidation, the observed transition could not result from transport limitation in the intermediate digenite layer. In fact, the thickness of the digenite layer adjusts itself to the flux of copper ions which diffuse through it: J when digenite only is formed, and $J_1 < J$ when both digenite and covellite are formed. It

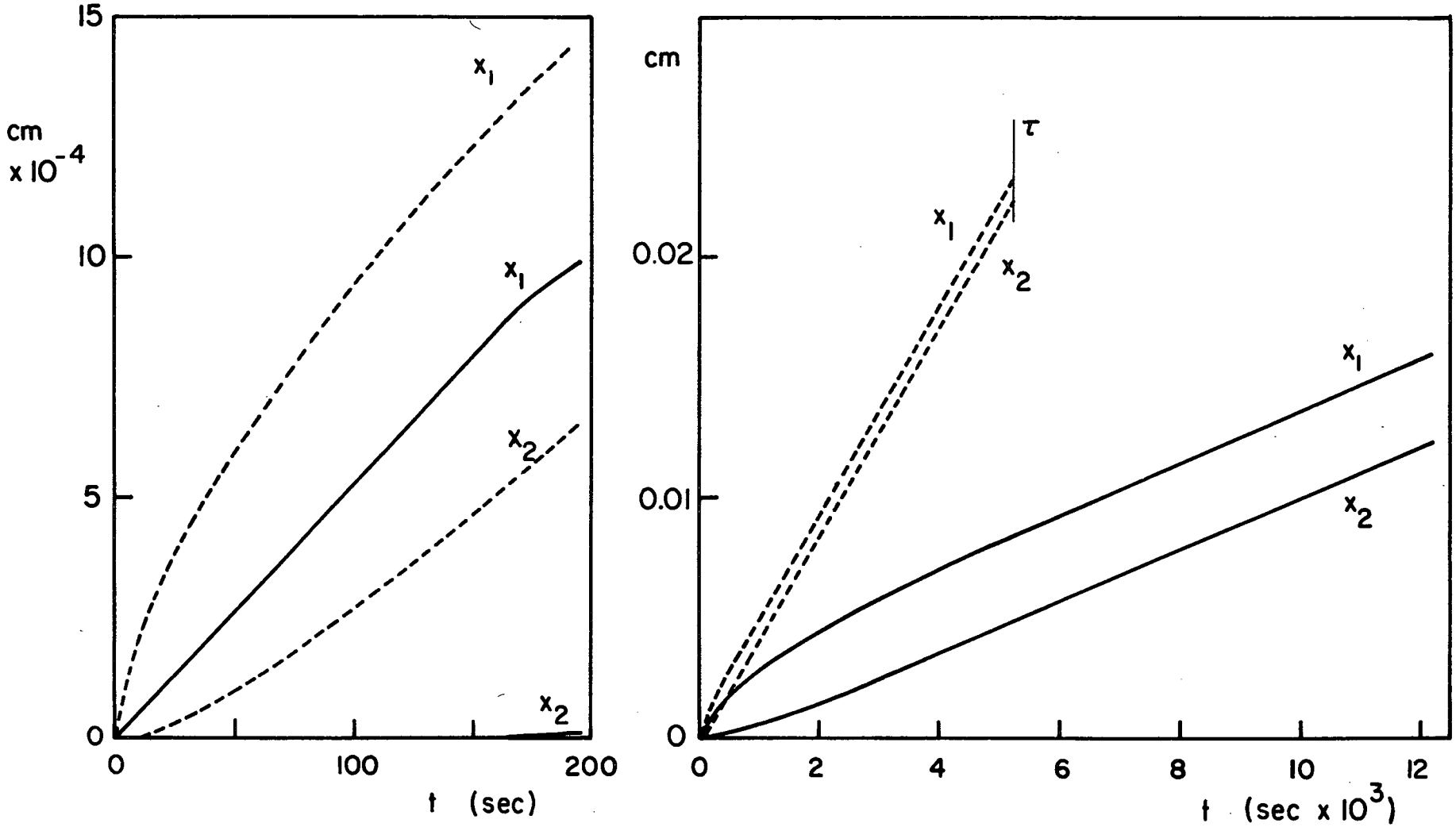

Figure 35 and 36. Depth of penetration of the chalcocite-digenite interface (x_1) and the digenite-covellite interface (x_2), during the oxidation of chalcocite.
----- I = 30 mA cm^{-2} _____ I = 7.5 mA cm^{-2}

follows from the theoretical analysis that the thickness of the digenite layer converges towards a constant (Eq. (5.6)) and that the depth of penetration of the covellite is linear and given by Eq. (5.9) for times larger than 90 t_D (Eq. (5.1)).

Since the product $I^2\tau$, relevant to the chalcocite electrolysis, was observed to be constant in Kuxmann's experiments, it may be proposed that the covellite had reached its steady rate of growth (Eq. 5.9) when the transition occurred. This would indicate that the observed transition time, τ, is larger than 90 t_D and therefore that the constant of dissolution through the digenite layer, k_D, is much smaller than the constant of dissolution through the covellite layer, k_C,

$$k_C > 20\ k_D,$$

as can be calculated from the equations (5.9), (5.1), (4.6).

It would be meaningless to compare the value of the constant of dissolution through the covellite layer calculated from the present work (Eq. (4.6)) with the constant that could be calculated from Kuxmann's work, interpreted by Eq. (5.9) and the data of Figure 21.:

- In a solution containing 250 g/l of H_2SO_4 and 30 g/l $CuSO_4$ the migration current is likely to be negligibly small while it is far from being so in a 0.1 M $CuSO_4$-0.1 M H_2SO_4 solution.

- The cupric salt which precipitates in the pores in the case of the 0.1 M $CuSO_4$-0.1 M H_2SO_4 solution may be a basic sulphate while it is more likely to be a sulphate in the case of the 30 g/l $CuSO_4$-250 g/l H_2SO_4 solution.

- The theoretical porosity of the covellite resulting from the oxidation of the chalcocite and of the digenite is 25.5% and 19.7% respectively. As the dissolution constant depends on the effective fraction of the cross section occupied by the pores, it must be corrected to take that effect into account.

If the model proposed for the dissolution of chalcocite and digenite is correct, it would be of interest to attempt the direct electrolysis of copper matte in a chloride or a mixed chloride-sulphate electrolyte since the solubility of cupric chloride in water is 6.6 M at 55°C (63) while the solubility of cupric sulphate is 2.2 M at 55°C (60,63).

5.2 Leaching of covellite with acidic ferric solutions: electrochemical oxidation

An electrochemical process, involving two simultaneous reactions, has often been proposed to account for the aqueous oxidation of sulphides (1,27,5,65): the reduction of the oxidant and the oxidation of the sulphide take place at different sites of the mineral and the electrons are transferred through the sulphide lattice. The process is analogous to the corrosion of metals and the electronic conductivity of many sulphides makes this feasible.

Thomas and Ingraham (5) leached rotating disks of covellite in 0.1 M Fe^{3+}-0.1 M H_2SO_4 solutions, their experiments were usually continued until 20% of the copper was dissolved. Up to this point, the disks retained their smooth surfaces, shape, dimensions and electrical conductivity. The reacted disks were a mixture of elemental sulphur and unreacted covellite similar to what was observed after the electrolysis

of covellite anodes (4.7.1); the covellite persisted on the outer surface of the specimen. The morphology of the leached specimens suggested that the interface where the covellite was oxidised to sulphur was penetrating the disk while the electrons released by the oxidation reaction were travelling through the persisting network of covellite particles towards the specimen surface where the ferric ions could be reduced.

During leaching, copper sulphides should assume mixed electrode potentials which depend on the nature and magnitude of the electrochemical reactions taking place and which could be directly measured. In the case of an aqueous electrochemical oxidation, the leaching rates and the corresponding mixed potential taken by the sulphide can be estimated from the current-voltage curves obtained during anodic polarization of the sulphide and cathodic polarization of the oxidant. This calculation has been made in the case of the leaching of a covellite disk rotating at 500 r.p.m. in acidic ferric solutions at 55°C; these conditions correspond to the leaching experiments conducted by Thomas and Ingraham (5).

The electrode kinetics of the Fe^{+++}/Fe^{++} couple, which has been abundantly investigated on platinum electrodes, result from the interplay of diffusion and charge-transfer resistances (49). The contribution of the diffusion resistance can be calculated in the case of a rotating disk electrode. All the data which are necessary for the calculation of the current density-potential curves of the Fe^{+++}/Fe^{++} couple have been compiled from the available literature and are reported in Appendix 6. The cathodic curves calculated in that fashion

for a ferric ion concentration of 0.1 M and for a ferrous ion concentration of 10^{-3} and 10^{-2} M are plotted on Figure 37 (these concentration values have been selected to match Thomas' experimental leaching conditions), and can be confronted with the polarization curve of covellite anode determined in the present work (Fig. 25).

The leaching rate derived, at 55°C, from Thomas' and Ingraham's experiments is equivalent to a current density of 1.97 mA cm^{-2}; the leaching rates remained constant after a transient period of several hours. They studied the effect of the variation of the ferric ion concentrations at 50°C and found that the leaching rate was independent of ferric ion concentration for concentrations larger than 0.1 M. This results from a limiting dissolution rate of the covellite and could correspond to the limiting current density observed during the electrolysis of covellite anodes ($I_{lim} \simeq 1.40$ mA cm^{-2} , see Section 4.7.1), since the potential exerted by the Fe^{+++}/Fe^{++} couple is not sufficient to force the transition to occur.

An attempt that was made to derive the variation of the leaching rate of covellite at 55°C against the ferric ion concentration will be described with the experimental polarization curve for a covellite anode using I_{lim} = 2 mA cm^{-2} and a set of calculated current density potential curves for various Fe^{+++} concentrations, the ratio Fe^{+++}/Fe^{++} being assumed constant (Figure 38).

This estimation leads only to semi-quantative information since it is derived from polarization curves which have not been precisely established for the leaching conditions:

- The polarization curve for a covellite anode remains somewhat

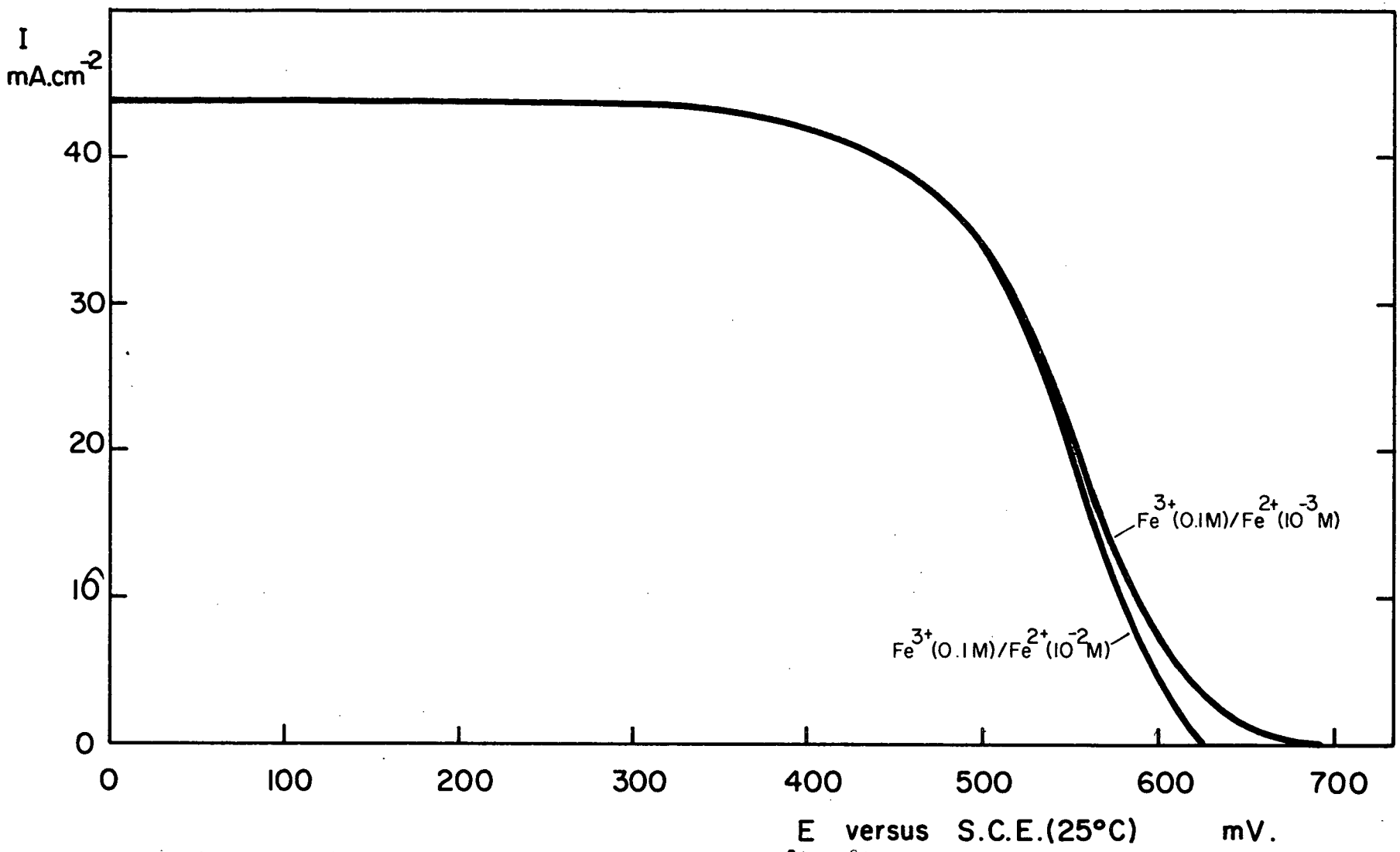

Figure 37. Current density-potential curves for the Fe^{3+}/Fe^{2+} couple. Platinum electrode rotating at 500 r.p.m., 55°C.

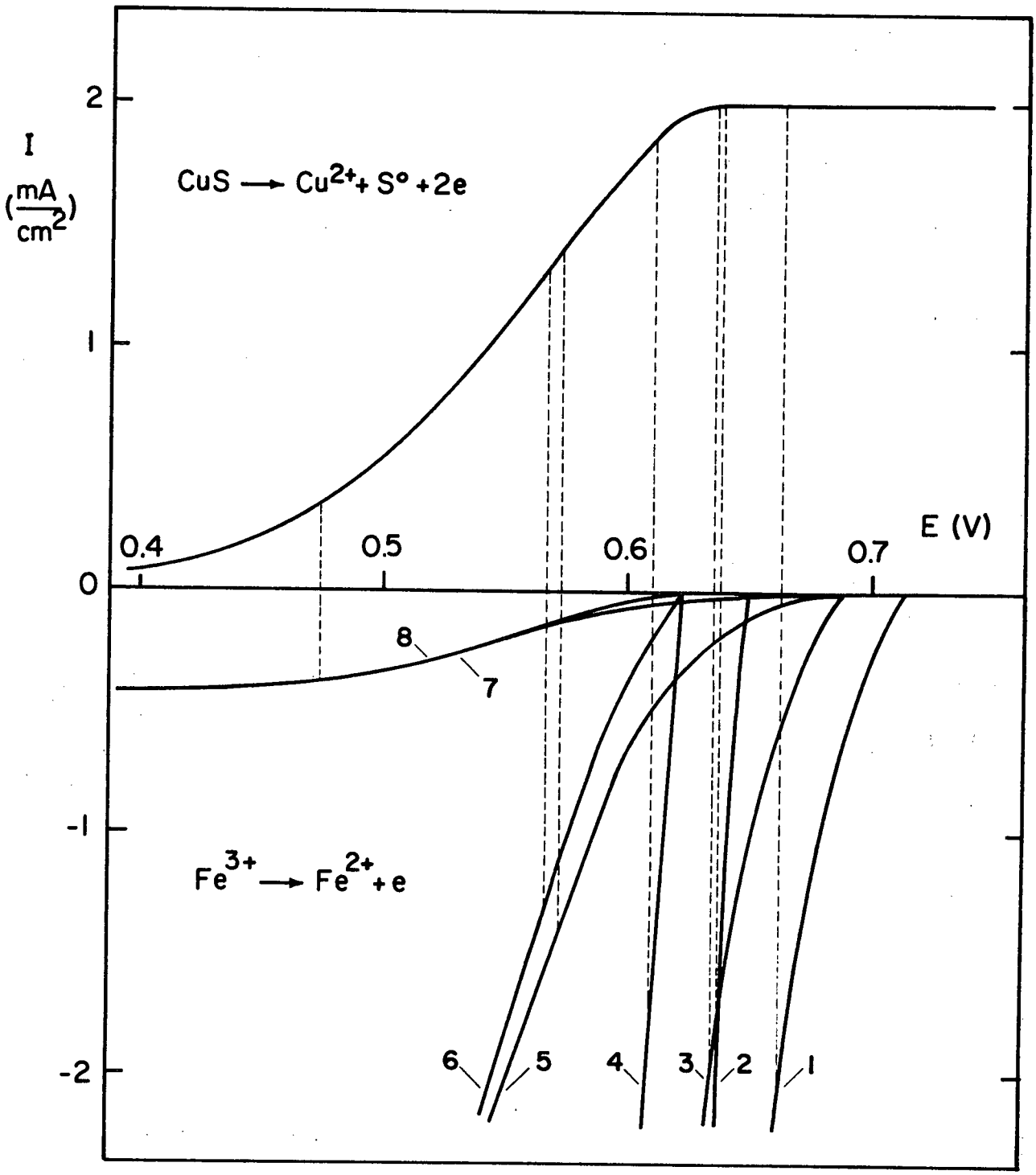

Figure 38. Electrochemical oxidation of CuS by ferric sulphate solutions
R.D.E. spinning at 500 r.p.m., 55°C.

1, 2 | Fe^{3+} (0.25 M) } / Fe^{2+} (10^{-3} M) / Fe^{2+} (10^{-2} M)

3, 4 | Fe^{3+} (0.1 M) } / Fe^{2+} (10^{-3} M) / Fe^{2+} (10^{-2} M)

5, 6 | Fe^{3+} (10^{-2} M) } / Fe^{2+} (10^{-4} M) / Fe^{2+} (10^{-3} M)

7, 8 | Fe^{3+} (10^{-3} M) } / Fe^{2+} (10^{-5} M) / Fe^{2+} (10^{-4} M)

approximate since it depends upon the actual interfacial area which, in turn, is the result of the morphology of the sulphur growth.

- In addition, the polarization of covellite anode was studied in 0.1 M $CuSO_4$ solution while Thomas and Ingraham start their leaching experiment with a solution containing no copper.

- The charge-transfer parameters of the Fe^{+++}/Fe^{++} couple have been measured at a platinum electrode.

- The whole apparent sulphide area is supposed to be active for the reduction of ferric ions.

The leaching rates expressed in current densities were calculated from Figure 38 and are reported on Figure 39 in regard of the experimental leaching rates measured by Thomas and Ingraham. Both calculated and experimental curves seem to follow the same type of dependence upon the ferric ion concentration.

The leaching rate of covellite is independent of the ferric ion concentration above a certain value, which is likely to be temperature dependent, and is, then, controlled only by the oxidation kinetics of the sulphide. In very dilute solutions, the leaching rate is determined by the limited rate of diffusion of the ferric ions towards the covellite. In the intermediate range of concentrations, the leaching rate results from both the oxidation kinetics of covellite and the reduction kinetics of ferric ions.

It follows from the foregoing discussion that, so far, an electrochemical mechanism appears to be adequate to explain the oxidation of covellite in acidic ferric solution.

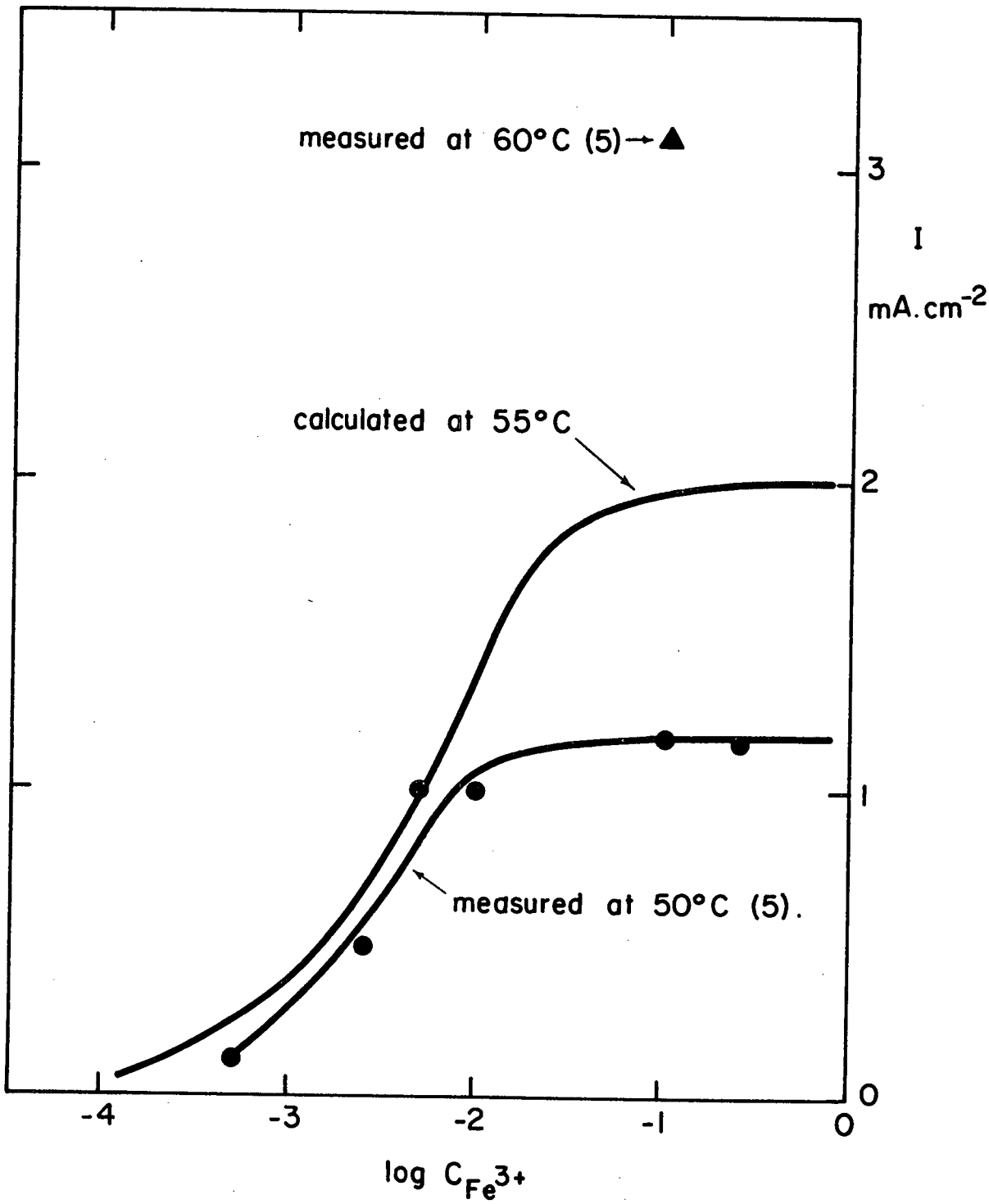

Figure 39. Leaching rate of rotating covellite disks (500 r.p.m.) versus ferric ion concentration in solution.

5.3 Leaching of chalcocite and digenite with acidic ferric solutions: constant potential oxidation

The driving force exerted by acidic ferric solutions is large enough to oxidise any copper sulphide to elemental sulphur but the sulphur formation, which has to overcome a nucleation stage, is sufficiently resistive to occur only to a negligible extent during the chalcocite and digenite oxidation, either until these sulphides are completely exhausted (ground minerals) or until the diffusion resistance of the covellite layer (solid sample) has markedly slowed down the reaction (4.3). This explains the characteristic two stage reaction generally observed during the leaching of chalcocite and covellite.

In the following discussion, the first leaching stage of digenite and chalcocite will be treated as a reaction controlled by the transport of copper ions across the oxidation products, as it follows from the model proposed at the beginning of this chapter.

Except for the initial period, this leaching reaction can be approximated as an oxidation at constant potential, the rate of which is controlled by diffusion through the reaction products. Theoretically the problem consists in calculating the thickness of the various sulphide layers as a function of time. At this point, the analogy between the first leaching stage of chalcocite and digenite and the oxidation of metals is obvious.

Theoretical model: constant current multiplelayer oxidation (Fig. 40)

The preliminary assumptions are the same as the ones stated for constant current oxidation model.

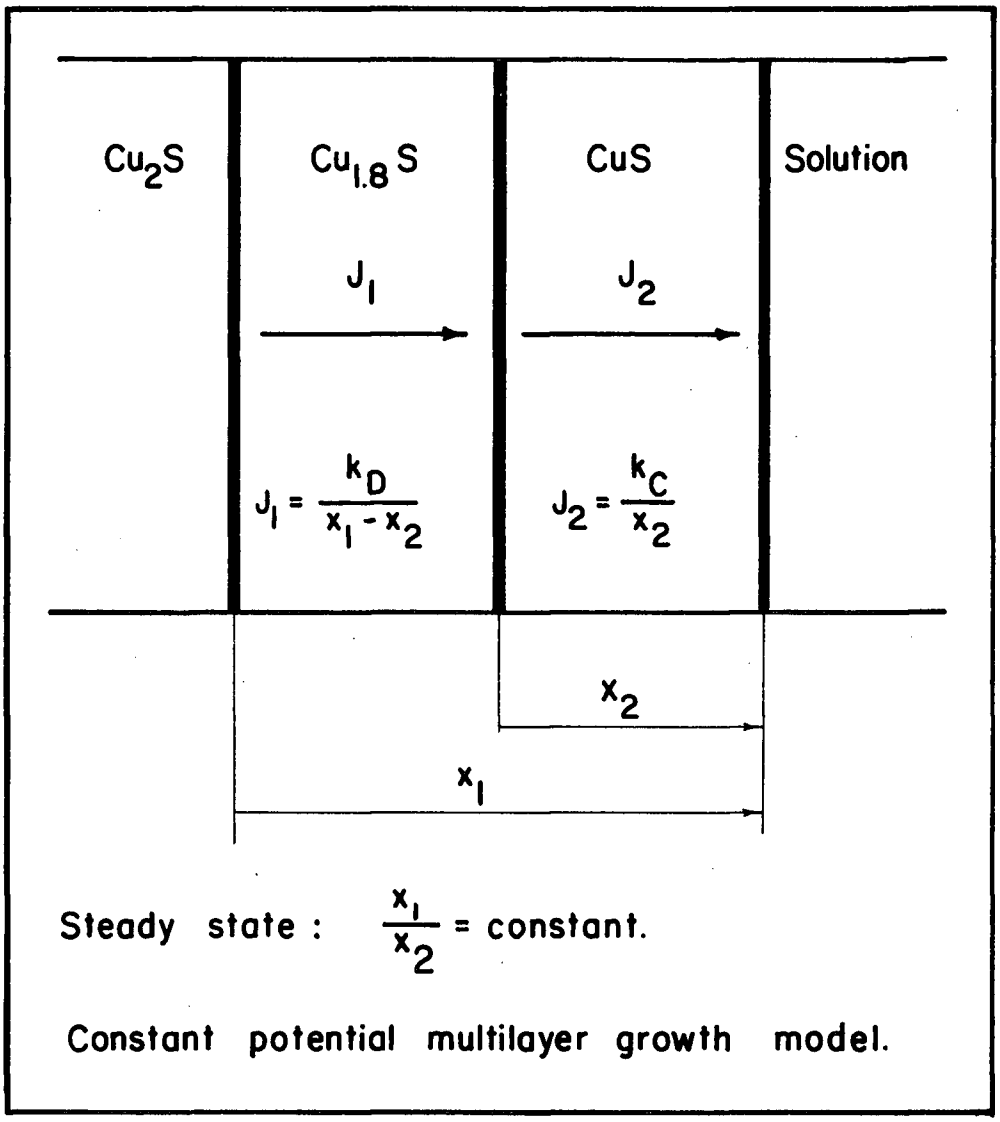

Constant potential multilayer growth model.

Figure 40

During the oxidation of digenite, the covellite grows according to the parabolic law

$$x = (2k_{C,D}\alpha)^{1/2} t^{1/2}$$

where $k_{C,D}$ is the constant of dissolution through the covellite layer defined by Eq. (4.6) and $\alpha = (\frac{M}{d})_D \frac{1}{0.78}$.

The copper flux crossing the covellite layer is inversely proportional to its thickness

$$J = \frac{k_{C,D}}{x} \quad \text{or} \quad J = (\frac{k_{C,D}}{2\alpha})^{1/2} t^{-1/2} \tag{5.10}$$

During chalcocite oxidation, the growth of the digenite (subscript 1) and covellite (subscript 2) layers will obey the two following differential equations which translate a material balance between the copper fluxes and the interface motions (Fig. 40),

$$\frac{dx_1}{dt} = \frac{k_D \alpha_1}{x_1 - x_2} \qquad \alpha_1 = (\frac{M}{d})_{Ch} \frac{1}{0.22} \tag{5.11}$$

$$\frac{dx_2}{dt} = \frac{k_{C,Ch}\alpha_2}{x_2} - \frac{k_D \alpha_2}{x_1 - x_2} \qquad \alpha_2 = (\frac{M}{d})_{CH} \frac{1}{0.78} \tag{5.12}$$

where k_D is the dissolution constant through the digenite layer as defined by Eq. (5.1). The division of equation (5.12) by equation (5.11) yields

$$\frac{dx_2}{dx_1} = \frac{k_{C,Ch}\alpha_2}{k_D \alpha_1} \frac{x_1}{x_2} - \frac{\alpha_2}{\alpha_1}(1 + \frac{k_{C,Ch}}{k_D}). \tag{5.13}$$

The most general solution of this classical, first order homogeneous differential equation is (Appendix 7).

$$\frac{1}{C} = (x_2 - u_1 x_1)^{\frac{u_1}{u_2 - u_1}} \quad (x_2 - u_2 x_1)^{\frac{u_2}{u_1 - u_2}}, \tag{5.14}$$

where C is the integration constant, and u_1 and u_2 are the roots of the second degree equation

$$u^2 + \frac{\alpha_2}{\alpha_1}\left(1 + \frac{k_{C,Ch}}{k_D}\right)u - \frac{k_{C,Ch}}{k_D}\,\frac{\alpha_2}{\alpha_1} = 0.$$

The condition that x_1 and x_2 are strictly positive for $t > 0$ and zero at $t = 0$ simplifies equation (5.14) considerably to

$$x_2 = u_1 x_1 \qquad u_1 > 0 \tag{5.15}$$

or

$$x_2 = \frac{-\frac{\alpha_2}{\alpha_1}\left(1 + \frac{k_{C,Ch}}{k_D}\right) + \left[\left(\frac{\alpha_2}{\alpha_1}\right)^2\left(1 + \frac{k_{C,Ch}}{k_D}\right)^2 + 4\,\frac{k_{C,Ch}}{k_D}\,\frac{\alpha_2}{\alpha_1}\right]^{1/2}}{2}\, x_1$$

The relationship (5.15) has already been proposed by Valensi (66,67) for metal oxidation leading to the formation of several oxide layers and controlled by diffusion through the oxidation product.

The integration of equations (5.11) and (5.12) yields

$$x_1 = \left(2\,\frac{k_D \alpha_1}{1 - u_1}\right)^{1/2} t^{1/2}, \tag{5.16}$$

$$x_2 = \left[2\left(k_{C,Ch}\alpha_2 - \frac{k_D \alpha_2}{\frac{1}{u_1} - 1}\right)\right]^{1/2} t^{1/2}. \tag{5.17}$$

Both phases grow according to a parabolic law and the ratio between the quantity of the two phases remains constant.

The flux crossing the covellite layer is inversely proportional to its thickness and equals

$$J = k_{C,Ch}\left[2\left(k_{C,Ch}\alpha_2, - \frac{k_D\alpha_2}{\frac{1}{u_1} - 1}\right)\right]^{-1/2} t^{-1/2} \qquad (5.18)$$

It follows from the calculations or from the analogy with metal oxidation that the depth of penetration of the digenite and of the covellite varies as a parabolic function of time (Eq. (5.16) and (5.17)) and that the ratio between the depth of penetration of the two phases remains constant (Eq. (5.15)).

The rate of the first leaching stage of digenite and chalcocite will be calculated from equation (5.10) and from equations (5.18) and (5.15) using the following dissolution constants: As it has already been pointed out earlier, the dissolution constant, k_C, through the covellite layer depends upon the fraction of the cross section occupied by the pores and is assumed to be proportional to it. As the covellite resulting from the oxidation of digenite and covellite theoretically contains 19.7% and 25.5% of pores, respectively, it follows that

$$k_{C,Ch} = \frac{25.5}{19.7}\ k_{C,D},$$

where $k_{C,D} = 2.35\ 10^{-9}$ mole $cm^{-1}sec^{-1}$ was derived from the experimental results reported in section (4.6.2). The value of k_D relevant to the leaching of chalcocite has already been discussed in section (5.1) (theoretical model). In the absence of other data, k_D was calculated in

the case of solid state diffusion to be 3.1 10^{-11} mole $cm^{-1}sec^{-1}$. The molar volumes $(\frac{M}{d})$ of chalcocite and digenite are 27.5 and 25.4 cm^3mole^{-1}, respectively (59). The calculated rates for times equal to 1 and 5 hours, as well as the rate averaged over this time interval,

$$\bar{J}_{\Delta t} = \int_{t_1}^{t_2} J dt, \qquad (5.19)$$

are reported in Table 7.

Table 7

Rates of the first leaching stage of massive digenite and chalcocite at 55°C in acid ferric solutions

	t (hr)	I_D mA cm^{-2}	I_{Ch} mA cm^{-2}
calculated	1	19.3	24.1
	5	8.6	10.8
	averaged, Eq. (5.19)	11.9	14.9
measured (10)		12.9	18.2

Thomas and al. (10) measured dissolution rates of rotating disks of chalcocite and digenite during the first stage of leaching in 0.1 M Fe^{3+}-0.1 M H_2SO_4 solution. Their experimental values, which did not depend upon ferric ion concentration at 500 r.p.m., are reported in Table 7. Though the plot of the observed quantity of copper dissolved

against time was slightly curved, they calculated average dissolution rates for the range of 0.5 to 2.5 g of copper dissolved, which should approximately correspond to the selected time interval.

The agreement between the two sets of values is satisfactory given the assumptions which were introduced and given the uncertainty on the measured dissolution constant ($k_{C,D}$).

From the division of equation (5.10) by equation (5.18) it follows that digenite should dissolve at 80% of the chalcocite rate* in otherwise identical conditions. In Thomas and al's experiments, the rate of dissolution of digenite ranges between 70 and 84% of the rate of chalcocite.

It can be derived from Eq. (5.15) that, in the conditions stated for these calculations, the covellite represents approximately 96% of the oxidation products.

Therefore it appears that the rate of the first stage of dissolution of massive chalcocite and digenite may be reasonably accounted for by a model corresponding to a rate controlling transport of copper ions through the oxidation products.

The second leaching stage of these sulphides, which involves the oxidation of covellite, should follow the same mechanism as this latter. A difference resides in the fact that this particular covellite already contains 20 or 25% of porosity which explains the larger dissolution rates observed in this case (4,9).

---

* This rate ratio is affected relatively little by the value chosen for k_D. In fact, a value of 78% is calculated to correspond to $k_D = 3\ 10^{-10}$ mole $cm^{-1}sec^{-1}$, the covellite then representing 74% of the oxidation products.

CHAPTER 6.

CONCLUSIONS

6.1 Electrochemical parameters of the copper sulphides

Electrochemical studies performed on copper sulphides provided some fundamental information on the Cu-S system.

1. E.m.f. measurements were conducted in the range between 40 and 80°C on the following galvanic cells,

$$\text{S.C.E. (25°C)} \mid 0.1\ \text{M}\ CuSO_4,\ 0.1\ \text{M}\ H_2SO_4 \mid Cu \quad ,$$

$$\text{S.C.E. (25°C)} \mid 0.1\ \text{M}\ CuSO_4,\ 0.1\ \text{M}\ H_2SO_4 \mid Cu_yS.$$

The copper sulphide composition was selected to produce a two phase electrode having a fixed copper activity. The potentials of the investigated electrodes with respect to S.C.E. (25°C) (Stockholm Convention) were measured to be:

$$E(Cu) = (70.45 \pm 0.33) \times 10^{-3} + (0.632 \pm 0.025) \times 10^{-3}\ (T-328) \quad V,$$

$$E(D.-C.) = (251.50 \pm 0.35) \times 10^{-3} + (0.765 \pm 0.035) \times 10^{-3} (T-328) \quad V,$$

$$E(D.-Dj.) = (242.20 \pm 0.45) \times 10^{-3} + (0.62 \pm 0.060) \times 10^{-3} (T-343) \quad V.$$

The variation of the chemical potential of copper and sulphur across the Cu-S system could be assessed from the above measurements and from existing thermodynamic data. Consequently, the standard free enthalpy of formation of digenite and djurleite were calculated in the investigated range of temperature with the noted precision, as follows:

$$\Delta F^\circ(Cu_{1.765}S) = (-18{,}140 \pm 520) - (4.9 \pm 2.5)(T-328) \quad \text{cal mole}^{-1},$$

$$\Delta F^\circ(Cu_{1.965}S) = (-19{,}700 \pm 550) - (5.5 \pm 3.1)(T-343) \quad \text{cal mole}^{-1}.$$

The variation of the standard free enthalpy of formation of digenite was estimated as a function of composition ($1.765 < y < 1.83$):

$$\Delta F^\circ(Cu_yS) = (-18{,}140 \pm 520) - (4.9 \pm 2.5)(T-328) + (y - 1.765)[(-7{,}910 \pm 40) - (3.2 \pm 2.5)(T-328)] \quad \text{cal mole}^{-1}.$$

The major component (approximately 90%) of the final error on the above thermodynamic values originated from the error on the existing data for CuS.

2. Copper sulphides were grown on a copper anode from an acidic solution saturated with H_2S at constant current. The thickening of the copper sulphide film, at low electric field strength, was accounted for by electrolytic transport in the scale and a theoretical model for the scale growth was proposed for steady-state conditions. The diffusion coefficient of cuprous ions in chalcocite and digenite was calculated in the temperature range between 30 and 73°C from the slope of the electrode potential versus time relationship. The diffusion coefficient of cuprous ions in low chalcocite was found to be

$$D_{Cu^+} = 8.1 \times 10^{-3} \exp\left(-\frac{5870}{T}\right) \quad \text{cm}^2\text{sec}^{-1},$$

and in low digenite

$$D_{Cu^+} = 3.6 \times 10^{-2} \exp\left(-\frac{6100}{T}\right) \quad \text{cm}^2\text{sec}^{-1}.$$

The phase boundary reactions did not appear to be too resistive to interfere with these measurements.

3. Potential-time curves were recorded during the galvanostatic polarization of rotating disk anodes of digenite and covellite in 0.1 M $CuSO_4$-0.1 M H_2SO_4 solutions at 55°C, and were analysed.

Digenite anodes always underwent a potential discontinuity in a transition time, τ, such that the relationship between the current density and the transition time was

$$I^2\tau = 2.5 \qquad A^2cm^{-4}sec.$$

It was proposed that, at the transition, the rate of the overall electrode reaction, $Cu_{1.78}S \rightarrow CuS + 1.56e + 0.78Cu^{++}$, was limited by the transport of the copper ions released by the oxidation reaction, though the porous covellite layer; the main transport component was likely diffusion in the solution filling the shrinkage pores of the covellite. The dissolution constant, k_C, through the covellite layer has been defined ($J = \frac{k_C}{\ell_C}$) and calculated from the experimental data.

The interface reaction seemed to introduce little resistance in the overall oxidation process.

The anodic reaction on covellite, $CuS \rightarrow Cu^{++} + S^\circ + 2e$, appeared to be relatively resistive. During oxidation, covellite exhibited a limiting current of dissolution similarly to diffusion controlled reactions.

The apparent current density-potential curve has been established for the steady-state which occurred after long dissolution times of covellite.

6.2 Application to the electrolysis of matte anodes and to the leaching of copper sulphides

The discussion of the data existing in the literature on the constant current electrolysis of chalcocite anodes, supplemented by the information obtained in the present work, suggests that the rate of dissolution of chalcocite, as is the case of digenite, is limited by the diffusion of copper ions in the higher sulphide layer.

Leaching rates of covellite in acidic ferric solutions are estimated from the data established in the preceeding parts of this work on the basis of an electrochemical mechanism of oxidation, analogous to metal corrosion. This model appears adequate to explain the behaviour of covellite in the presence of an aqueous ferric oxidant, as observed by other researchers.

The rates of the first leaching step of chalcocite and digenite by an aqueous oxidant are calculated on the basis of a constant potential oxidation model, where the rate of the process is controlled by the transport of copper ions through the oxidation products. The results of these calculations are found to be in agreement with the relevant experimental data existing in the literature.

APPENDIX 1.

USE OF A GALVANIC CELL TO MEASURE THE IONIC CONDUCTIVITY OF A COPPER SULPHIDE MEMBRANE

a. Measurement method

The application of an electric field to an initially homogeneous copper sulphide gives rise to activity gradients and for larger fields, when the activity gradients tend to exceed the stability limits, to decomposition. The type of current (ionic, electronic or mixed) depends on the contacts or electrodes.

In a cell, where the copper sulphide is inserted between two ionic conductors, e.g.,

$$Cu \mid CuSO_4 \text{ aq} \mid Cu_yS \mid CuSO_4 \text{ aq.} \mid Cu \qquad \text{(AI)}$$

the application of a d.c. potential forces an ionic current through the copper sulphide. However the current is not exclusively ionic since copper is in the cupric form in solution and may exist in the cuprous form in the solid.

The flux of copper atoms, flowing through the copper sulphide depends on the total current flowing through the cell.

$$\frac{I}{2F} = J_{Cu}, \qquad \text{(A1.1)}$$

which is related to the Onsager coefficient through Eq. (3.7)

$$J_{Cu} = -M_{Cu} \frac{\partial \mu_{Cu}}{\partial x}. \qquad (3.7)$$

Integration of Eq. (3.7) over the thickness of the sulphide tablet yields

$$J_{Cu} = 2F \frac{\bar{M}_{Cu}}{\ell} \Delta E \qquad (A1.2)$$

where $\bar{M}_{Cu}$ is the average value of the Onsager coefficient in the activity gradient, and $\Delta\mu_{Cu} = -2F\ \Delta E$ represents the drop of electrochemical potential across the sulphide.

It appears from Eq. A1.1 and A1.2 that the average Onsager coefficient can be calculated from the experimental current-potential relations. The conversion of the Onsager coefficient in ionic conductivity or diffusion coefficient (Eq. 3.8) requires the determination of the charge of the diffusing species. The Onsager coefficient may depend upon the potential drop across the sulphide. Since the thermodynamic potentials are not fixed at the copper sulphide-electrolyte interface, the results may depend on the sample.

b. Experimental

Several designs and constructions of cell were attempted:

1. A first type of cell was made of two teflon cylinders pressed against a copper sulphide membrane by a vise. The teflon was creeping under the compression stress and the cell leaking.
2. A second type of cell was made of two pyrex tubes cemented to the copper sulphide membrane with epoxy resin. The leads of the two copper electrodes were sealed in the cell with epoxy resin and the cell was evacuated and sealed after having been filled wih the solution. The manufacture of these cells was extremely delicate and the thin epoxy joint was not standing the solution during more than one or two days.

3. A third type of cell, which was made of teflon, is pictured on Fig. 41. The experiments were performed with this last cell, which was open to the atmosphere.

The cell was filled with a boiled solution (0.5 M $CuSO_4$, 0.5 M H_2SO_4), deaerated under vacuum and kept under a helium atmosphere. This treatment was intended to prevent the evolution of bubbles, which were dragging the solution out of the cell during the course of the experiments. In spite of this precaution many experiments were discontinued by bubbling. This gas evolution however could not be attributed to an electrode reaction.

Each half cell was divided by a fritted polyethylene disk into an anodic and cathodic compartment (see section 4.5).

The cell was enclosed in a pyrex tube closed at both ends with metallic covers. The electrical leads were cased in rubber tubings fitted to one of the covers. A helium atmosphere was maintained in the tube. The above assembly was immersed in a thermostat-regulated ethylene glycol bath.

An electroscan,Beckman 30, was used as a constant current source. The current was measured by a Keithley, model 153, microvoltammeter. The potential drop across the two terminal copper electrodes was measured with a Keithley, model 630, electrometer.

The copper electrodes were made of 0.99999 pure copper plate. The covellite membrane was synthesized and shaped in the way described in section 4.5.

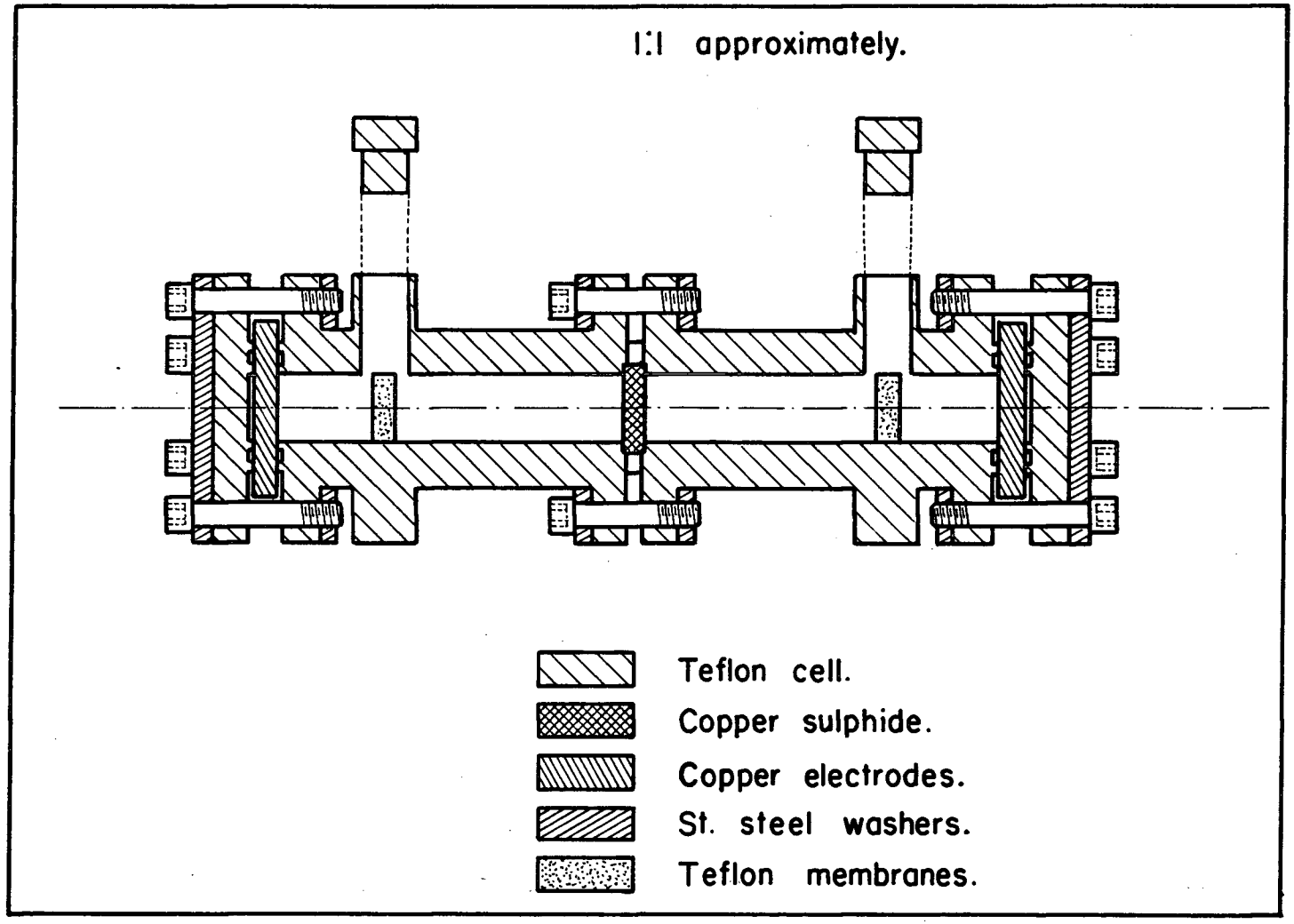

Figure 41. Design of a galvanic cell to measure the ionic conductivity of a copper sulphide membrane.

c. Results and discussion

The cell was first calibrated with a copper membrane. The potential drop between the two terminal copper electrodes of the cell

$$Cu \mid CuSO_4, H_2SO_4 \text{ aq.} \mid Cu \mid CuSO_4, H_2SO_4 \text{ aq.} \mid Cu$$

remained smaller than 1 mV up to currents of 10 μA. Consequently, the difference of electrochemical potential across the sulphide membrane could be directly measured by the potential drop occurring in cell AI for currents smaller than 10 μA. The data reported for digenite in Chapters 2 and 3 indicate that this range of current could be adequate.

At 55°C, the maximum potential difference that can be imposed on digenite is 20 mV and its cuprous conductivity is $7.5\ 10^{-5}\ \Omega^{-1}cm^{-1}$. Eq. (A1.2) allows the calculation of the maximum current that can be forced through a digenite disk, 3 mm thick by 9.55 mm in diameter.

$$i = \frac{4 \times 7.5\ 10^{-5} \times 2\ 10^{-2}}{0.3} \simeq 14\ \mu A$$

Any current higher than this value would cause the electrolysis of the sulphide. The maximum potential difference that can exist across a covellite membrane is approximately 75 μV, but its ionic conductivity may be expected to be smaller than that of digenite. So, in first approximation, the same range of current can be used for this experiment.

A certain quantity of coulombs must be passed through the specimen in order to establish the copper activity gradient necessary to support the steady-state flow of copper. If, in first approximation, a

linear concentration gradient is assumed across the membrane, the time necessary to establish the steady-state in a digenite membrane, in the above conditions, can be estimated. The initial composition of digenite is assumed to be $Cu_{1.7825}S$, its stability limits being $Cu_{1.8}S$ and $Cu_{1.765}S$ at 55°C. A quantity of copper equal to $\Delta C_{Cu} \frac{S\ell}{2} (\frac{d}{M})_{Cu_yS}$ is necessary to shape the concentration gradient across the disk,

$$i\ t = \frac{(1.8-1.7825) \times 0.72 \times 0.3}{2 \times 25.4} \quad 2\ 10^5$$

$$t \simeq 12 \text{ days.}$$

By that time, the cell, which contains only about 4 cm^3 of solution, will be dryed off by evaporation. Since covellite is reported to be stoichiometric, the time necessary to establish the steady-state flow should be considerably smaller.

Measurements made on covellite membrane, approximately 2 mm thick, at current below 10 μA were not reproducible either in time on the same sample, or on different samples. The potential drops measured in identical conditions could be as different as 1 to 10. The residual porosity of the disk could short-circuit the membrane and account for the low values. The very high potential drop observed immediately after the switching of the current, which was decaying, thereafter, seemed to indicate that sulphur was probably formed at the anodic side of the covellite. In fact, the synthetic covellite is very close to sulphur saturation, and current flow should cause the sulphur formation at the anode during the transient period. As the covellite-sulphur electrode appears irreversible (Section 4.7), the sulphur formation would remove all significance to the potential measurements.

APPENDIX 2.

DIVISION OF THE TOTAL OVERVOLTAGE IN THE VARIOUS COMPONENTS

The various overvoltages are clearly defined when there is only one rate-controlling step in the electrode process but the definitions are still controversial when several resistances arise concurrently during the reaction (50). If either concentration overvoltage or crystallization overvoltage occurs alone, the electrode potential during current flow can be calculated with the help of the Nernst's equation for equilibrium potentials, since the charge-transfer reaction is in equilibrium. In the mixed control case, this equation is, strictly speaking, no longer applicable.

K.J. Vetter (49) gave a definition for the division of the measured overvoltage in its diffusion, reaction, crystallization and charge-transfer components, which is based on the requirement that upon the disappearance of all overvoltage types but one, the residual overvoltage must agree with the definition for the single remaining overvoltage type.

The determining quantity for charge-transfer control is the exchange current density I_o; when I_o becomes infinitely great, charge-transfer rate-control no longer exists, so that for $I_o \to \infty$, $\eta_t \to 0$. The reaction overvoltage will vanish if the determining exchange reaction rate $v_{0,r} \to \infty$, as will the diffusion component for $D \to \infty$. The crystallization component will disappear if the crystallization is infinitely rapid ($v_{o,c} \to \infty$). The order in which these limits are taken is important for precise overvoltage definitions. Vetter proposed the following sequence,

$I_o \to \infty$	$\eta \to \eta_r + \eta_D + \eta_C$	$\Delta\eta = \eta_t$	
$v_{o,r} \to \infty$	$\eta_r + \eta_D + \eta_C \to \eta_D + \eta_C$	$\Delta\eta = \eta_r$	
$D \to \infty$	$\eta_D + \eta_C \to \eta_C$	$\Delta\eta = \eta_D$	(A2.1)
$v_{o,C} \to \infty$	$\eta_r + \eta_D + \eta_C \to \eta_D + \eta_r$	$\Delta\eta = \eta_C$	
	$\eta_D + \eta_C \to \eta_D$		
	$\eta_C \to 0$		

The charge-transfer component, because it depends upon the concentrations at the electrode surface, is influenced by the existence of the other overvoltage. Therefore the limit $I_o \to \infty$ should be carried out first.

On the basis of this definition, the current-potential relationship (50) for simultaneous occurrence of charge-transfer and concentration overvoltage will be treated.

$$I = I_o\left[\prod_i \left(\frac{C_i}{\bar{C}_i}\right)^{z_{r,i}} \exp\frac{\alpha z F}{RT}\eta - \prod_i\left(\frac{C_i}{\bar{C}_i}\right)^{z_{o,i}} \exp -\frac{(1-\alpha)zF}{RT}\eta\right] \quad \text{(A2.2)}$$

C_i and $\bar{C}_i$ are the concentrations of species i at the electrode surface and in the bulk of the solution, respectively. I_o is the exchange current density, $z_{o,i}$ and $z_{r,i}$ the electrochemical reaction orders, z the charge transfer valence, and α the charge transfer coefficient.

$$I_o \to \infty, \quad \prod_i\left(\frac{C_i}{\bar{C}_i}\right)^{z_{r,i}} \exp\frac{\alpha z F}{RT}\eta = \pi_i\left(\frac{C_i}{\bar{C}_i}\right)^{z_{o,i}} \exp -\frac{(1-\alpha)zF}{RT}\eta$$

$$\exp -\frac{zF}{RT}\eta = \pi_i\left(\frac{C_i}{\bar{C}_i}\right)^{z_{r,i}-z_{o,i}}$$

with $z_{o,i} - z_{r,i} = \nu_i \frac{z}{n}$ (49)

where ν_i is the stoichiometric coefficient of the reaction and, n the electrode reaction valence change.

$$\eta_D = \frac{RT}{nF} \ln\left(\frac{C_i}{\bar{C}_i}\right)^{\nu_1}$$

This equation coincides with the Nernst equation for a concentration cell.*

---

* This is in contradiction with the theory of concentration overvoltage proposed recently by M. Enyo and T. Yokoyama (50) who used equation (A2.2) to demonstrate their point, but took the limits (A2.1) in the inverted sequence.

APPENDIX 3.

ESTIMATION OF THE POTENTIAL DROP IN A DIFFUSION LAYER OF A PARTIALLY IONIZED ELECTROLYTE

The set of equations (4.9) describing the diffusion in a $CuSO_4$ electrolyte are:

$$J_1 = -D_1 \frac{\partial C_1}{\partial x} \tag{A3.1}$$

$$J_2 = -D_2 \frac{\partial C_2}{\partial x} - \frac{2F}{RT} D_2 C_2 \frac{\partial \phi}{\partial x} \tag{A3.2}$$

$$J_3 = -D_3 \frac{\partial C_3}{\partial x} + \frac{2F}{RT} D_3 C_3 \frac{\partial \phi}{\partial x} \tag{A3.3}$$

The subscripts 1, 2, 3 stand for $CuSO_4$, Cu^{++}, SO_4^{--} respectively.

The electroneutrality condition is $C_2 = C_3$

The flow requirement is $J_1 = -J_3$

The chemical equilibrium statement is $C_1 = KC_2^2$

Addition of Eq. (A3.1) and Eq. (A3.3) yields after rearrangement of the variables

$$2 \frac{D_1}{D_3} K \frac{\partial C_2}{\partial x} + \frac{1}{C_2} \frac{\partial C_2}{\partial x} = \frac{2F}{RT} \frac{\partial \phi}{\partial x} \tag{A3.4}$$

For steady-state diffusion across a boundary layer, of defined thickness, integration of Eq.(A3.4) with respect to the thickness of the layer yields

$$\Delta\phi = \frac{RT}{F} \frac{D_1}{D_3} K (C_2 - \bar{C}_2) + \frac{RT}{2F} \ln \frac{C_2}{\bar{C}_2} \tag{A3.5}$$

When the saturation in a cupric salt is reached at the electrode-electrolyte interface, $C_1 + C_2 = C_S$, and C_2 can be calculated from $K C_2^2 + C_2 - C_S = 0$.

The potential drop in the diffusion layer is estimated from Eq. (A3.5) taking the following values for the physical parameters.

- C_s = 2.2 mole $^{-1}$ corresponds to the saturation of the solution with $CuSO_4 \cdot 5H_2O$ at 55°C (60,63).

- $D_1 = D_2$ this assumption has been proposed in section (4.6.2)

Since the transport number of Cu^{++} has been measured to be 0.36 in 0.1 M $CuSO_4$ at 25°C (75) and should not be temperature dependent, it can be assumed that $\frac{D_1}{D_3} = \frac{0.36}{0.74} = 0.485$.

- The complexation constant, K, has been estimated to be 127 at ambient temperature by Nasanen and Klaile (61) but the appropriate value of this constant in concentrated solutions at 55°C is not known. In these conditions, the potential drop amounts to 76 mV, 185 mV and 249 mV for values of the complexation constant of 10, 100 and 200 respectively.

APPENDIX 4.

CALCULATION OF THE DIFFUSION OVERVOLTAGE AT A ROTATING DISK ELECTRODE.

The concentration overvoltage arising at a R.D.E. from limited diffusion rate across the electrode boundary layer can be calculated from Eq. (4.1) and the Nernst equation.

Hsueh and Newman (58) measured the limiting current density for the deposition of copper from a 0.1 M $CuSO_4$ solution as a function of the angular velocity of the rotating disk electrode.

$$I_D = 72 \text{ mA cm}^{-2} \qquad \text{at } 25°C \text{ and } 250 \text{ r.p.m.}$$

Since the transport number of the cupric ions in a 0.1 M $CuSO_4$ solution, is 0.36 (75), it is possible to extrapolate from this measurement, the corresponding limiting current density in the presence of an excess of indifferent electrolyte. This case is hypothetical since the presence of an excess of indifferent electrolyte would modify the physical properties of the solution.

$$I_D = 46 \text{ mA cm}^{-2} \qquad \text{at } 25°C \text{ and } 250 \text{ r.p.m.}$$

A 0.1 M $CuSO_4$-0.1 M H_2SO_4 solution is intermediate between these two cases; its physical properties are very close to a 0.1 M $CuSO_4$ solution (62). The limiting diffusion current density derived from

Marathe's and Newman's experiments in a 0.1 M $CuSO_4$-0.1 M H_2SO_4 solution is (56)

$$I_D = 59 \text{ mA cm}^{-2} \qquad \text{at } 25°C \text{ and } 250 \text{ r.p.m.}$$

It follows from Eq. (4.1) that

$$\frac{C}{\bar{C}} = 1 - \frac{I}{I_D} \qquad \begin{matrix} I > 0 \text{ at an anode} \\ I < 0 \text{ at a cathode} \end{matrix}$$

The diffusion overvoltage will be calculated at 55°C in the case of a 0.1 M $CuSO_4$ solution and in the hypothetical case of 0.1 M Cu^{++} in the presence of an excess of indifferent electrolyte.

Since the limiting current density is given by Eq. (4.1)

$$I_D = 0.62\, D^{2/3}\, \nu^{-1/6}\, \omega^{1/2}\, 2F\, \bar{C}$$

it can be extrapolated to 55°C, D and ν being the only temperature dependent parameters.

- $D = A \frac{T}{\mu}$ A is a constant and μ is the viscosity of water (76)

$$D_{55} = D_{25} \frac{328}{298} \frac{\mu_{25}}{\mu_{55}}$$

- $\nu = \frac{\mu}{d}$

$$\nu_{55} = \nu_{25} \frac{\mu_{55}}{\mu_{25}} \frac{d_{25}}{d_{55}}$$

The viscosity and density of water are tabulated in chemical handbooks (77).

$$D_{55} = 1.945\ D_{25} \qquad \nu_{55} = 0.573\ \nu_{25}$$

$$I_D(55) = 1.71\ I_D(25)$$

	Binary electrolyte: $I_D = 123$ mA cm^{-2}		Excess of indifferent electrolyte $I_D = 79$ mA cm^{-2}	
I (mA cm^{-2})	$1 + \frac{I}{I_D}$	η_D (mV)	$1 + \frac{I}{I_D}$	η_D (mV)
75.3	1.61	6.7	1.95	9.4
56.5	1.46	5.3	1.71	7.6
37.7	1.31	3.8	1.48	5.5
18.8	1.15	2.0	1.24	3.0
15.1	1.13	1.7	1.19	2.5
11.3	1.09	1.2	1.14	1.9
7.5	1.07	1.0	1.09	1.2

The average value of the diffusion overvoltage over the two extreme cases was selected for use in other calculations in this thesis. Though such a calculation is only an approximation, the magnitude of the diffusion overvoltage remains small and is likely smaller than the experimental error on the potential.

A resistance polarization is generally associated with a concentration gradient in solution: this term which is zero in the presence of excess of indifferent electrolyte equals the diffusion overvoltage in a binary electrolyte. In the present case, however, it has been shown in Appendix 3 that this value, calculated for a dissociated electrolyte, was not appropriate. The ohmic drop calculated with the

resistivity of the bulk solution is already taken into account in the term, η_{Ω}. The small concentration variation in the boundary layer is unlikely to modify much of the resistivity of the solution, and the remaining part of the resistance polarization is neglected.

APPENDIX 5.

INTEGRATION OF EQUATION (5.3)

$$\frac{d(x_1-x_2)}{dt} = \frac{k_D(\alpha_1+\alpha_2)}{x_1-x_2} - J\alpha_2 \qquad (5.3)$$

Let us set $x_1-x_2 = y$

$$k_D(\alpha_1+\alpha_2) = A$$

$$J\alpha_2 = B$$

Eq. (5.3) can then be written

$$y\, dy = (A-By)\, dt$$

which can be directly integrated

$$\int \frac{y}{(A-By)}\, dy = t + C$$

Let us set $A - By = z$

$$-B\, dy = dz$$

It follows

$$\frac{1}{B^2} \int \frac{z-A}{z}\, dz = t + C$$

or

$$\frac{1}{B^2} (z-A \ln z) = t + C$$

Replacing z by its value yields

$$\frac{1}{B^2}\,[A-B(x_1-x_2)] - \frac{A}{B^2}\,\ln\,[A-B(x_1-x_2)] = t + C$$

The solution (5.5) can be written, after taking into account the initial condition $x_1-x_2 = x_D$ at $t = t_D$

$$-\frac{x_1-x_2-x_D}{J\alpha_2} - \frac{k_D(\alpha_1+\alpha_2)}{J^2\alpha_2^2}\,\ln\frac{k_D(\alpha_1+\alpha_2) - J\alpha_2(x_1-x_2)}{k_D(\alpha_1+\alpha_2) - J\alpha_2\,x_D} = t - t_D$$

APPENDIX 6.

THE Fe^{3+}/Fe^{2+} ELECTRODE

The current density-potential relationship is expressed in the case of the Fe^{3+}/Fe^{2+} electrode by

$$I = I_o[(1 - \frac{I}{I_{D,2}}) \exp \frac{\alpha F}{RT} \eta - (1 - \frac{I}{I_{D,3}}) \exp - \frac{(1-\alpha)F}{RT} \eta] \quad (49)$$

This equation translates the effect of charge-transfer and diffusion resistances.

Parameters of the charge-transfer process (measured at a platinum electrode)

I_o, the exchange current density was determined to satisfy the relationship

$$I_o = k_o[Fe^{2+}] \exp \frac{\alpha F}{RT} E_{eq.} = k_o[Fe^{3+}] \exp - \frac{(1-\alpha)F}{RT} E_{eq.} \quad (49,68,69)$$

If the selected reference is the standard Fe^{3+}/Fe^{2+} electrode itself ($\varepsilon_o = 0$), the expression of I_o is simplified to

$$I_o = k_o[Fe^{3+}]^{\alpha} [Fe^{2+}]^{1-\alpha}$$

The following experimental data are available:

$$\alpha = 0.58 \quad (68)$$

$$k_o(25°C) = 300 \quad mA\ cm^{-2} mole^{-1}\ l \quad (68)$$

$$\frac{\partial \ln I_o}{\partial(\frac{1}{T})} = - \frac{\Delta H}{R} \qquad \Delta H = 7{,}500 \text{ cal mole}^{-1} \qquad (70,71)$$

Parameters of the diffusion process: case of a rotating disk electrode (section 4.2).

In the presence of an excess of indifferent electrolyte, the limiting diffusion current densities of the ferrous and ferric ions towards a R.D.E. are given by (Eq. 4.1)

$$I_{D,2} = 0.62\ D_2^{2/3}\ \nu^{-1/6}\ \omega^{1/2}\ F\ [Fe^{2+}]$$

$$I_{D,3} = 0.62\ D_3^{2/3}\ \nu^{-1/6}\ \omega^{1/2}\ F\ [Fe^{3+}]$$

The diffusion coefficients of ferrous and ferric ions (D_2, D_3, respectively) in sulphuric solutions have been measured to be

$$D_2(25°C) = 5.4\ 10^{-6}\ cm^2 sec^{-1} \qquad (72)$$

$$D_3(25°C) = 4.4\ 10^{-6}\ cm^2 sec^{-1} \qquad (72)$$

The other parameters were chosen to fit the conditions of Thomas' and Ingraham's leaching experiments (5).

$$\omega = \frac{2\pi \times 500}{60} \text{ radian sec}^{-1}$$

The kinematic viscosity of the solution was approximated by the kinematic viscosity of a 0.1 M H_2SO_4 solution.

$$\nu(25°C) = 0.99\ 10^{-2} \quad cm^2 sec^{-1} \qquad (62)$$

Temperature corrections for the diffusion coefficients and kinematic viscosity were done according to the method described in Appendix 4.

Equilibrium potential of the Fe^{3+}/Fe^{2+} couple

The standard electrode potential of the Fe^{3+}/Fe^{2+} couple is at 25°C (Stockholm Convention)

$$\varepsilon_o\ (25°C) = 771\ mV \qquad (2)$$

or if the S.C.E. (25°C) is chosen as reference

$$\varepsilon_o\ (25°C) = 529.5\ mV$$

The electrode potential of the normal Fe^{3+}/Fe^{2+} couple at 55°C with respect to the S.C.E. (25°C) can then be calculated with the help of the thermal temperature coefficient of the electrode,

$$\left(\frac{d\varepsilon_o}{dt}\right)_{th} = +2.059\ mV\ (°C)^{-1} \qquad (32),$$

$$\varepsilon_o\ [S.C.E.\ (25°C)] = 592\ mV \text{ at } 55°C$$

The actual electrode potential still depends upon the ionic strength of the solution (2,73,74) and is approximately 30 mV lower than the theoretical value in solution of ionic strength larger than 0.3 (73).

A correction taking into account the difference in activity coefficients of the ferric and ferrous ions, resulting from the concentration difference, was not made because of the lack of data.

APPENDIX 7.

INTEGRATION OF EQUATION (5.13)

$$\frac{dx_2}{dx_1} = \frac{k_{C,Ch}\ \alpha_2}{k_D\ \alpha_1}\ \frac{x_1}{x_2} - \frac{\alpha_2}{\alpha_1}\ (1 + \frac{k_{C,Ch}}{k_D}) \qquad (5.13)$$

Let us set

$$A = \frac{k_{C,Ch}}{k_D}\ \frac{\alpha_2}{\alpha_1}$$

$$B = \frac{\alpha_2}{\alpha_1}\ (1 + \frac{k_{C,Ch}}{k_D})$$

$$\frac{x_2}{x_1} = u$$

It follows that

$$dx_2 = u\,dx_1 + x_1\,du$$

or

$$\frac{dx_2}{dx_1} = x_1\ \frac{du}{dx_1} + u$$

$$\frac{du}{dx_1} = \frac{Au^{-1} - B - u}{x_1}$$

Integration of the former equation yields

$$x = C\ \exp.\ \int \frac{du}{Au^{-1} - B - u} \qquad (A7.1)$$

$$\int \frac{du}{Au^{-1} - B - u} = -\int \frac{u\,du}{u^2 + Bu - A}$$

or after reduction in simple fractions

$$- \int \frac{\frac{u_1}{u_1-u_2}}{u-u_1} \, du \quad - \int \frac{\frac{u_2}{u_2-u_1}}{u-u_2} \, du \tag{A7.2}$$

where u_1 and u_2 are the roots of the second degree equation

$$u^2 + Bu - A = 0$$

It follows after integration of Eq. (A7.2)

$$\frac{u_1}{u_2-u_1} \ln (u-u_1) + \frac{u_2}{u_1-u_2} \ln (u-u_2) \tag{A7.3}$$

and replacement of Eq. (A7.3) in Eq. (A7.1)

$$x = C(u-u_1)^{\frac{u_1}{u_2-u_1}} (u-u_2)^{\frac{u_2}{u_1-u_2}}$$

Replacement of u by $\frac{x_2}{x_1}$ yields

$$\frac{1}{C} = (x_2-u_1x_1)^{\frac{u_1}{u_2-u_1}} (x_2-u_2x_1)^{\frac{u_2}{u_1-u_2}} \tag{5.14}$$

which is the proposed solution, Eq. (5.14).

REFERENCES

1. J.T. Woodcock, Proceedings the Aus. I.M.M. 198, 47 (1961).
2. W.M. Latimer, The oxidation states of the elements and their potential in aqueous solutions, Prentice-Hall, Inc., N.Y. (1952).
3. F. Loewen, M.A.Sc. thesis, University of British Columbia (1967).
4. J. Sullivan, U.S. Bur. Mines Tech. Paper 487 (1930).
5. G. Thomas, T.R. Ingraham, Canadian Met. Quarterly, 6, 153 (1967).
6. K.J. Jackson, J.D.H. Strickland, Trans. Met. Soc. A.I.M.E. 212, 373 (1958).
7. I.H. Warren, Aust. J. Appl. Sci., 9, 36 (1956).
8. J. Dahms, J. Gerlach, F. Pawlek, Erzmetall 20, 203 (1967).
9. J. Sullivan, U.S. Bur. Mines Tech. Paper 473 (1930).
10. G. Thomas, T.R. Ingraham, R.J.C. MacDonald, Can. Met. Quarterly, 6, 281 (1967).
11. E. Roseboom Jr., Econ. Geol. 61(4), 641 (1966).
12. P. Cavalloti, G. Salvago, Electrochim. Metal. IV(3), 181 (1969).
13. J.A. King, Ph.D. thesis, University of London (1966).
14. A.R. Burkin, Min. Sci. Engng. 1, 4 (1969).
15. U. Kuxmann, H. Biallass, Erzmetall 22, 53 (1969).
16. L.S. Renzoni, R.C. McQuire, W.V. Barker, J. of Metals 10, 414 (1958).
17. Symposium on the Thompson operation, The Canadian Mining and Metallurgical Bulletin 57, 1181 (1964).
18. A.G. Losharev, A.F. Vozinov, J. of applied Chemistry U.S.S.R. 26, 49 (1953).

19. S. Venkatachalam, R. Mallikarjunan, Inst. Min. Met. Trans. section C 77, C45 (1968).

20. F. Habashi, N. Torres-Acuna, Trans. Met. Soc. A.I.M.E. 242, 780 (1968).

21. J.H. Schloen, S.S. Forbes, Industry report on modern tank house practices, Extractive metallurgy of copper, nickel and cobalt, edited by P. Queneau, Interscience Publishers (1961).

22. E. Frenay, L'élaboration des métaux non ferreux à partir de leurs minerais, Université de Liège (1961).

23. L. Eisenmann, Ann. Phys. 10, 129 (1952).

24. E. Hihara, J. Phys. Soc. Japan 6, 422 (1951).

25. T. Kamigaishi, J. Sci. HIroshima Univ. A16, 325 (1952).

26. O. Kubaschewsky, E. Evans, C. Alcock, Metallurgical thermochemistry, Pergamon Press (1967).

27. H. Majima, E. Peters, Proceedings of the 8th International Mineral Processing Congress, Leningrad, Vol. 2, p. 6, June 1969.

28. M.J. Fraser, M.A.Sc. thesis, University of British Columbia (1965).

29. M. Sato, Economic Geology, 55, 1202 (1960).

30. P. Ruetschi, R.F. Amlie, J. of the Electrochemical Society, 112, 665 (1965).

31. R. Bacon, R. Fanelli, Ind. and Eng. Chemistry 34, 1043 (1942).

32. A. de Bethune, T. Licht, N. Swendeman, J. Electrochem. Soc. 106, 616 (1959).

33. S. Djurle, Acta Chem. Scand. 12, 1415 (1958).

34. H. von Wartenberg, Z. physikal. Chem. 67, 446 (1909).

35. F. Weibke, O. Kubaschewsky, Therchemie der Legierungen, Springer-Verlag, (1943).

36. C.T. Anderson, J. Am. Chem. Soc. 54, 107 (1932).

37. K.K. Kelley, U.S. Bur. Mines Bulletin 584 (1960); U.S. Bur. Mines bulletin 592 (1961).

38. A. Dumon, A. Casalot, E. Poquet, S. Gromb, C.R. Acad. Sc. (Paris) série B, 269 (17), 835 (1969).

39. F. Richardson, J. Antill, Trans. Faraday Soc. 51, 22 (1955).

40. A. Brooks, J. Am. Chem. Soc. 74, 2464 (1953).

41. J.B. Wagner, C. Wagner, J. Electrochem. Soc. 104, 509 (1957).

42. W. Jost, Diffusion in solids, liquids, gases, Academic Press, Inc., N.Y. (1960).

43. J. Mikulski, S. Mrowec, I. Stronski, T. Werber, Z. phys. Chem. (Frankfurt) N.F. 22, 20 (1959).

44. V. Wehefritz, Z. phys. Chem. (Frankfurt) N.F. 26, 359 (1960).

45. D.A. Vermilyea, Anodic films, Advances in Electrochemistry and Electrochemical Engineering, P. Delahay and C.W. Tobias editors, Interscience Publishers, N.Y. (1963).

46. C. Wagner, J. Chem. Phys. 21, 1819 (1953).

47. F.A. Kroger, The Chemistry of imperfect crystals, North Holland Publishing Co. (1964).

48. D.M. Barrer, Trans Faraday Soc. 37, 590 (1941); Trans Faraday Soc. 38, 78 (1942).

49. K.J. Vetter, Electrochemical Kinetics, Theoretical and experimental aspects, Academic Press, N.Y. (1967).

50. M. Enyo, T. Yokoyama, Electrochimica Acta 15, 183 (1970).

51. V. Levich, Physicochemical hydrodynamics, Prentice Hall, Englewood Cliffs, New Jersey (1962).

52. A.C. Riddiford, The rotating disk system, Advances in electrochemistry and electrochemical engineering (Vol 4), Delahay and Tobias editors, Interscience Publishers, N.Y. (1963).

53. D.P. Gregory, A.C. Riddiford, J. Chem. Soc. 3756 (1956).

54. J. Newman, L. Hsueh, Electrochimica Acta 12, 417 (1967).

55. J. Newman, J. Electrochem. Soc. 113, 1235 (1966).

56. V. Marathe, J. Newman, J. Electrochem. Soc. 116, 1704 (1969).

57. J. Newman, J. Electrochem. Soc. 113, 501 (1966).

58. L. Hsueh, J. Newman, Electrochimica Acta 12, 429 (1967).

59. A.S.T.M. X-ray diffraction data file.

60. A. Seidell, Solubilities of inorganic and metal organic compounds, Van Nostrand Co. (1940).

61. R. Nasanen, B. Klaile, Suomen Kemistilehti B27, 50 (1954).

62. J.R. Selman, L. Hsueh, J. Newman, Physical properties of $CuSO_4$-H_2SO_4 solutions, Inorganic Materials Research Division Annual Report 1966, p. 49 (U.C.R.L.-17330, March 1967).

63. Chemical Engineer's Handbook, J.H. Perry editor, McGraw-Hill Book Co. 1950.

64. H.K. Richardson, F.D. Taylor, Trans. of the Am. Electrochem. Soc. 20, 179 (1911).

65. E. Peters, H. Majima, Annual meeting of the A.I.M.E., New York February 25-29, 1968.

66. G. Valensi, Métaux et Corrosion 12 (145), 145 (1937).

67. G. Valensi, Métaux et Corrosion 12(146), 195 (1937).

68. H. Gerisher, Z. Elektrochem. 54, 366 (1950).

69. J.V. Petrocelli, A.A. Paolucci, J. Electrochem. Soc. 98, 291 (1950).

70. E. Lewartowicz, J. Chim. Phys. 49, 564 (1952).

71. E. Lewartowicz, J. Chim. Phys. 49, 573 (1952).

72. A.M. Baticle, F. Perdu, P. Vennerau, C.R. 264, C12 (1967).

73. W.C. Schumb, M.S. Sherill, S.B. Sweetser, J. Amer. Chem. Soc. 59, 2360 (1937).

74. W.C. Bray, A.V. Hershey, J. Am. Chem. Soc. 56, 1889 (1934).

75. J.J. Fritz, C.R. Fuget, J. Phys. Chem. 62, 303 (1958).

76. R.C. Reid, T.K. Sherwood, The properties of gases and liquids, McGraw Hill Book Co. (1958).

77. Handbook of Chemistry and Physics, R.C. Weast editor, The Chemical Rubber Co. (1968).